ELASTIC TESTS ON STEEL BEAMS WITH ECCENTRIC
RECTANGULAR WEB OPENINGS

by

SHUAIB HAROON AHMAD

B.S., N.E.D. Engineering College, Karachi, Pakistan, 1974

———————————

A MASTER'S THESIS

submitted in partial fulfillment of the
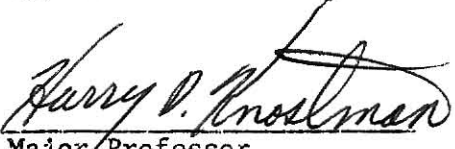
requirements of the degree

MASTER OF SCIENCE

Department of Civil Engineering

KANSAS STATE UNIVERSITY
Manhattan, Kansas

1975

Approved:

Major Professor

TABLE OF CONTENTS

LIST OF FIGURES

LIST OF TABLES

NOMENCLATURE

<u>Symbols</u>

A	cross sectional area
E	modulus of elasticity
G	shear modulus
I	moment of inertia
L	length
M	moment
Q	resultant force
P	applied load
V	shear
2a	length of the opening
f	stress
2h	depth of the opening
k	kip
m	moment due to unit load
t	thickness
v	shear due to unit load
x	longitudinal distance from the center line of the opening
y	transverse distance from centrodial axis to any fiber
δ	deflection
σ	normal stress
τ	shearing stress
$(U_o)_s$	shearing strain per unit volume
U_s	total shearing strain
$(U_o)_b$	bending strain per unit volume
U_b	total bending strain

Subscripts

B	bottom section
N	net section
T	top section
W	web

Abbreviations

BHMS	Bottom High Moment Section
BLMS	Bottom Low Moment Section
D.G	Dial gage
HME	High Moment Edge
HMS	High Moment Section
in.	inch, inches
ksi	kips per square inch
LME	Low Moment edge
LMS	Low Moment Section
N.A	Neutral Axis
THMS	Top High Moment Section
TLMS	Top Low Moment Section

INTRODUCTION

During recent years, architects and engineers have more frequently been specifying that openings be provided in the webs of beams and girders. These openings accommodate the passage of utility components, thereby minimizing the story height and consequently the cost of the buildings. The openings cut in the web may be concentric or eccentric with respect to mid-depth of the structural steel members. The position of the opening depends upon the level of the utilities components and the level of the beam or girder. When the practice of cutting openings in the web first started, little information was available regarding the effect of the opening on the strength of the members. In the past few years considerable effort has been made by the steel industry, university investigators and ASCE to develop theoretical and experimental information on steel beams with web openings.

Most of the previous investigations (3,5,6,12) have been restricted to reinforced and unreinforced concentric web openings and a suggested design guide (16) is available for this case. However, until recently little attention had been paid to openings which are eccentric with respect to mid-depth of the beam. Some work has been done on eccentric circular web openings (4) and a design guide (13) has been published. Papers (1,2,8,9,11) have been published on the strength of beams with eccentric rectangular web openings. The papers (2,8,9) take into consideration only the unreinforced web openings, whereas (1,11) deal with both the reinforced and the unreinforced cases.

This investigation deals with the stress analysis and deflections of beams with eccentric, rectangular, unreinforced and reinforced web openings. Although plastic design methods may be preferred because of their rationality and because their application to rectangular holes have been explored

extensively (3,6,9,15,17), the allowable stress approach may be necessary in some cases. In particular, openings in non-compact sections require elastic analysis. In this report attention is restricted to determining the elastic stresses and the deflections, and it is assumed that buckling does not occur.

The Vierendeel method of analysis is perhaps the most popular theoretical method used to compute the normal stresses in the vicinity of the opening. This analysis was originally developed for rigid trusses with posts normal to the main longitudinal chords of the truss. The Vierendeel analysis estimates the normal stress at the opening as a summation of the primary bending stress and the secondary bending stress (Vierendeel stress). The primary bending stress is due to the bending moment at the centerline of the opening, while the secondary bending stresses are due to the shearing forces carried by the sections above and below the opening. This method has its limitations, first it can only be applied to rectangular web openings, and second it does not account for the stress concentration at the corners of the openings. Cooper and Snell (5) performed sixteen elastic tests on beams with reinforced concentric rectangular web openings and obtained good agreement with the results predicted by the Vierendeel method of analysis. For its application to beams with eccentric rectangular web openings, it is necessary to know the shear distribution ratio V_T/V_B, i.e., the ratio between the shearing force carried by the section above the opening (V_T) to that carried by the section below the opening (V_B). Four recent papers have presented methods to determine this shear distribution ratio V_T/V_B.

Frost (9) conducted tests on four A36 steel W16 x 40 beams having rectangular openings at different eccentricities and moment shear ratios. No

consistent value of the shear force distribution ratio V_T/V_B could be obtained, although considerable data was recorded during the tests.

Bower (2) used data based on experimental tests conducted by Frost (10) to compare five different analytical methods for determining the shear force distribution ratio V_T/V_B at unreinforced eccentric openings. Bower concluded that the best shear force ratio was that determined by equating the shear deformation in the sections above and below the opening when the shear coefficients of Cowper (7) are used.

Brice-Nash and Snell (1) used finite element computer programs to determine the shear force above and below the opening for both the unreinforced and the reinforced cases. During these investigations the moment-shear ratios and the eccentricity of the opening were varied to determine the effect on the shear force distribution ratio V_T/V_B. Six theoretical methods of calculating the shear force distribution were compared with the results of the finite element investigation. None of these methods gave results which were entirely consistent with the finite element results, however, the method preferred by Bower (2), discussed above, did seem to give the best agreement.

Douglas and Gambrell (8) developed a design procedure for beams with unreinforced eccentric web openings based on the interaction curves which were derived using the Vierendeel method of elastic stress analysis and von Mises yield theory. By treating the sections above and below the opening as fixed-end beams they determined an equation for shear ratio V_T/V_B. This equation is almost the same as that used by Frost (9), which was based on relative stiffness of the two sections, except that Douglas and Gambrell used the shear coefficient of Cowper (7) to determine the shear deflection.

The main objective of the elastic tests was to determine experimentally the shear distribution ratio V_T/V_B and the effect the opening reinforcing had on this ratio. The elastic tests in this report deal with W16 x 40 and W16 x 45 steel beams. McNew (11) conducted both elastic and ultimate load tests on the W16 x 45 steel beams. The beams had 9" x 6" rectangular openings with an eccentricity of 2 inches above the mid-depth, but differed in the amount of reinforcing. Beam 1 was unreinforced, whereas the opening in Beam 2 was reinforced with 0.5 sq. in. reinforcing bars. In this report the experimental and finite element elastic test results of Beams 1 and 2 are revised and presented along with the results of the present investigation on W16 x 40 steel beams.

Elastic tests were conducted on steel beams having four different opening configurations, which were named as Beams 3, 4, 5 and 5a. All four beams had eccentrically positioned rectangular web openings of the same size, but differed in the amount of reinforcing or eccentricity of the opening. The beams were each subjected to elastic tests at three different moment shear ratios, hence in all data was taken for twelve elastic tests. During the elastic tests, both deflection and strain data were recorded. Deflections were measured at three sections, namely at the edges of the openings and at the mid-span of the beam. Experimental results of mid-span deflections and relative deflections across the opening have been compared with those predicted by theory and were found to be in good agreement. Longitudinal linear strains were measured at sections four and one half inches either side of the vertical centerline of the opening. The cross-sectional stresses were determined from these strains and were used to evaluate the shear force

carried by the sections above and below the opening. This experimental value of shear distribution V_T/V_B was used as input data for Vierendeel analysis in estimating the stresses in the vicinity of the opening.

Theoretical investigation included the determination of the shear distribution ratio V_T/V_B by finite element analysis. The finite element analysis is an elastic-plastic computer program. Only the elastic portion of the program was used. For Beams 1 and 2 finite element runs were made for four moment-shear ratios and for Beams 3, 4, and 5 runs were made for three moment-shear ratios resulting in a total of seventeen finite element computer runs. No finite element computer run was made for Beam 5a. In the finite element analysis, the shear distribution was calculated by numerically integrating the normal as well as the shearing stress curves. The normal stresses were compared with those obtained by Vierendeel analysis and experimental tests and good agreement was obtained. The shear distribution ratio V_T/V_B obtained experimentally compared reasonably well with the results predicted by the finite element analysis. Results from several analytical methods for predicting the shear force distributions have been compared with the results predicted by finite element and those obtained experimentally.

Equations for predicting the mid-span deflection and relative deflection across the opening have been developed and presented in this report. The theoretically predicted deflections compare reasonably well with experimental results.

EXPERIMENTAL PROGRAM

Introduction

The elastic tests were conducted on a single 14 ft. – 6 in. length of
W16 x 40 steel beam. The four different opening configurations which were
studied were referred to as Beam 3, 4, 5 and 5a. All the tests utilized the
same web opening but variations were made in the amount of reinforcing for
Beams 3, 4, and 5 and in the position of the opening for Beam 5a. The beams
were simply supported and were subjected to a single concentrated load at
mid-span. By varying the span each beam was tested at three different
moment to shear ratios (M/V = 20, 40, 60 inches). Hence in all, strain and
deflection data was taken for twelve elastic tests.

Web Opening

To minimize the effect of the concentrated load the vertical centerline
of the opening was located at 25 inches from the mid-span of the beam. The
opening was a 12 inch long by 6 inch deep rectangle with 17/32 inch radius
corner fillets. It was located at an eccentricity of 2 inches, with respect
to the mid-depth of the beam. The centerline of the opening was above mid-
depth for Beams 3, 4 and 5 and below for Beam 5a. The web opening was cut
by first drilling 17/16 inch diameter holes at all the four corners of the
opening and then flame cutting between the holes. Except where strain
gages were placed the irregularities in the edges of the openings were left
in order to make the specimen more representative of commercial fabrication.

Reinforcement

To be able to analyze the effect of adding reinforcing around the opening
the unreinforced beam was first tested elastically and was named Beam 3.

Beam 4 was fabricated by adding 1/2 sq. in. of reinforcement above and below the opening on only one side of the web. Beam 5 was obtained from Beam 4 by adding the same amount of reinforcing to the other side of the web. Beam 5a is Beam 5 inverted, so that the opening is eccentric below the mid-depth of the beam. The reinforcing for Beam 4, 5 and 5a consisted of steel bars of rectangular cross sections running parallel to the beam flanges and welded to the beam with 3/16 inch fillet welds. Reinforcing bars were made from 1/4 inch thick by 2 inch wide bar stock and were 18 inches long so that they extended 3 inches on either side of the opening. This size of the reinforcing bar was used to minimize the possibility of local buckling according to the AISC Specifications for width-to-thickness (18). The bars were placed 1/4 inch from the top and the bottom edges of the opening. The welds ran the full length of the bar on the sides nearest the opening and lapped back 1-1/2 inches on the other sides at the ends. The details of the reinforcement are shown in Fig. 7. No bearing stiffeners were used during the elastic tests.

The cross-sectional dimensions of the beams were measured at sections 1-1/2 inches away from the edges of opening, i.e., at the low and high moment sections. These sections were chosen for measuring the dimension because experimental strain data was to be recorded at these sections. Figure 6 shows the sections where the dimensions were measured. These cross-sectional dimensions were used in the Vierendeel analysis, in the numerical integration program (experimental) and to find the theoretical mid-span deflection and the relative deflection across the opening. Slight variations exist between the measured dimensions and those found in the AISC manual for W16 x 40. The width of the flange was found to vary quite a bit along the length of the beam, but the average value was within 0.4%

of the nominal value in the manual. The web of the test beam was found to be 8.08% thicker than the nominal dimension. The thickness of the flange was 5.5% thinner than the nominal. The average values of the cross-sectional dimensions measured at the low and high moment sections are presented in Table 1.

Tensile specimens (Coupons) were cut from each beam and from the reinforcing bar stock. The Coupons for the tensile tests were taken from a one foot length cut from one end of each beam, two from the web, and two from each flange. As the reinforcing bars were cut from the same length of bar stock, two one foot lengths were cut from the same piece for the tensile tests. Figure 8 shows the locations from which the Coupons were taken and their dimensions. The tension tests were conducted on a Riehle screw type, 20,000 pound universal testing machine, using a 2 inch extensometer and an automatic load-elongation recorder. The tests results are presented in Table 2 and consist of the static yield point σ_y (yield point corresponding to zero strain rate), the tensile strength σ_u, the percent elongation in 2 inch and the percent reduction in area.

Instrumentation

Two types of instrumentation were used during the elastic test program. The purpose of the first type was to measure the strain which was accomplished by the use of 1/4 inch gage length, epoxy backed, foil type electrical resistant strain gages. These were Micro Measurement NO EA-06-250BG-120. Strain gages were oriented parallel to the longitudinal axis of the test beam and were used on the flanges, web and reinforcing bars at the low and high moment sections, which were 9 inches apart. In all 42, 58, 76, and 76 strain gages were used on Beams 3, 4, 5 and 5a, respectively. The location

of the strain gages on Beams 3, 4, and 5 are shown in Figs. 9, 10, and 11. As Beam 5a was obtained by inverting Beam 5, there was no change in the strain gage locations for Beam 5a.

The purpose of the second type of instrumentation was to measure the vertical deflections. This was achieved by using mechanical dial gages having dial divisions of one-thousandth of an inch and a maximum deflection of 2 inches. During the elastic test on the beams, vertical deflections were recorded at three sections, the low moment edge (LME), the high moment edge (HME) and at the mid-span of the beam. The dial gages were supported by a 4 inch steel channel. In order to eliminate the necessity of correcting the deflection readings due to the settlement of the support arms of the machine, the channel and the beam were supported on the same support pedestals. The location of the dial gages are shown in Fig. 7.

Test Procedure

The elastic tests on the beams were conducted in a 200,000 lb capacity, Tinius-Olsen screw type testing machine, with a lever-type load measuring system. The machine is equipped with centilever arms for holding the pedestal supports for the beams, and is well suited for testing the beams at different moment shear ratios, since the pedestals can be moved with ease. The pedestals had rounded top and bottom surfaces, thus permitting the rotation of the beam and rocking of the pedestal as the load was applied. During the loading a 3" x 7" x 1" bearing plate was placed on top of the beam at the load point. The beam was loaded with a 10 kips load before the strain gages and the dial gages were "zeroed." The 10 kips load was applied in order to make sure that the beam was seated properly on the pedestal supports before recording any data. By "zeroing" the instruments at the 10 kips load, the

nonlinearity in the strain and deflection data, which was found to occur

while seating the beam, was avoided. Before recording any data at each

moment-shear ratio the beams were loaded and unloaded three or four times

to allow the gage backing and adhesive to adjust. The load was applied in

two equal increments of 15 kips each, up to a maximum load of 40 kips. The

same load increments were used during the unloading, ending the test with

10 kips load. The proper functioning of the instruments was checked by

comparing the data recorded during loading and unloading cycles.

THEORETICAL METHODS

Finite Element Analysis

The finite element analysis is an approximate method for obtaining solutions to the problems in mechanics. Due to the complexities of the matrices involved, it is only practical to obtain solutions with the help of computers. The computer program (14) used in this investigation was a two-dimensional elastic-plastic program developed jointly by the Illinois Institute of Technology Research Institute and the Air Force Flight Dynamics Laboratory. Since elastic conditions were under consideration, only the elastic portion of the program was used.

For the application of this method, the beam is idealized by dividing it into small triangles and bars called elements. The accuracy of the solution depends upon the size of the elements, and in general, the smaller the elements the better the accuracy. Since the time to obtain a solution depends upon the number of elements, the tests beams were divided in such a fashion that the elements were comparatively bigger at sections away from the opening but in the vicinity of the opening (area of prime interest) the elements were made smaller for better accuracy. Constant strain triangles and bar elements were used to represent the beams. The complete structure is obtained by connecting these elements at points called nodes. Triangular elements are connected at the corners and the bar elements are connected at the ends. Finite element discretization of Beam 5 is shown in Fig. 1a and 1b, as a typical example. Beam 4 was idealized in the same manner and Beam 3 was the same except there were no reinforcing bar elements immediately above and below the opening.

THIS BOOK
CONTAINS
NUMEROUS PAGES
WITH DIAGRAMS
THAT ARE CROOKED
COMPARED TO THE
REST OF THE
INFORMATION ON
THE PAGE.

THIS IS AS
RECEIVED FROM
CUSTOMER.
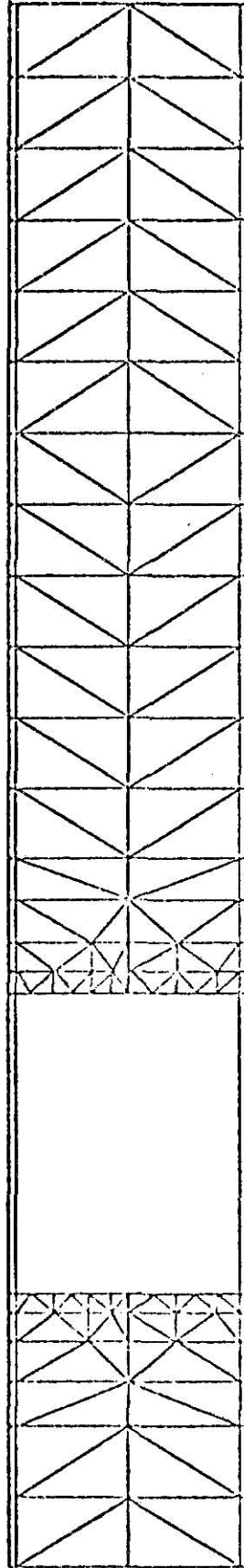
Fig. 1a Finite element discretization of Beam 5
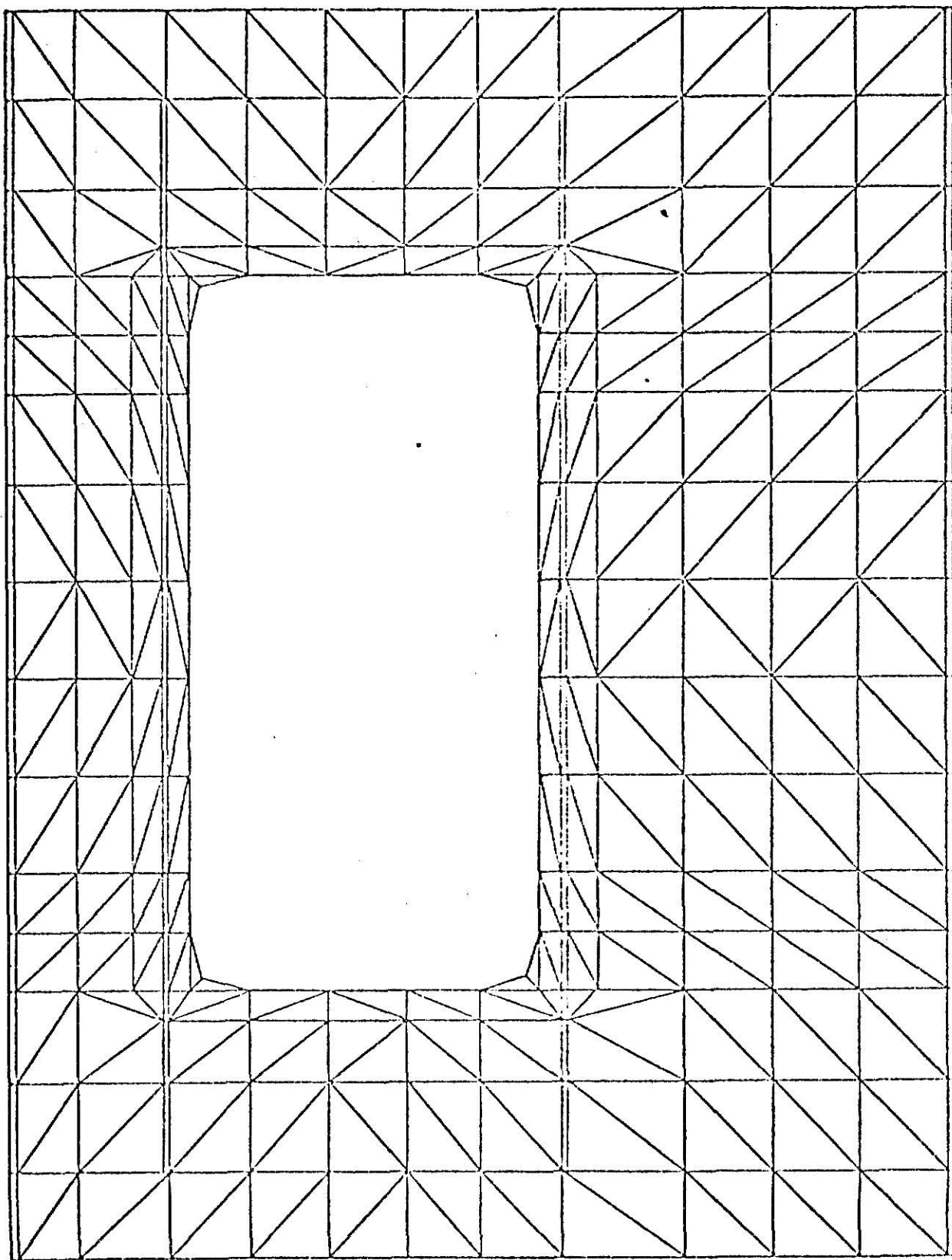
Fig. 1b Finite element discretization at the web opening of Beam 5

In order to apply the two-dimensional finite element program to a three dimensional structure, certain modifications had to be made. The actual flanges and web reinforcing were replaced by equivalent bar elements. These bar elements run between nodes along the path of actual flange and web reinforcement. The bar elements do not have thickness, hence in determining the equivalent flange area either the flange area or the moment of inertia of the beam could be maintained. To maintain the bending stiffness of the beam the equivalent flange area was determined so that the moment of inertia remained constant.

A coordinate system for the entire beam was set up, with the origin at the left end of the bottom flange. Thus each triangular element could be specified by the X and Y coordinates of its nodes, and the thickness of the elements. In the case of bar elements, the cross-sectional area was specified, instead of thickness. Since each of the bar or triangular elements has to satisfy equilibrium, the force vector can be equated to the product of the stiffness matrix and the displacement matrix. The displacement of each node is determined, and then used to obtain element strains and stresses. A more detailed description of the method of application of the finite element method is given in Ref. (1).

Finite element computer runs were made for Beams 1, 2, 3, 4 and 5. For Beams 1 and 2 four moment shear ratios were tested and for the remaining beams three moment-shear ratios were investigated. No finite element computer run was made for Beam 5a. In all, seventeen finite element models were investigated. Figure 2a shows the position of a vertical section of elements at the low moment section (LMS) of Beam 3, when M/V = 20 inches.
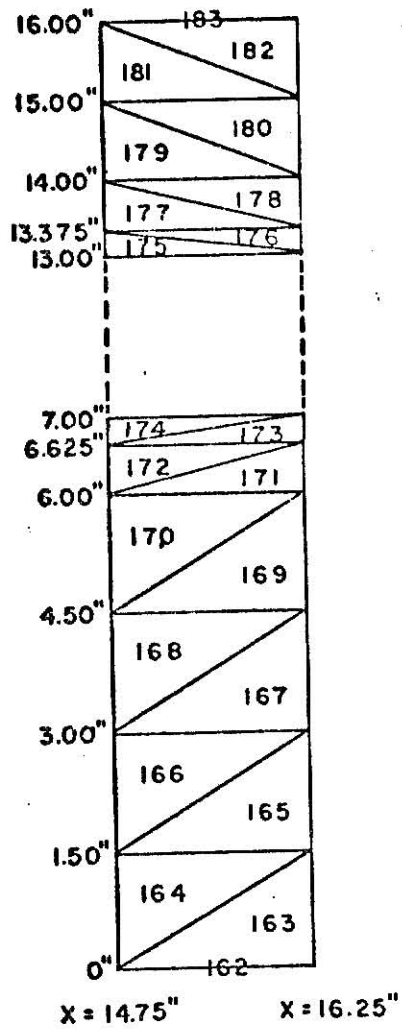
Fig. 2a Element discretization for M/V = 20" at X = 15.50" (LMS), Beam 3 (unreinforced)
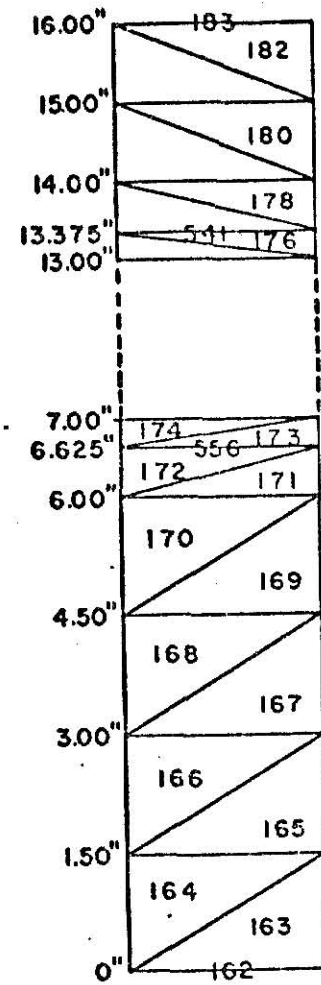
Fig. 2b Element discretization for M/V = 20" at X = 15.50" (LMS), Beam 4 (reinforced)

Since Beam 3 is unreinforced, the only bar elements are numbers 162 and 183, which represent the beam flanges. For the reinforced beams the only change in the idealized section is the addition of the reinforcing bar elements. These bar elements have the same location and cross-sectional area as the actual reinforcing and are shown by element number 541 and 556 in Fig. 2b. The strains obtained for this set of elements and for a similar set at the high moment section (HMS) were used to determine the amount of shearing force distributed to the top section (V_T) and the bottom section (V_B) at the web opening.

The vertical centerline of these elements is at X = 15.50 in. which is the section to be investigated. The actual size of the opening is 12 in. x 6 in. for Beams 3, 4, and 5, but to stay away from the effect of stress concentrations at the corner, the section selected for the investigation was chosen to be 1.50 in. away from the edge of the opening. The centroid of each of the triangular elements is the point where stress is determined. For example the stress in elements 163 and 164 are combined and averaged to obtain the stress which acts halfway between the centroids of the elements 163 and 164, which falls at coordinates X = 15.50" and Y = 0.75".

By averaging the stresses between the adjacent elements, ten stress points at X = 15.50" (LMS) were obtained. The curves of normal stresses were plotted and a numerical integration program was used to obtain the shear force distribution V_T/V_B. This program was also used for numerical integration of the experimental data to obtain the experimental V_T/V_B.

Numerical Integration Program

The numerical integration computer program divides the normal stress curves into small areas and calculates the force (Q_i) acting on each of

these small areas. The summation of all these forces give the resultant

force (Q) acting on the section. The same procedure is repeated for all

four sections; namely top and bottom at low and high moment sections.

Figure 3 shows the resultant forces and their locations on all the four

sections.
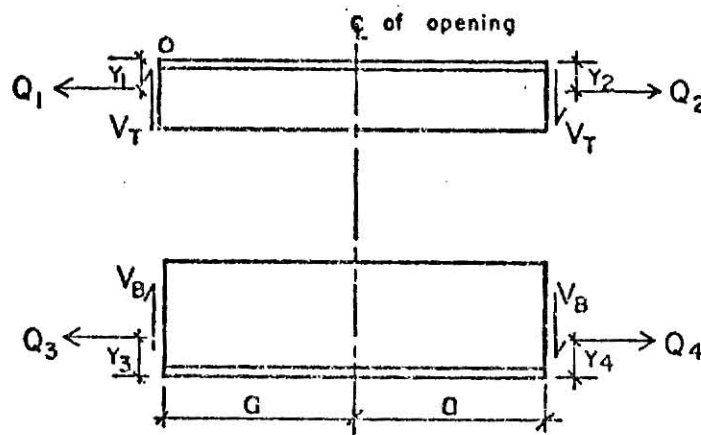
Fig. 3. Equilibrium of tee sections.

In the computer program the shear force above the opening (V_T) is

determined by writing the moment equilibrium equation about point 0, giving

$$V_T(2a) = Q_2 Y_2 - Q_1 Y_1 \quad - - - - - - - - - - \quad (1)$$

$$V_T = \frac{Q_2 Y_2 - Q_1 Y_1}{2a} \quad - - - - - - - - - - \quad (2)$$

where V_T = shear in the section above the opening

Q_1 = resultant force acting on the top low moment section

Q_2 = resultant force acting on the top high moment section

Y_1 = distance from the top to the point where the resultant force

    Q_1 acts

Y_2 = distance from the top to the point where the resultant force

Q_2 acts.

The expression Q times Y can be replaced by moments, hence

$$V_T = \frac{M_2 - M_1}{2a} - - - - - - - - - - - \quad (3)$$

Similarly the shear in the bottom section (V_B) can be expressed as

$$V_B = \frac{Q_3 Y_3 - Q_4 Y_4}{2a} - - - - - - - - - \quad (4)$$

$$V_B = \frac{M_3 - M_4}{2a} - - - - - - - - - - - \quad (5)$$

The total shear force acting on the section is the summation of the shear in

the section above the opening (V_T) and the shear below the opening (V_B).

Hence the total shear at the section is given by

$$V = V_T + V_B - - - - - - - - - - - \quad (6)$$

A more detailed description of the method is given in Ref. (11).

The shear force distribution V_T/V_B was also determined from the shear

stress distribution curves. The area under the curve above the opening

multiplied by the thickness of the element gives the shear force above the

opening, and the area under the shearing stress curve below the opening

multiplied by the thickness of the element gives the shear force below the

opening.

Vierendeel Method of Analysis

This analysis was originally developed for rigid concrete trusses with

posts normal to main longitudinal chords of the truss. It was later used

for rigid steel trusses of the same nature. This approximate elastic analysis,

when applied to beams with rectangular web opening, predicts quite accurately

the stresses in the vicinity of the opening. For its application to beams
with web openings, the following assumptions have to be made:

(i) The beam section above and below the opening are fixed at their
ends.

(ii) Points of inflection occur in the sections at the vertical center-
line of the opening.

(iii) The amount of shearing force distributed to the sections above and
below the opening must be assumed.

Figure 4 shows the portion of the beam between the reaction and the
centerline of the opening. Since this portion is in equilibrium, the internal
bending moment is equal to the reaction V times the distance L_o, and the
internal shear V_T and V_B add up to reaction force V.
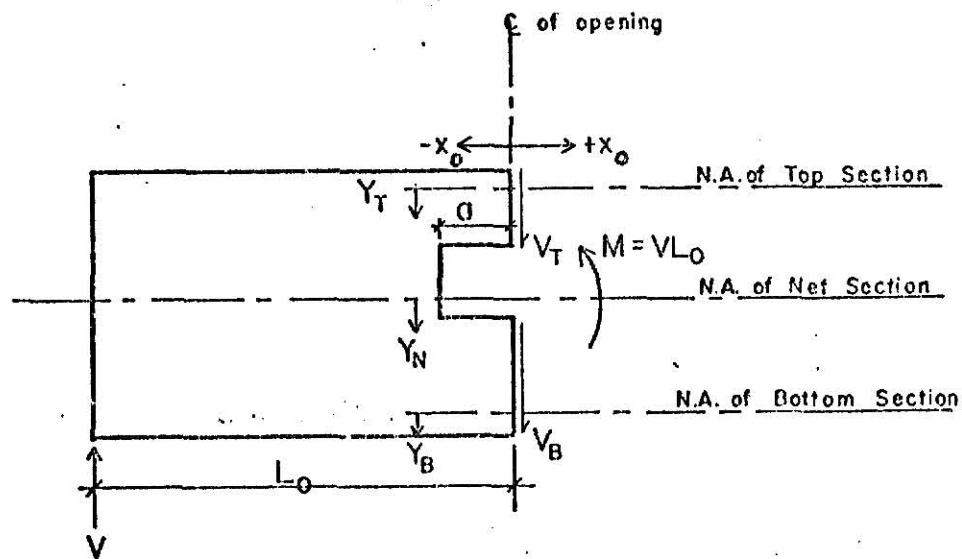
Fig. 4. Free body diagram.

According to Fig. 4 the general equation for the combined stress at any
point in the top or bottom section is given as the summation of the primary

bending stress and the secondary stress (Vierendeel stress). The combined stress for the top section may be expressed as

$$f_T = \frac{MY_N}{I_N} + \frac{V_T \cdot X_o \cdot Y_T}{I_T} \quad - - - - - - - - - \quad (7)$$

and for the bottom section

$$f_b = \frac{MY_N}{I_N} + \frac{V_B \cdot X_o \cdot Y_B}{I_B} \quad - - - - - - - - - \quad (8)$$

where M = primary bending moment at the centerline of the opening and is equal to V times L_0.

Y_N = distance from neutral axis of the net beam section to any fiber, and is measured positive down.

I_N = moment of inertia of the net section.

V_T, V_B = shear in the top and bottom section, respectively.

X_o = distance from the centerline of the opening and measured positive, towards the right.

Y_T, Y_B = distance from the neutral axes of top and bottom sections, respectively, to any fibre in the section and are measured positive down.

I_T, I_B = moments of inertia of the top and bottom sections.

As is obvious from the above equations, for the application of Vierendeel analysis; the shear distribution ratio V_T/V_B should be known. In the case of beams with concentric web openings, the value of V_T/V_B is one, and hence the Vierendeel analysis can be applied directly. But in the case of beams with eccentric web opening, the shear distribution ratio V_T/V_B must be obtained from experimental investigation; or from finite element analysis, then used as input data for obtaining stresses around the opening. The Vierendeel method of analysis is restricted to rectangular web openings and does not

account for the stress concentration around the corners of the opening. A detailed description of the method is given in Ref. (11).

Equilibrium Check

According to Eqs. (7) and (8), the normal stress at the centerline of the opening may be written as

$$f_x = \frac{M Y_N}{I_N} - - - - - - - - - - - - \quad (9)$$

where f_x = normal stress

M, Y_N, and I_N are the same as in Eqs. (7) and (8).

The normal stress f_x may be integrated over the total area of the top tee section to give the resultant axial force (Q) acting on the section.

Hence

$$Q = \int_{A_T} f_x \cdot dA = \frac{M}{I_N} \int_{A_T} Y_N \cdot dA - - - - - - - \quad (10)$$

or

$$Q = \frac{M}{I_N} A_T \bar{Y}_{NT} - - - - - - - - - - - \quad (11)$$

where A_T = area of the top tee section

$\bar{Y}_{NT}$ = distance from the centroid of the net beam section to the centroid of the top tee section.

The resultant axial force (Q) only varies with the moment M at the vertical centerline of the opening. Hence for a given load P the above equation may be written as

$$Q = C \cdot M - - - - - - - - - - - - \quad (12)$$

where C = constant, which depends upon A_T, I_N and $\bar{Y}_{NT}$ (section properties). To satisfy equilibrium, the resultant axial forces at all four sections, see Fig. 3, must be equal. Hence, the evaluation of Q for one section is all that is required.

DEFLECTIONS

Mid-span Deflections

During the elastic tests on the beams, mid-span deflections were recorded along with the deflections at the low moment edge (LME) and the high moment edge (HME). The mid-span deflections may be theoretically predicted using Castigliano's theorem on deflections. If the effect of the opening, the opening reinforcement, and the cover plates are neglected. The mid-span deflection of a simply supported beam with load P at the center may be written as

$$y_p = \frac{PL^3}{48EI} + \frac{PL}{4A_W G} \; - - - - - - - - - - - \; (13)$$

where   P = point load at the mid-span of the beam

L = span length of the beam.

E = Young's modulus of elasticity (E = 29,600 ksi)

I = moment of inertia of the gross beam section.

A_W = area of the web.

G = shear modulus (G = 11,500 ksi)

The first term in the above equation represents the deflection due to the moments, the second term shows the deflection due to the shear. The shear correction factor (k) which is normally applied to shear deflection has been taken as A/A_W.

If the flange cover plates are taken into account, the above equation takes the form

$$y_{p_1} = \frac{P}{48EI_R}\left[L^3 + (L-L_R)^3\left(\frac{I_R}{I} - 1\right)\right] + \frac{P}{4GA_{WR}}\left[L - (L-L_R)\left(\frac{A_{WR}}{A_W} - 1\right)\right]$$

where L_R = length of the cover plates.

I_R = moment of inertia with flange plates added.

A_{WR} = web area found by taking the beam depth including the thickness

of the cover plates time the web thickness.

The above two equations were used by McNew (11) for predicting the mid-span

deflections for Beams 1 and 2.
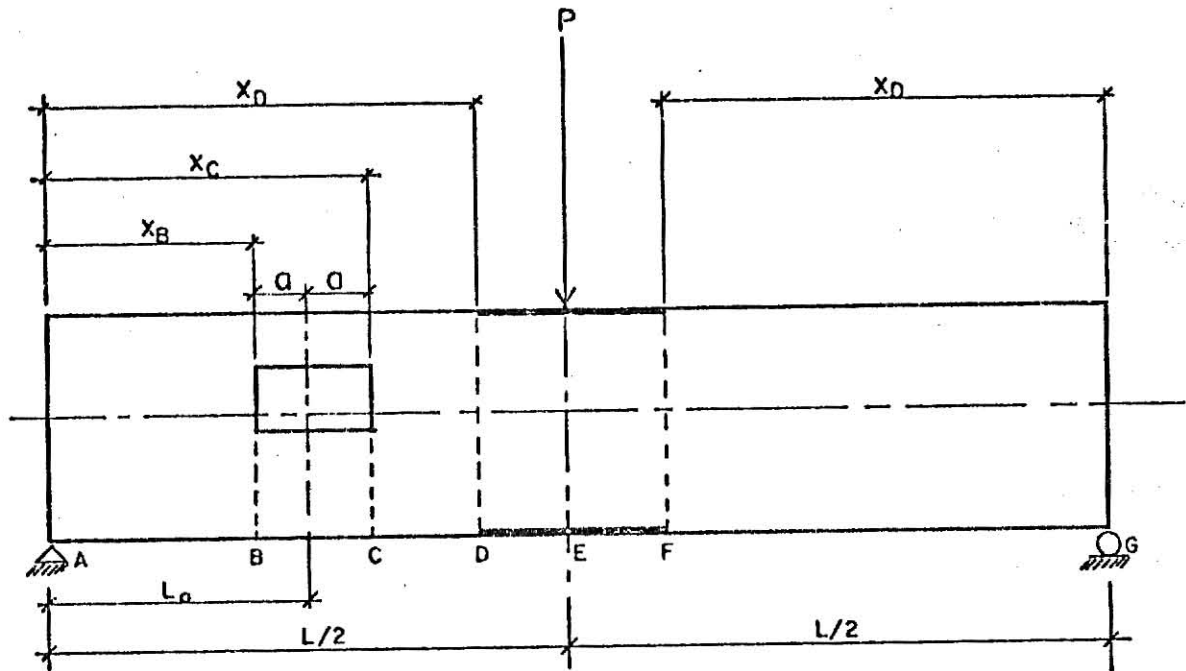
Fig. 5

If the effect of the web opening and the opening reinforcement are taken

into account and the flange reinforcement is present the mid-span deflection

may be written as

$$y_{P_2} = \frac{P}{12EI}\left[X_B^3 + 2X_D^3 - X_C^3 + 2\,\frac{I}{I_R}\left(\frac{L^3}{8} - X_D^3\right)\right] + \frac{PL_0^2 a}{2EI_N} + V_T\left(\frac{2a^3}{3EI_T} + \frac{k_T(2a)}{A_T G}\right)$$

$$+ \frac{kP}{4AG}(X_B + 2X_D - X_C) + \frac{k_R P}{4A_R G}\left(\frac{L}{2} - X_D\right) - - - - - - - - - - - - (15)$$

where k_T, k, and k_R are the shear deflection coefficients for the top tee
section, the gross section and the flange reinforced gross section, respec-
tively. The other dimensions used in the above equation are shown in Fig. 5
and the derivation of Eq. (15) is presented in Appendix A.

Relative Deflection Across the Opening

In an attempt to better understand the behavior of beams at web openings,
deflections were measured at the high and low moment edges at the center of
the bottom flange. Mechanical dial gages with the smallest division of
one-thousandth inch were used. More accurate gages could have been used
to an advantage since for the lower loads and M/V ratios the opening deflec-
tions were but a few thousandths of an inch.

Castigliano's theorem on deflections (strain energy principle of virtual
forces) was used to derive the equations for the deflection across the opening.
For a detailed explanation of the derivation see Appendix A. Because of the
reduced area of the opening cross-section, shear deformation becomes important.
If we assume that shearing stress is proportional to shearing strain the
shear strain energy per unit volume may be written as

$$(U_o)_s = \tau^2/2G \quad - - - - - - - - - - - (16)$$

where τ is the shearing stress and G is the shearing modulus.

By assuming that the basic strength of materials equation for the transverse
shearing stress is sufficiently accurate we can write the total shear strain
energy as

$$U_s = \int_o^\ell \frac{kV^2 dx}{2AG} \quad - - - - - - - - - - (17)$$

where A is the cross section area and k is the shear deflection coefficient. The derivation of the shear deflection coefficient k for the shapes involved in this report are given in Appendix B.

Assuming that normal stress is proportional to normal strain, the strain energy of bending per unit volume may be written as

$$(U_o)_b = \sigma^2/2E \quad - - - - - - - - - - \quad (18)$$

where σ is the normal stress and E is the modulus of elasticity. When the normal stress is given by the flexure formula, $\sigma = MY/I$, the total strain energy of bending becomes

$$U_b = \int_o^\ell \frac{M^2 dx}{2EI} \quad - - - - - - - - - - - \quad (19)$$

where M is the moment at x and I is the centroidal moment of inertia.

The bending moments and shearing forces in regions other than at the opening are well defined and the strain energy may be determined using Eqs. (17) and (19). The normal stresses at the opening are obtained by assuming that the Vierendeel method of analysis, as explained in Ref. (11), is correct. The strain energy is then determined by substituting the equations for normal stress into Eq. (18) and integrating over the volume. In order to apply this method it is necessary to know the amount of the shearing force carried above and below the opening. Although there are a number of theoretical methods for determining this ratio, the method based on the Vierendeel assumptions seems to give the best results. This procedure assumes that the sections above and below the opening behave as fixed end beams with center inflection points which must deflect equally. Applying

Castigliano's Theorem to the strain energy derived using these assumptions

results in the following equation for the relative opening deflection:

$$y_{BC} = \frac{2Pa}{E}\left[\frac{x_C^3 - x_B^3}{6IL} - \frac{x_C^2}{4I} + \frac{L_o a}{I_N L}(\frac{L}{2} - L_o) + \frac{kaE}{ALG} + \frac{L^2}{16I_R}\right.$$

$$\left. + \frac{x_o^2}{4I}(1 - \frac{I}{I_R}) + V_T(\frac{2}{3}\frac{a^3}{EI_T} + \frac{k_T(2a)}{A_T G})(1 - \frac{2a}{L})\right] \text{ --- (20)}$$

where P is the applied load, the subscript T refers to top section, and I,

I_N, and I_R are the centroidal moments of inertia of the gross beam, the net

section at the opening and of the flange reinforced beam.

The equations for the theoretical relative deflection across the opening

and the mid-span deflection were programmed for a digital computer. In the

deflection calculations, the modulus elasticity was taken as 29,600 ksi.

ANALYTICAL METHODS FOR CALCULATING SHEAR DISTRIBUTION RATIO V_T/V_B.

For concentric web openings in steel beams, the shear force at the

opening is equally distributed between the upper and lower tee sections,

hence the shear distribution ratio V_T/V_B is 1.0. An eccentric opening in

the web creates a section as shown in Fig. 6. The unequal tee sections

cause unequal shearing forces to be distributed to the web sections above

and below the opening. Several methods of calculating unequal shear force

distribution ratios V_T/V_B were presented by Bower (2). One method assumes

that shear forces are proportional to the bending stiffnesses of the tees.

Two other methods considered V_T/V_B as an exclusive function of the beam web

instead of the tee sections, and another method takes into account the

effect of the beam flanges in altering the shear stress distribution in a

normal wide flange beam. In another method Bower equated the shear deflec-

tion of the upper and the low sections, but he did not consider shear and

bending deflections at the same time, hence the length of the opening did

not enter the calculations. His theoretical ratios were compared with the

experimental results obtained from four W16 x 40 steel beams having a

12.80" x 6.50" rectangular opening with one and two inch eccentricities.

Brice-Nash (1) summarized the methods of Bower in his report and compared

the ratio of V_T/V_B that he obtained by the finite element method to Bower's

theoretical methods. Brice-Nash applied the finite element method to six

W16 x 40 steel beams. All beams had the same size opening (12.80" x 6.50")

but the openings were reinforced on three of the beams and the opening

eccentricities varied from one to three inches. Brice-Nash concluded that

the ratio V_T/V_B predicted by equating the shear deflections of the two

sections, when the shear shape factors of Cowper (7) were used, gave good

agreement with the results of the finite element analysis. Brice-Nash extended

the work of Cowper to include the unsymmetrical "I" sections, which were used

to obtain the shear coefficients for the reinforced tee sections.

Five different methods for calculating the unequal shear force distri-

bution in the case of eccentric rectangular web openings are presented here,

and the results obtained by applying them to particular problems are compared

with finite element and experimental results. Three of these methods are

quite similar and differ only in the shear deflection coefficient used. These

methods consider both shear deflection and bending deflection and are derived

by equating the deflections of the two sections. The shear distribution

ratio V_T/V_B in a general form may be written

$$\frac{V_T}{V_B} = \left(\frac{\dfrac{a^2}{3I_B E/G} + \dfrac{k_B}{A_B}}{\dfrac{a^2}{3I_T E/G} + \dfrac{k_T}{A_T}} \right) \quad - - - - - - - - - - (21)$$

where   a = one-half the opening width

       A = cross-sectional area

       I = moment of inertia

       k = shear deflection coefficient

       E = modulus of elasticity

       G = shear modulus

       T = subscript referring to top section

       B = subscript referring to bottom section

Method 1 uses a shear deflection coefficient k based on strain energy.

The derivation of the coefficient is presented in Appendix B.

Method 2 was presented by Frost (9) and suggests using a constant value

of 1.20 for the shear deflection coefficient k.

In Method 3, whose derivation is presented in Douglas and Gambrell (8), the coefficient k is replaced by 1/R, where R is the shear shape factor of Cowper (7). Cowper's coefficient R is derived on the basis of theory of elasticity.

The two other methods considered are derived by equating the shear deflection in the sections above and below the opening. Method 4 uses the shear deflection coefficient based on strain energy and takes the form

$$\frac{V_T}{V_B} = \frac{k_B A_T}{k_T A_B} \quad - - - - - - - - - - - - \quad (22)$$

Method 5, which uses the shear coefficient of Cowper is written as

$$\frac{V_T}{V_B} = \frac{R_T A_T}{R_B A_B} \quad - - - - - - - - - - - - \quad (23)$$

DISCUSSION AND PRESENTATION OF RESULTS

Normal and Shearing Stresses

Linear strains parallel to the axis of the beam were measured at the
cross sections 4.50 inches either side of the vertical centerline of the
opening, as shown in Fig. 9a. The strain gages were located at these sections,
which are 1.50 inches from the edges of the opening, so that the effect of
stress concentrations at the corners of the opening would be reduced. The
positions of the strain gages for beams 3, 4, 5 and 5a are shown in Figs. 9,
10 and 11. Measured strains were multiplied by the modulus of elasticity
($E = 29,600$ ksi) to obtain normal stresses. These normal stresses were then
plotted with respect to cross-sectional position, and numerically integrated
to determine the shearing force distribution V_T/V_B. The normal stress
curves for the experimental data are shown in Figs. 12-19. The three curves
in each of these figures correspond to the different M/V ratios tested and
for each beam the stresses at the low moment section and the high moment
section are shown in different figures. The plotted points in these curves
have been connected by straight lines and no attempt was made to draw smooth
curves. The stress plotted for the flanges are the average values except in
Figs. 16 and 17 where the web stress in the region of the flange is shown by
a dashed line for Beam 5. Similar curves obtained from the *finite element*
solution are presented in Figs. 20-25. Curves comparing the experimental
normal stresses to those obtained by the finite element solution and Vierendeel
method of analysis are shown in Figs. 28 and 29. The shear distribution
V_T/V_B, which was determined experimentally, was used in the Vierendeel
analysis to determine the stresses shown in these figures. The shearing

stress curves for Beam 3 which were obtained by the finite element method are shown in Figs. 30-31. These curves are typical of the shearing stress distribution of the other beams. Consideration of the normal stress curves, Figs. 26 and 27, shows that the main effect of adding reinforcing at the opening is to reduce the stresses toward the edge of the opening. For example at M/V = 60 inches, top low moment section (TLMS), the stress at the opening is 19.29 ksi for Beam 3, 15.50 ksi for Beam 4 and 10.38 ksi for Beam 5. The same pattern of results is predicted by the finite element analysis. It may be noted from the normal stress curves that finite element analysis tends to overestimate the stresses at the top and the bottom edges of the opening, while the Vierendeel analysis tends to underestimate the stresses, since it does not take into account the effect of stress concentration.

The normal stresses from the elastic tests and the normal and shearing stresses from the finite element analysis were numerically integrated to determine the shearing force present in the section above and below the opening. Tables 3a-4b presents the resulting shearing forces at the opening, for all M/V ratios tested for each beam. The numerical integration procedures were unable to account for the total 10 kip shearing force that should exist at the opening. It can be seen in Table 5 that the amount of shearing force accounted for is always less than that due to the applied load. It is felt that neglecting the flange fillets in the real beams could account for some of this difference but the same argument doesn't apply to the finite element solutions. However, checking the equilibrium according to Eq. (11) from the section Equilibrium Check, indicated beam equilibrium to be within 5%. To be more realistic, the forces in the reinforcing bars

were considered to act at the position of the weld on the side of the bar
nearest to the opening, approximately 1/4 inch from the edge of the opening.
Dimensions used in the numerical integration of the finite element data were
the same as those used in the finite element analysis. The actual dimensions
shown in Table 1 were used in the numerical integration program to determine
the experimental shear distribution ratio V_T/V_B. So that the effect of
adding reinforcing bars at the opening could be studied, slight adjustments
were made in the position of the openings for Beams 1 and 2. Although the
dimensions shown in Table 1 for Beams 1 and 2 are approximately the same, they
turned out to be sufficiently different to cause the change in the shear
distribution ratio V_T/V_B to appear inconsistent. However when the dimen-
sions at the opening were made equal, i.e., $d_T = 3.05"$ and $d_B = 7.05"$, the
change in the ratios V_T/V_B between the two beams became consistent with the
finite element results and those obtained for beams 3, 4 and 5. The initial
as well as the adjusted results are shown in Table 7a where a comparison of
the shear distribution ratio obtained by the different methods are shown.
Table 7a shows that the change in the value of shear distribution ratio V_T/V_B
increases with the addition of reinforcing to the web opening.

During the elastic tests on the beams, the strain gages were placed on
either side of the web to check bending of the web about the vertical axis.
As would be expected the variation in the strain across the web was greatest
in Beam 4, which was reinforced on only one side of the web. The strain
variation across the web, which was obtained for M/V ratio of 40, is shown
in Fig. 39, as a typical example. This figure shows that the side of the
web without the reinforcing experienced greater strain. When gages existed
on opposite sides of the web their average was used as the strain at that

position, but when only one gage existed the average was obtained from the curve.

For Beams 4 and 5 the strain variation curves of the reinforcing bars are shown in Figs. 34-37. These curves represent the average strains in the bars. As shown in Figs. 10 and 11, linear strain gages were placed on the edges of the reinforcing bars and on the top and bottom of the bar mid-day between the edge and the web. Also Beam 4 had a gage on the web directly opposite the reinforcing bar. The strain at the web centerline at the level of the reinforcing bar of Beam 5 was determined by linearly inter-polating between the gages on the web above and below the reinforcing bars. Consideration of Figs. 34-37 show the reinforcing bar strains to be slightly nonlinear. It is felt, however, that a linear interpolation between the value at the web and that at the edge of the reinforcing bar would give satisfactory results. An alternate method of handling the reinforcing bar strains would be to use the average of strains obtained from gages placed on the top and bottom of the bar halfway between the web and the edge of the bar.

Figure 38 shows the strain variation in the bottom flange at the low and high moment sections for Beam 5. Since no gages were placed at the edges of the top flange, their strain variations were not plotted. From the above graphs, it can be concluded that the average flange strain may be obtained to a reasonable accuracy by using the average of the gages placed 1-3/4 inches from the edges of the beam flanges.

Deflections

Deflection readings were recorded for each loading and unloading cycle, and the average of these are presented as the experimental values. The deflection

readings were recorded to the nearest thousandth of an inch and were taken at the edges of the opening and the centerline of the beam. Since the dial gages were connected to a steel channel, which was supported on the same pedestal as the beams, no corrections in the deflection readings were necessary because of support settlement.

Tables 8-10 presents the experimental and theoretical mid-span deflections and relative deflections across the opening for Beams 1, 2, 3, 4 and 5. The actual average dimensions as shown in Table 1 were used in the calculations. It is observed that mid-span deflections decrease when reinforcement is added to the web opening. For example at $M/V = 20$ inches, the experimental mid-span deflection decreases by 1.80% with the addition of unsymmetrical reinforcement (Beam 4), and by 3.72% with the addition of reinforcement to both sides of the web. The theoretically predicted value of mid-span deflection taking into account the web opening and the reinforcing agrees very well for $M/V = 20$ and $M/V = 40$, but are slightly high for the higher M/V values. One reason for this is probably the difference in the moment of inertia. Since the fillets are not taken into account in the computer program used to evaluate the deflection, the reduced moment of inertia tends to become more important as bending deflection terms become larger with length. The theoretical mid-span deflections for Beam 1 are plotted against the moment-shear ratio M/V in Fig. 40. Since the pattern of the curve remains the same for all beams, the plot of Beam 1 has been presented as a typical example. The curves of Figs. 41-45 show the theoretically predicted and experimental values of the relative deflections across the opening. Relative deflections were theoretically predicted using Eq. (20). Agreement between the theoretical and experimental deflections across the

opening seems to be the best for Beams 1 and 2, but in general seem to be pretty good.

Theoretical Values of the Shear Distribution Ratio V_T/V_B

Table 7a presents the shear distribution ratio results for beams 1 and 2. The experimental and finite element results obtained by McNew (11) are also presented along with the revised results. Table 7a also presents the results of the five different analytical methods described above. Results of Beams 3, 4 and 5 are recorded in Table 7b. The dimensions used in the calculations are given in Table 1.

Theoretical values of V_T/V_B were obtained for eccentricities of 1, 2, and 3 inches and M/V ratios of 20, 40 and 60 inches. Experimental tests were for the same M/V ratios but for only the 2 inch eccentricity. Methods 1 and 2 given values which are consistent with the experimental results. However Method 1 shows better agreement than Method 2. The shear distribution ratio obtained by Method 1 is always lower than the experimental value. For example, Method 1 predicts values of the ratio V_T/V_B which are approximately 17, 1, and 10 percent low for Beams 3, 4 and 5, respectively.

While Method 3 does not yield results as close to experimental results as Methods 1 and 2 it does show an increase in the shear distribution ratio V_T/V_B when the opening is reinforced. Methods 4 and 5, which equate the shear deflection above and below the opening, are not consistent. With the addition of reinforcement of the web opening the value of V_T/V_B as predicted by these methods decrease, whereas the experimental results show an increase in the same.

CONCLUSIONS

From this theoretical and experimental investigation, the following
conclusions can be reached.

1. The distribution of shear force above and below the web opening
   did not appear to be sensitive to the variation of the moment to
   shear ratio at the centerline of the web opening.

2. When the reinforcement was added above and below the opening, the
   shear distribution ratio V_T/V_B increased.

3. The addition of reinforcement to the web opening had the following
   effect on the stress: For the HMS (high moment section) and LMS
   (low moment section), the normal stresses are lowered toward the
   opening and only minor stress reduction occurs at the top and
   bottom flange.

4. The finite element analysis tends to overestimate the stress at
   the opening. However, the shear distribution ratios predicted by
   finite element analysis show good agreement with experimental
   results.

5. Normal stresses calculated on the basis of the Vierendeel method
   of analysis compare reasonably well with the experimental results.
   However since the Vierendeel analysis does not account for stress
   concentration at the opening, the stresses predicted are lower in
   magnitude than the measured stresses.

6. Among the theoretical methods of calculating the shear distribution
   ratio V_T/V_B, Method 1, which considers both bending and shear
   deformation and uses a shear coefficient based on strain energy,
   gave results which compared reasonably well with the experimental
   results.

7. The shear stresses obtained from the finite element analysis predicted higher values for V_T/V_B than the finite element normal stresses.

8. By changing the eccentricity from 2 inches above the mid-depth to 2 inches below mid-depth, the results obtained were approximately the inverse of each other.

9. Mid-span deflections and relative deflections across the opening can be predicted fairly accurately by using the Castigliano's theorem on deflections.

RECOMMENDATIONS FOR FURTHER RESEARCH

In this research project unreinforced and reinforced eccentric web openings were studied. All the openings were six inches deep and had a 2 inch eccentricity with respect to the mid-depth of the beam. The widths of the web openings were 9 inches for two beams and 12 inches for four beams. Further experimental investigation of the opening size and position are necessary before theoretical methods of determining the shear distribution ratio V_T/V_B can be substantiated. The length, depth and eccentricity of the opening are three parameters which need further investigation. Perhaps the finite element method of analysis could be refined so that the experimental and finite element results agree better. After refinement, the finite element method of analysis should be applied to openings with different lengths, depths and eccentricities and compared with the experimental results. In the experimental investigations the increase in the length or depth of the opening could be accomplished by just changing the opening size without disturbing the setup of the strain gages.

For the elastic tests it would be helpful to record deflection to one ten-thousandth of an inch, since the relative deflections across the opening are of extremely small magnitude. Two types of web reinforcement, symmetrical and unsymmetrical were considered, but in these cases the reinforcing bars were parallel to the flange. The effect of diagonally reinforcing the web opening upon the elastic stresses and ultimate strength should be investigated. Beams with opening depth greater than half the beam depth should be tested, and the validity of the Vierendeel method of analysis investigated for various opening lengths, eccentricities and reinforcement.

ACKNOWLEDGEMENTS

REFERENCES

1. Brice-Nash, R. L., R. R. Snell, and P. B. Cooper, "Shear force distribution in beams with eccentric web openings by finite element method," Research Project Report, Department of Civil Engineering, Kansas State University, May 1974.

2. Bower, J. E., "Analysis and Experimental Verification of Steel Beams with Unreinforced Web Openings," Applied Research Laboratory, U.S. Steel Corporation, Monroeville, Pa., Jan. 1970.

3. Bower, J. E. "Ultimate Strength of Beams with Rectangular Holes," Journal of Structural Division, ASCE, Vol. 94, No. St. 6, Proc. Paper 5982, June 1968, pp. 1315-1337.

4. Chan, Peter W. and Richard G. Redwood, "Stresses in Beams with Circular Eccentric Web Holes," Journal of Structural Division, ASCE Vol. 100, No. St. 1, Proc. Paper 10291, January 1974, pp. 231-248.

5. Cooper, P. B. and R. R. Snell, "Tests on Beams with Reinforced Web Openings," Journal of Structural Division, ASCE Vol. 98, No. St. 3, Proc. Paper 8791, March 1972, pp. 611-632.

6. Congdon, J. G. and R. G. Redwood, "Plastic Behaviour of Beams with Reinforced Holes," Journal of Structural Division, ASCE, Vol. 96, No. St. 9, Proc. Paper 7561, September, 1970, pp. 1933-1956.

7. Cowper, G. R., "The Shear Coefficient in Timoshenko's Beam Theory," Transactions, American Society of Mechanical Engineers, Series E, Vol. 33, June 1966.

8. Douglas, T. R. and S. C. Gambrell, Jr., "Design of Beams with Off-Center Web Openings," Journal of Structural Division, ASCE, Vol. 100, No. St. 6, Proc. Paper 10611, June 1974, pp. 1189-1203.

9. Frost, R. W., "Behaviour of Steel Beams with Eccentric Web Holes," Technical Report 46.019-400(1), Research Laboratory, United States Steel Corporation, February 1973.

10. Frost, R. W., Unpublished data, U.S. Steel Applied Research Laboratory, Monroeville, Pa., 1969.

11. McNew, J. L. and H. D. Knostman, "Experimental Tests on Beams with Eccentric Web Openings," Research Project Report, Dept. of Civil Engineering, Kansas State University, Sept. 1974.

12. Redwood, R. G. and J. O. McCutcheon, "Beam Tests with Unreinforced Web Openings," Journal of Structural Division, ASCE, Vol. 94, No. St. 1, Proc. Paper 5706, January 1968, pp. 1-17.

13. Redwood, R. G. and Peter W. Chan, "Design Aid for Beams with Circular Eccentric Web Holes," Journal of Structural Division, ASCE, Vol. 100, No. St. 2, Proc. Paper 10331, February 1974, pp. 297-302.

14. Salmon, M., L. Berke, and R. Sandhu, "An Application of the Finite Element Method to Elastic-Plastic Problems of Plane Stress," Illinois Institute of Technology Research Institute and the Air Force Flight Dynamics Laboratory, Project No. 1467, "Structural Analysis Methods," January 1967 through December 1968.

15. Scritchfield. Roberta and P. B. Cooper, "Strength of beams with eccentric Reinforced Holes," Research Project Report, Department of Civil Engineering, Kansas State University, April 1975.

16. "Suggested Design Guide for Beams with Web Holes," Journal of Structural Division, ASCE, Vol. 97, No. St. 11, Proc. Paper 8536, Nov. 1971, pp. 2707-2728.

17. Wang, Tsong-Miin, Robert R. Snell, and P. B. Cooper, "Strength of Beams with Eccentric Reinforced Holes," Research Project Report, Department of Civil Engineering, Kansas State University, July 1974.

18. "Manual of Steel Construction," American Institute of Steel Construction, New York, 1970.
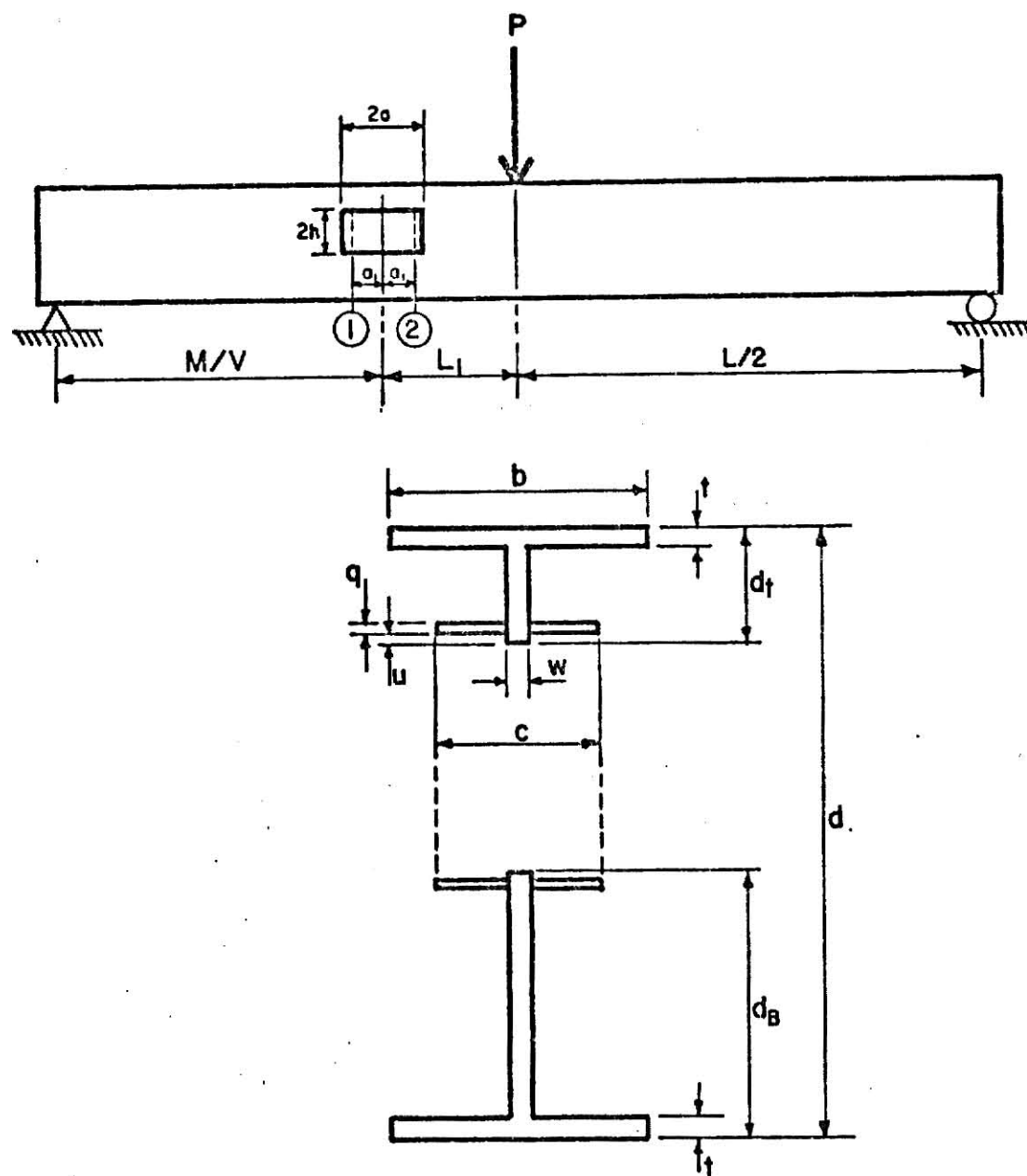
Fig. 6   Test setup and cross-sectional dimension locations

TABLE 1. BEAM DIMENSIONS IN INCHES (AVERAGE OF THE VALUES MEASURED AT SECTIONS 1 AND 2).

Beam	Size	$2a$	a_1	$2h$	d	d_T	d_B	b	t	w	c	q	u	L_1
1	W16 x 45	9.0	3.0	6.04	16.11	3.14	6.93	7.00	.539	.382	.382	---	---	24.0
2	W16 x 45	9.0	3.0	6.01	16.11	3.02	7.08	6.99	.539	.380	2.350	0.241	0.27	24.0
3	W16 x 40	12.0	4.5	6.09	16.10	3.01	7.00	7.03	.475	.334	.334	---	---	25.0
4	W16 x 40	12.0	4.5	6.09	16.10	3.01	7.00	7.03	.475	.334	2.334	0.25	0.25	25.0
5	W16 x 40	12.0	4.5	6.09	16.10	3.01	7.00	7.03	.475	.334	4.334	0.25	0.25	25.0
5a	W16 x 40	12.0	4.5	6.09	16.10	7.00	3.01	7.03	.475	.334	4.334	0.25	0.25	25.0

THIS BOOK WAS
BOUND WITH
NUMEROUS PAGES
THAT HAVE THE
PAGE NUMBER
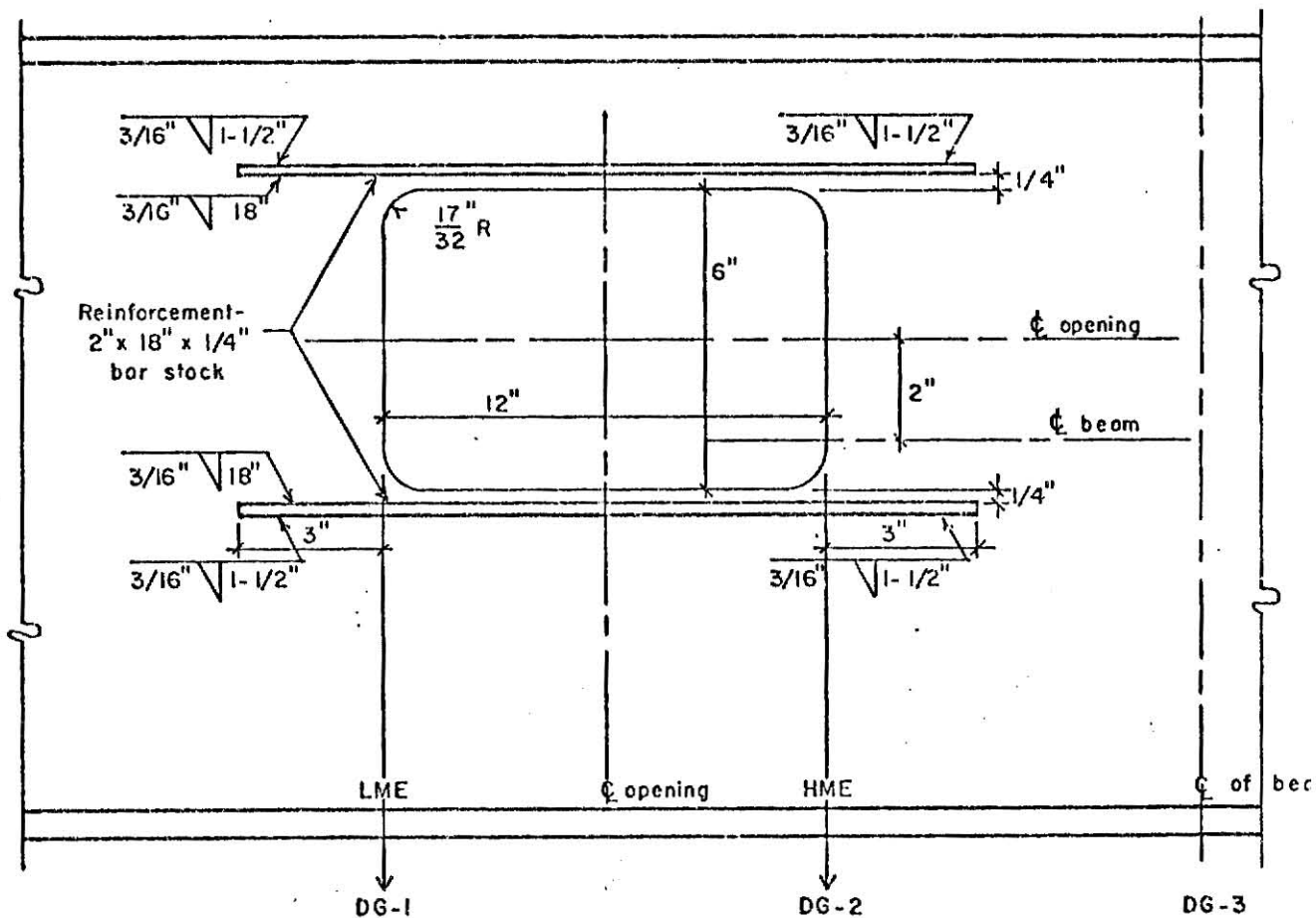PRINTED ON THE
PAGE TWICE.

THIS IS AS
RECEIVED FROM
CUSTOMER.

Fig. 7 Opening, reinforcement details, and dial gage locations

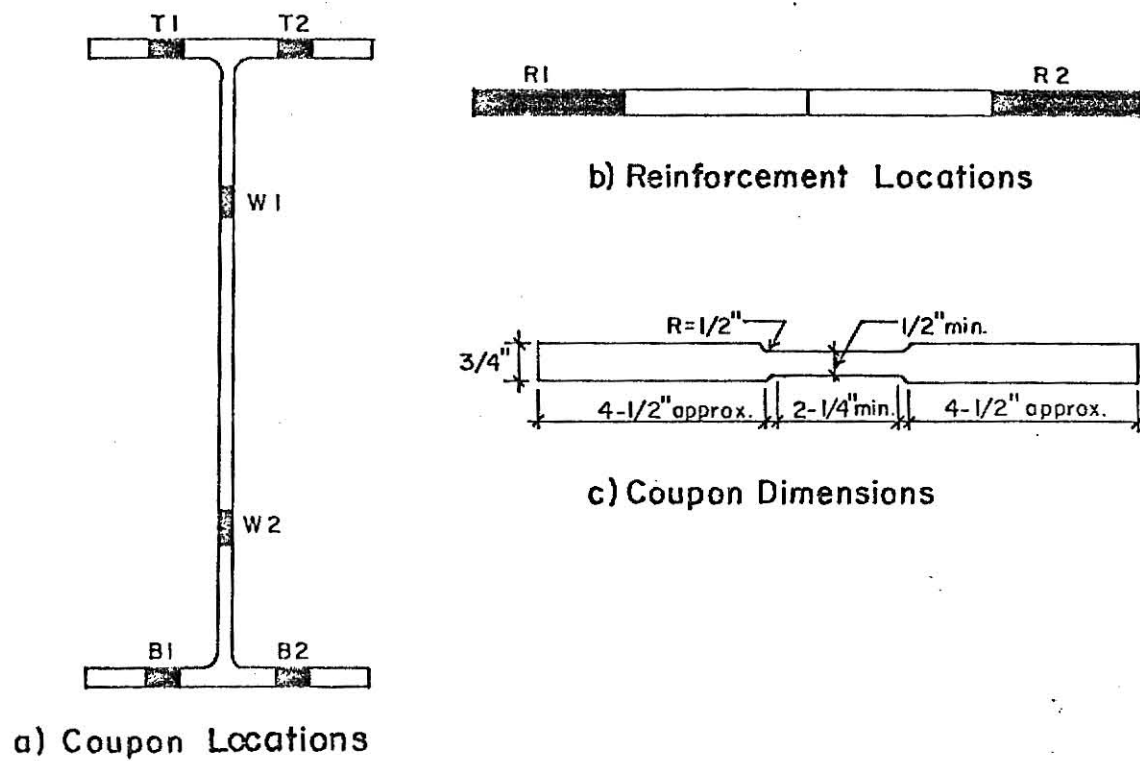a) Coupon Locations

b) Reinforcement Locations

c) Coupon Dimensions

Fig. 8   Tensile specimen details

TABLE 2. TENSILE TEST RESULTS.

Beam	Coupon	Yield Point (ksi)	% Red. Area	% Elong. (in. 2")	Ult. Tensile Str. (ksi)
1	T1	43.12	56.4	27.9	Not Measured
	T2	42.98	57.8	32.5	80.07
	B1	43.94	57.4	31.3	80.11
	B2	43.89	58.1	31.3	80.59
	W1	43.65	54.7	31.5	76.61
	W2	41.46	60.9	35.3	75.68
2	T1	42.77	56.8	31.5	81.97
	T2	42.60	57.1	32.0	80.37
	B1	43.02	55.4	26.4	83.91
	B2	42.24	52.0	32.5	80.29
	W1	42.40	55.7	33.0	76.15
	W2	43.72	56.5	33.0	76.44
	R1	40.36	57.1	35.0	66.35
	R2	38.48	55.2	36.5	64.96
3,4,5 and 5a	T1	40.42	62.1	37.8	69.71
	T2	39.65	63.3	38.3	69.48
	B1	41.92	60.3	35.3	70.72
	B2	40.13	62.4	36.3	69.83
	W1	41.47	62.9	33.3	69.65
	W2	41.24	61.8	37.3	69.06
	R1	38.39	65.4	35.3	64.72
	R2	38.17	63.0	37.8	64.88
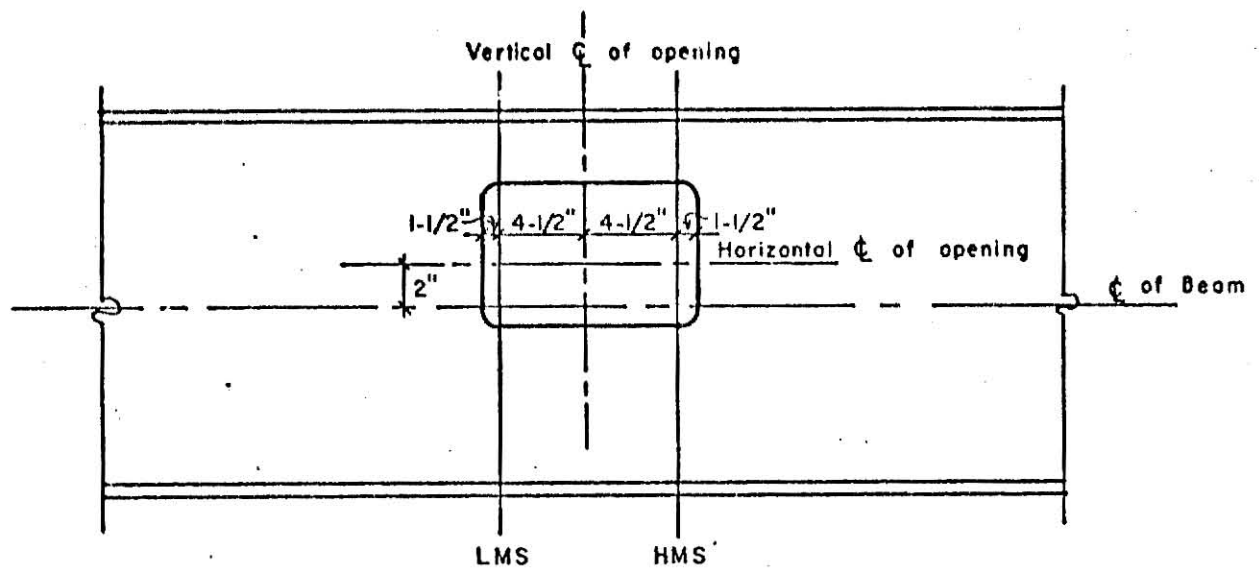
a) Opening Elevation
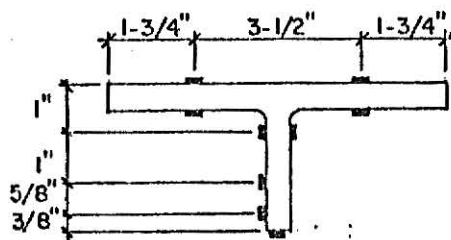
b) Low Moment Section
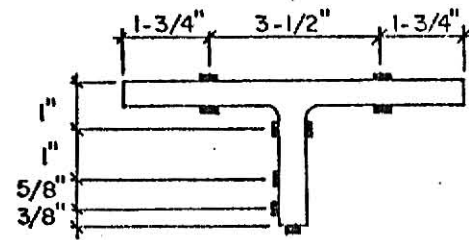
c) High Moment Section

Fig. 9   Strain gage locations -- Beam 3

a) Opening Elevation
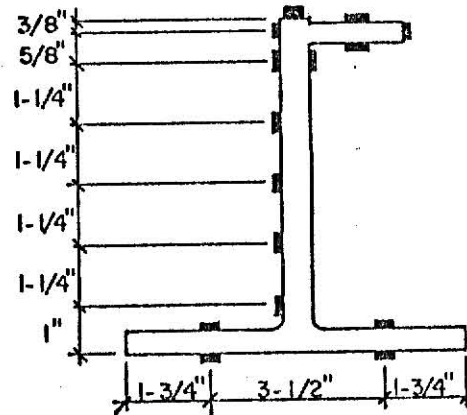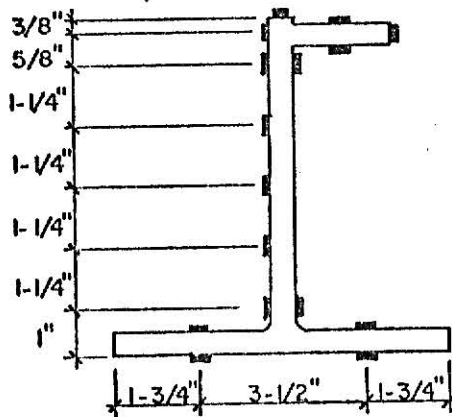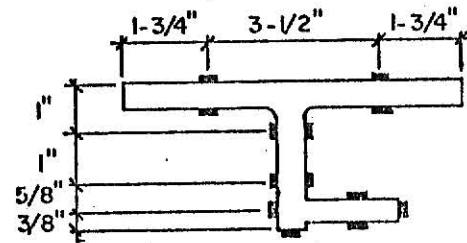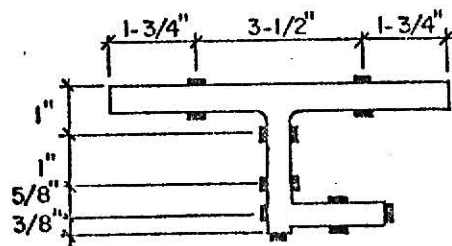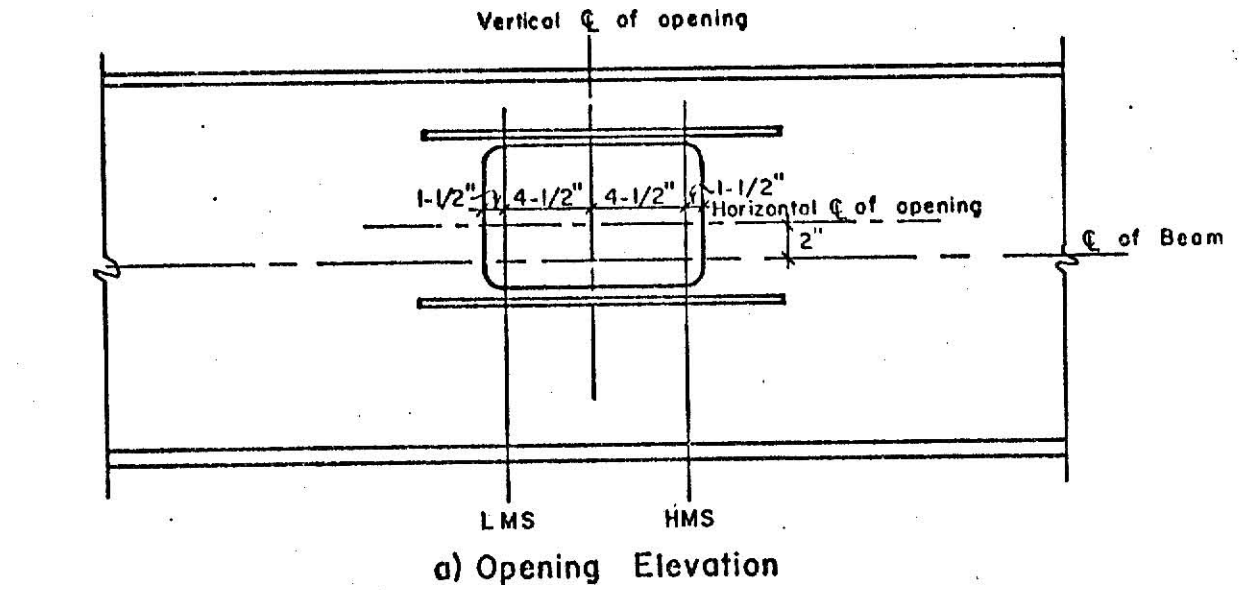
b) Low Moment Section

c) High Moment Section

Fig. 10   Strain gage locations -- Beam 4

a) Opening Elevation
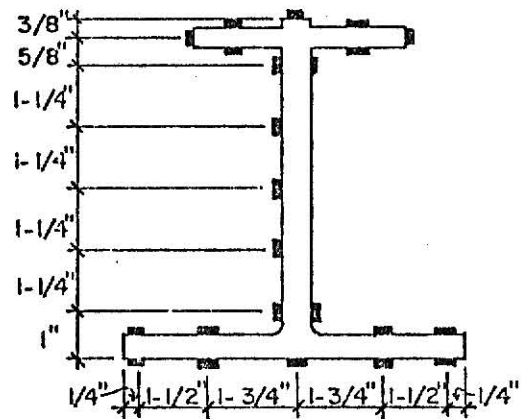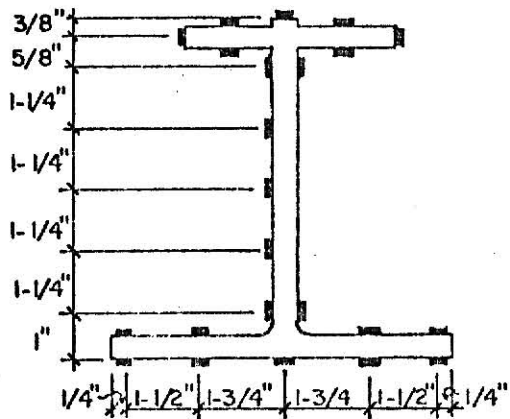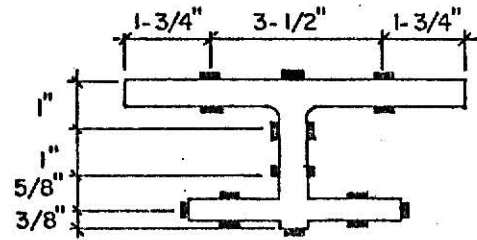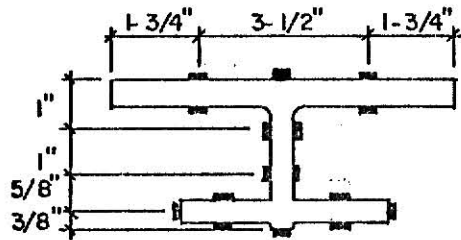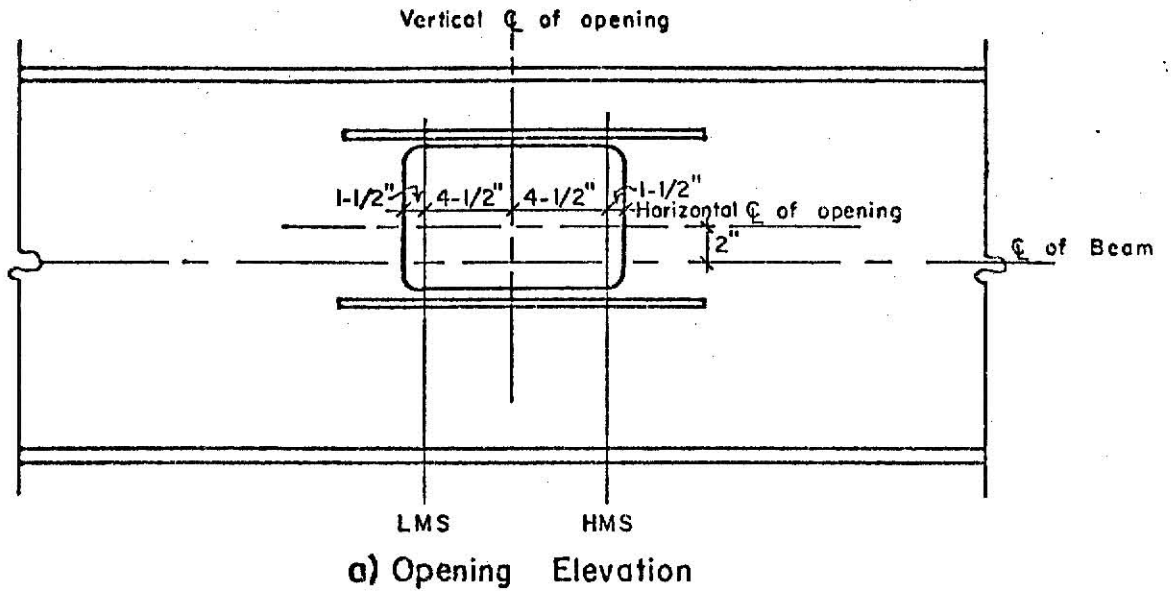
b) Low Moment Section

c) High Moment Section

Fig. 11   Strain gage locations -- Beam 5

Fig. 12 Experimental stress distribution curves for 20 kip load,
low moment section: Beam 3 (M/V = 20, 40, and 60)
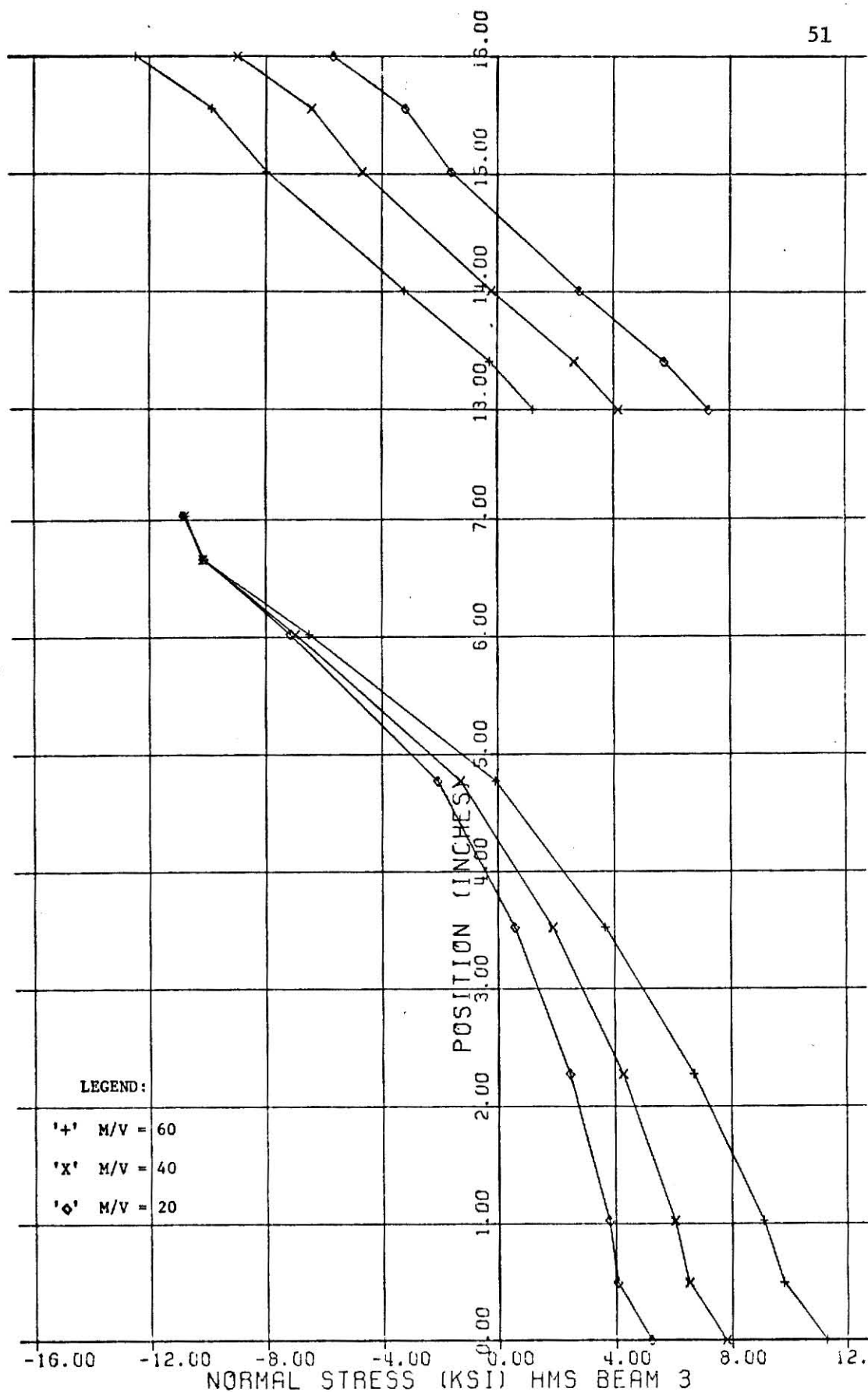
Fig. 13 Experimental stress distribution curves for 20 kip load, high moment section: Beam 3 (M/V = 20, 40, and 60)
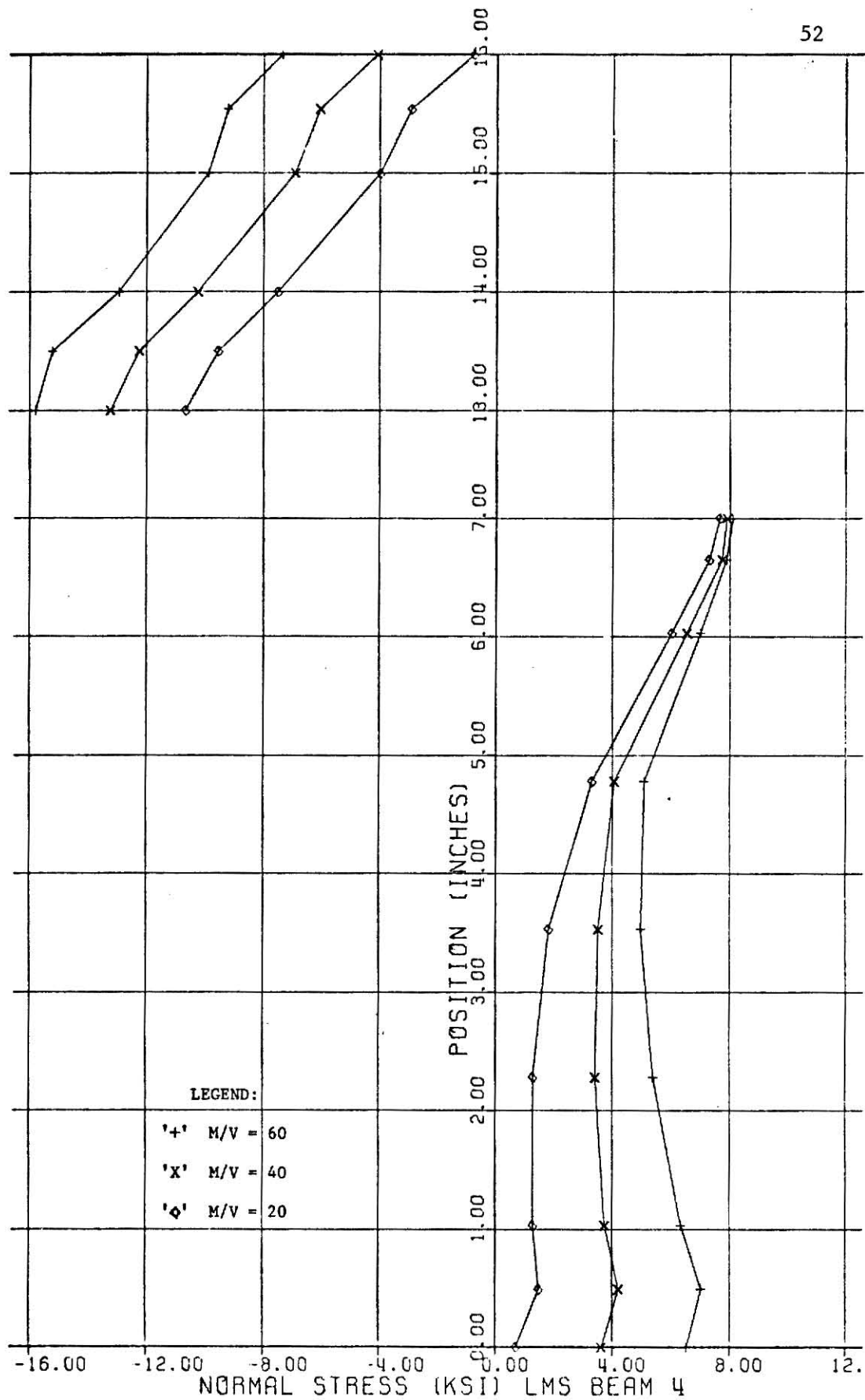
Fig. 14   Experimental stress distribution curves for 20 kip load,
low moment section: Beam 4 (M/V = 20, 40, and 60)
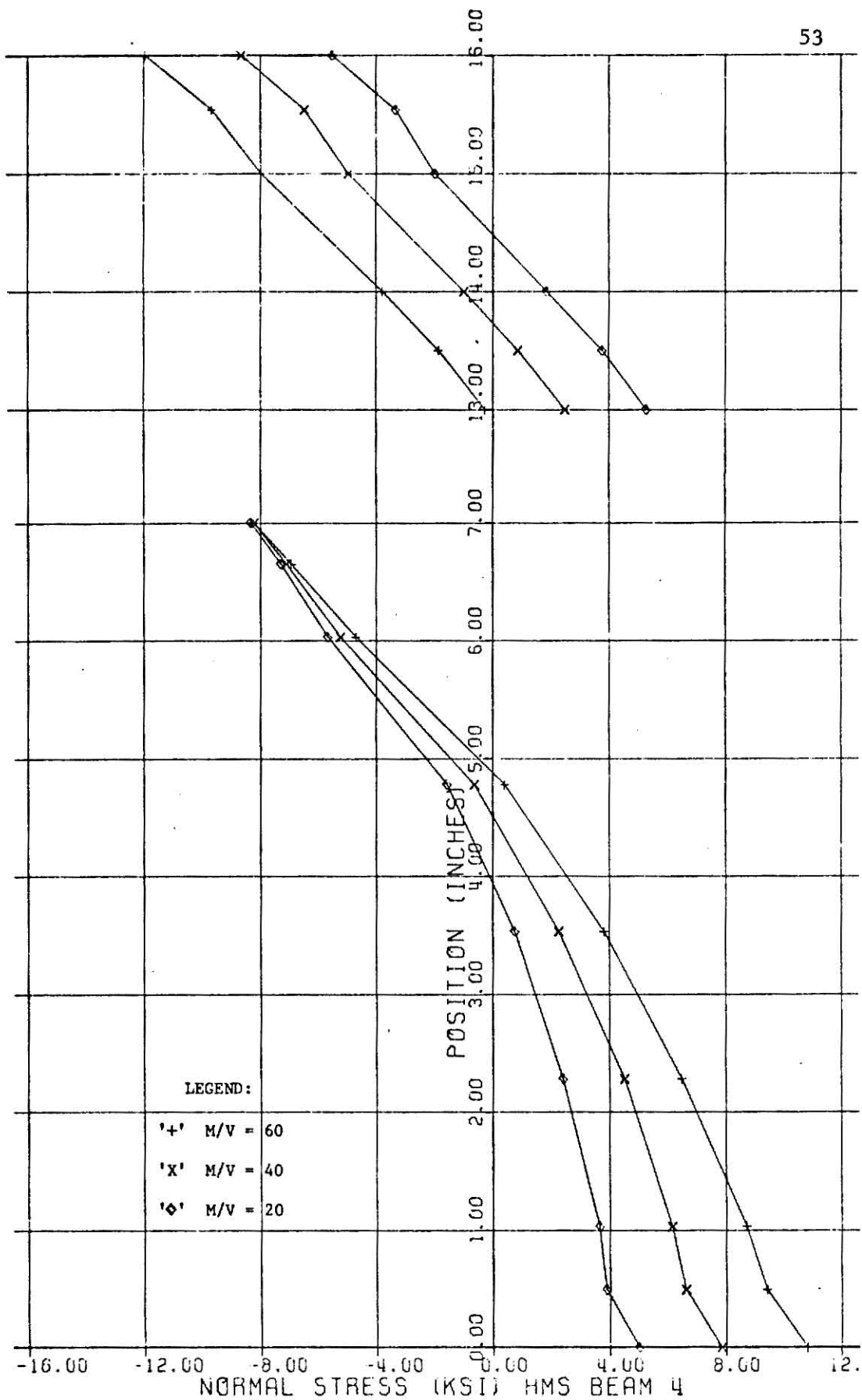
Fig. 15 Experimental stress distribution curves for 20 kip load,
high moment section: Beam 4 (M/V = 20, 40, and 60)
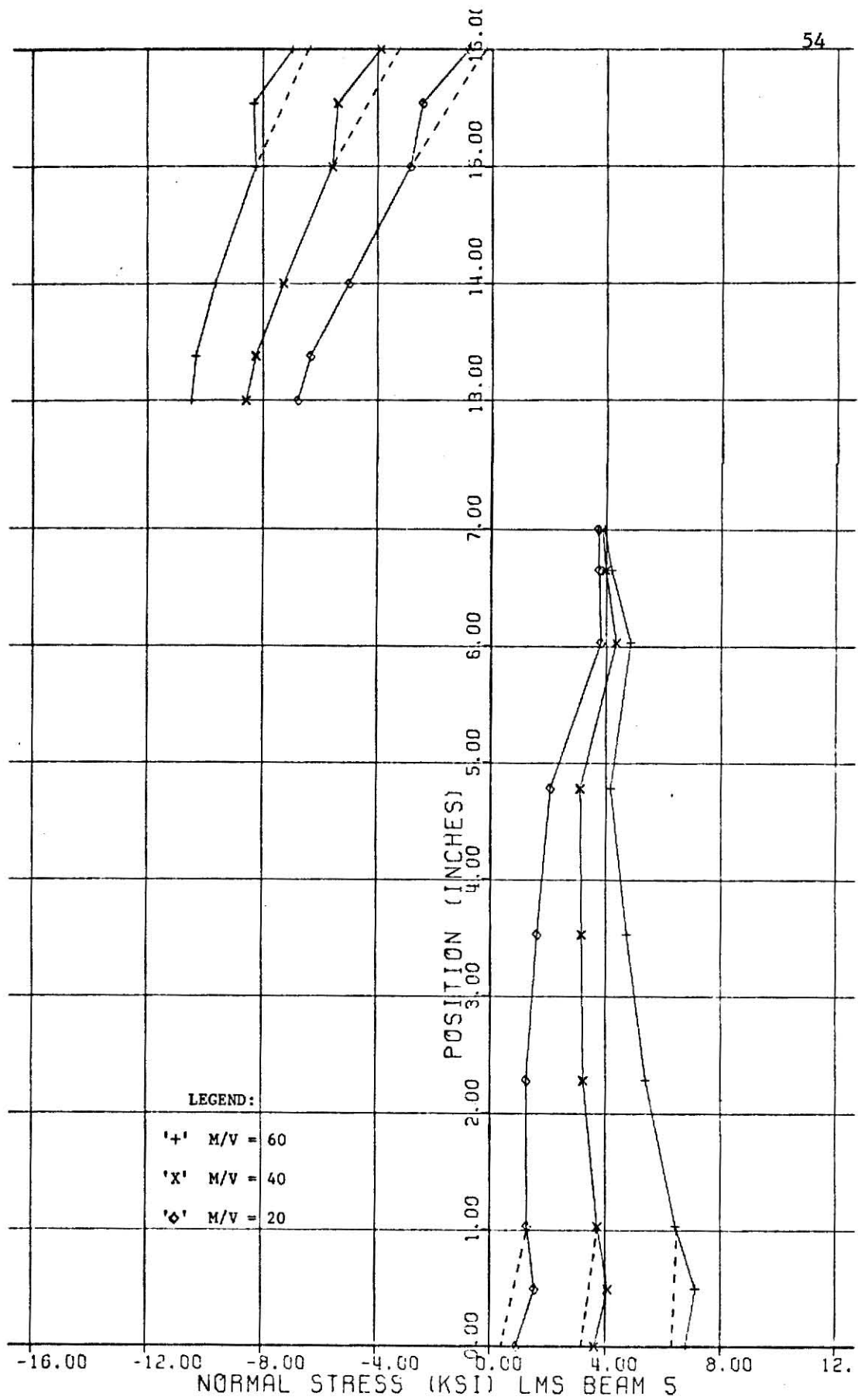
Fig. 16   Experimental stress distribution curves for 20 kip load,
low moment section: Beam 5 (M/V = 20, 40, and 60)
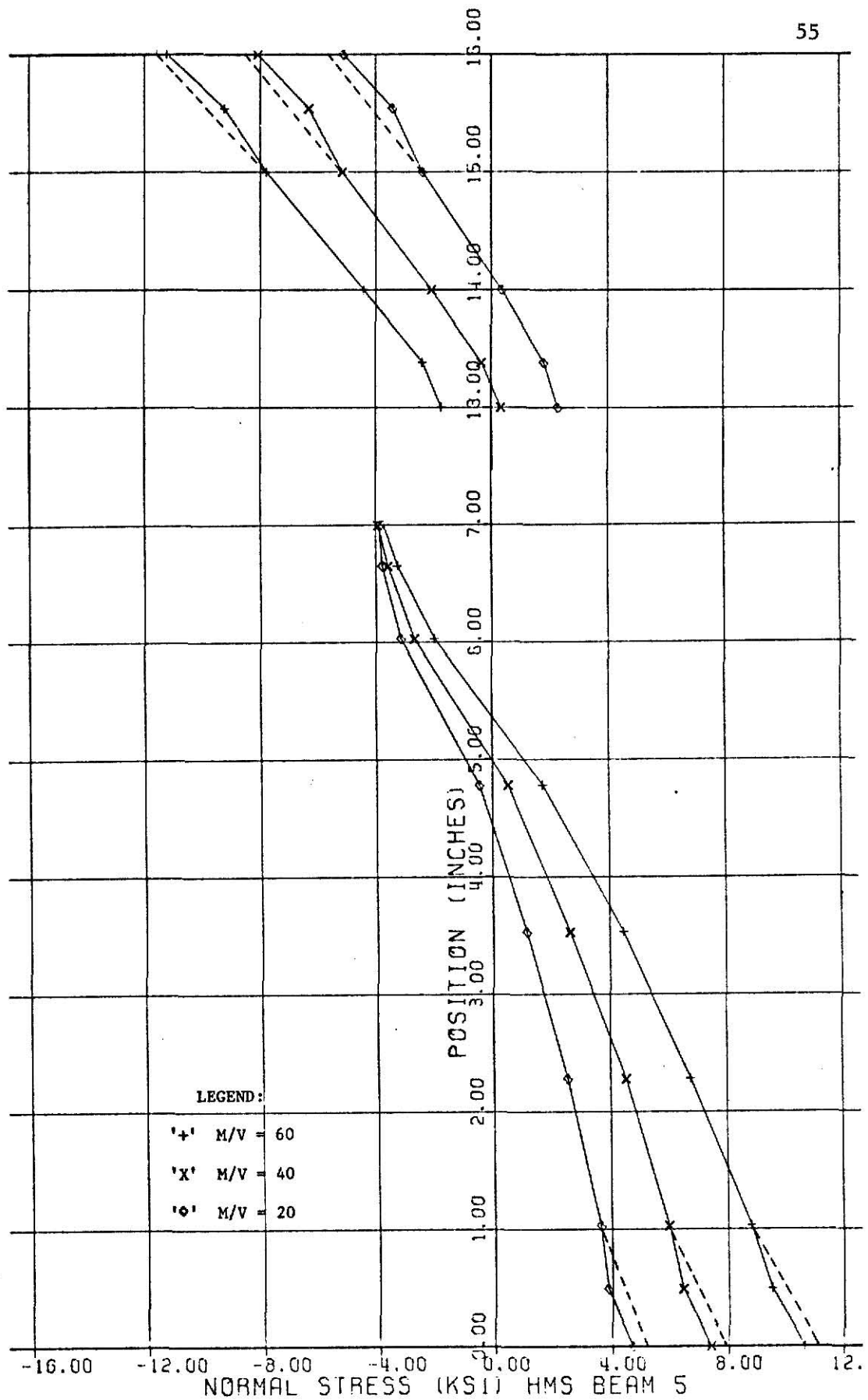
Fig. 17 Experimental stress distribution curves for 20 kip load, high moment section: Beam 5 (M/V = 20, 40, and 60)
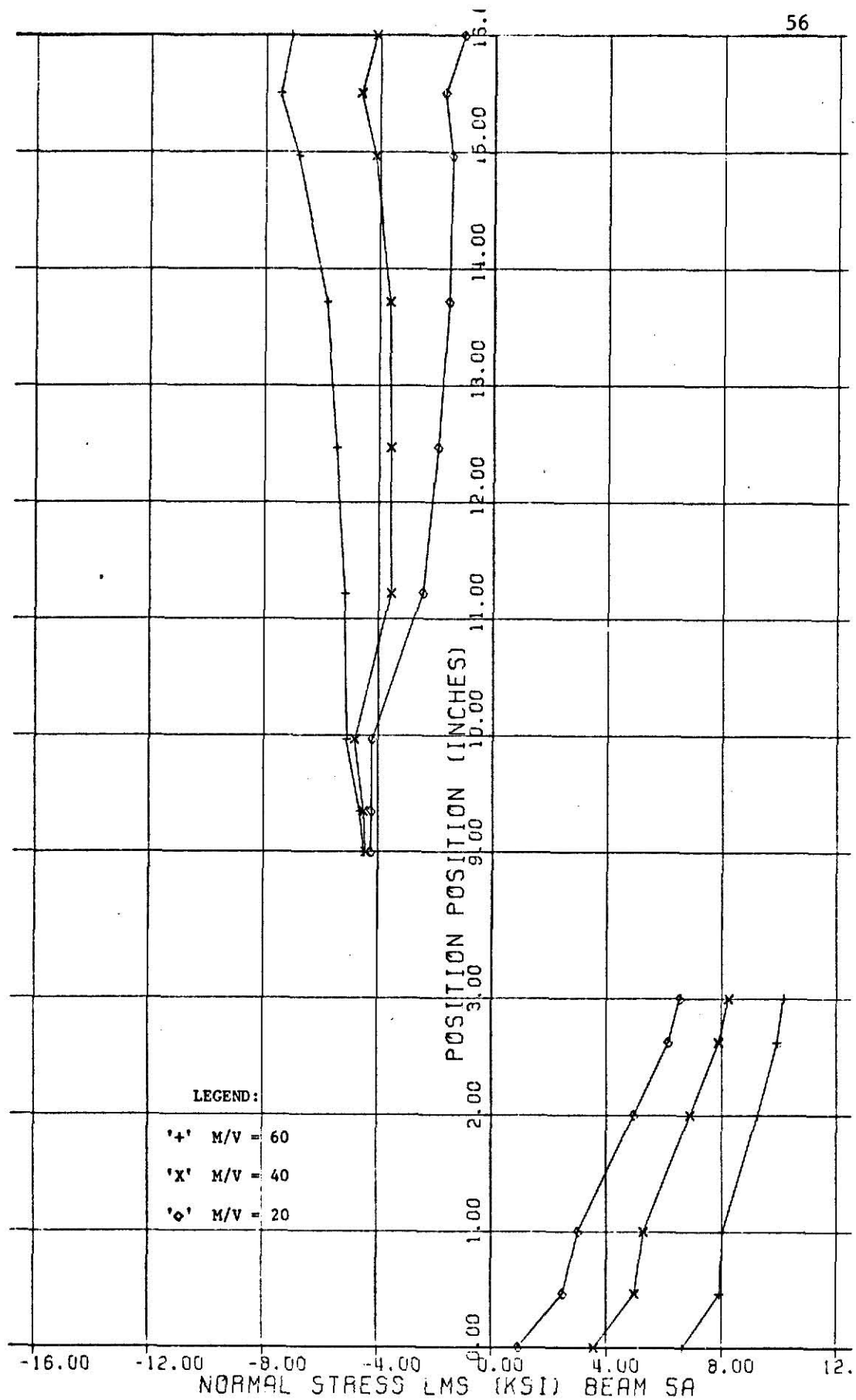
Fig. 18 Experimental stress distribution curves for 20 kip load,
low moment section: Beam 5a (M/V = 20, 40, and 60)
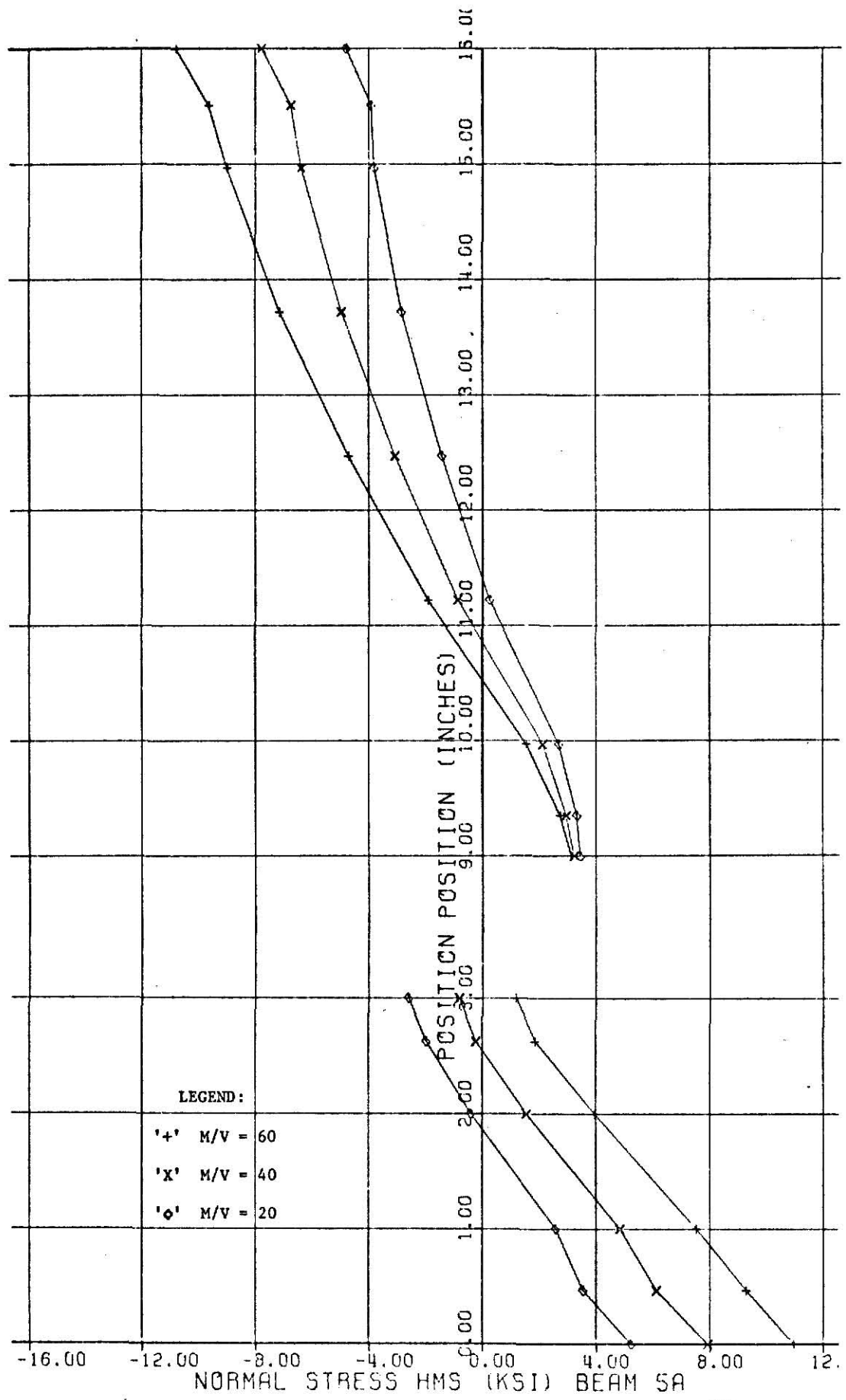
Fig. 19 Experimental stress distribution curves for 20 kip load,
high moment section: Beam 5a (M/V = 20, 40, and 60)
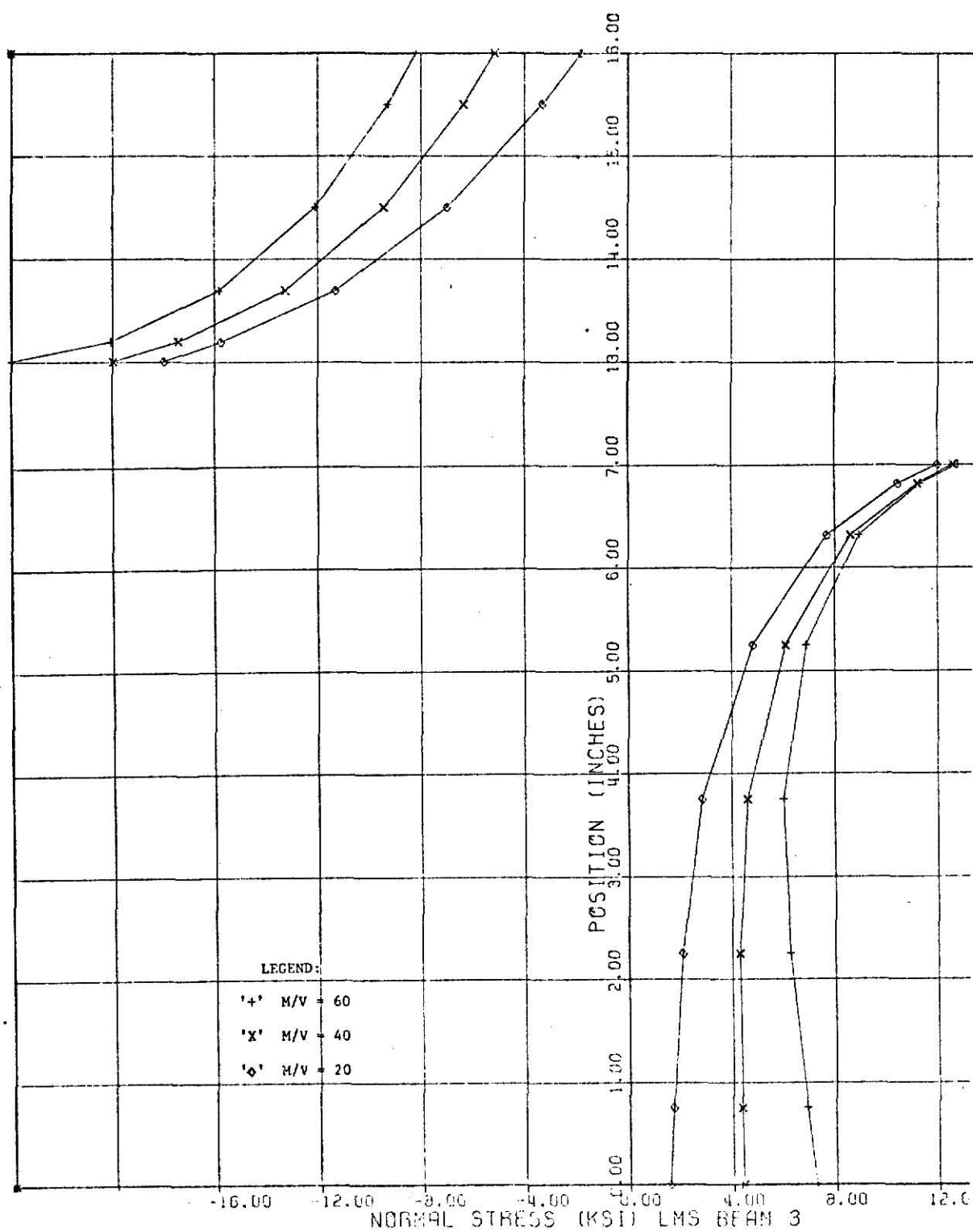
Fig. 20 Finite element stress distribution curves for 20 kip load,
low moment section: Beam 3 (M/V = 20, 40, and 60)
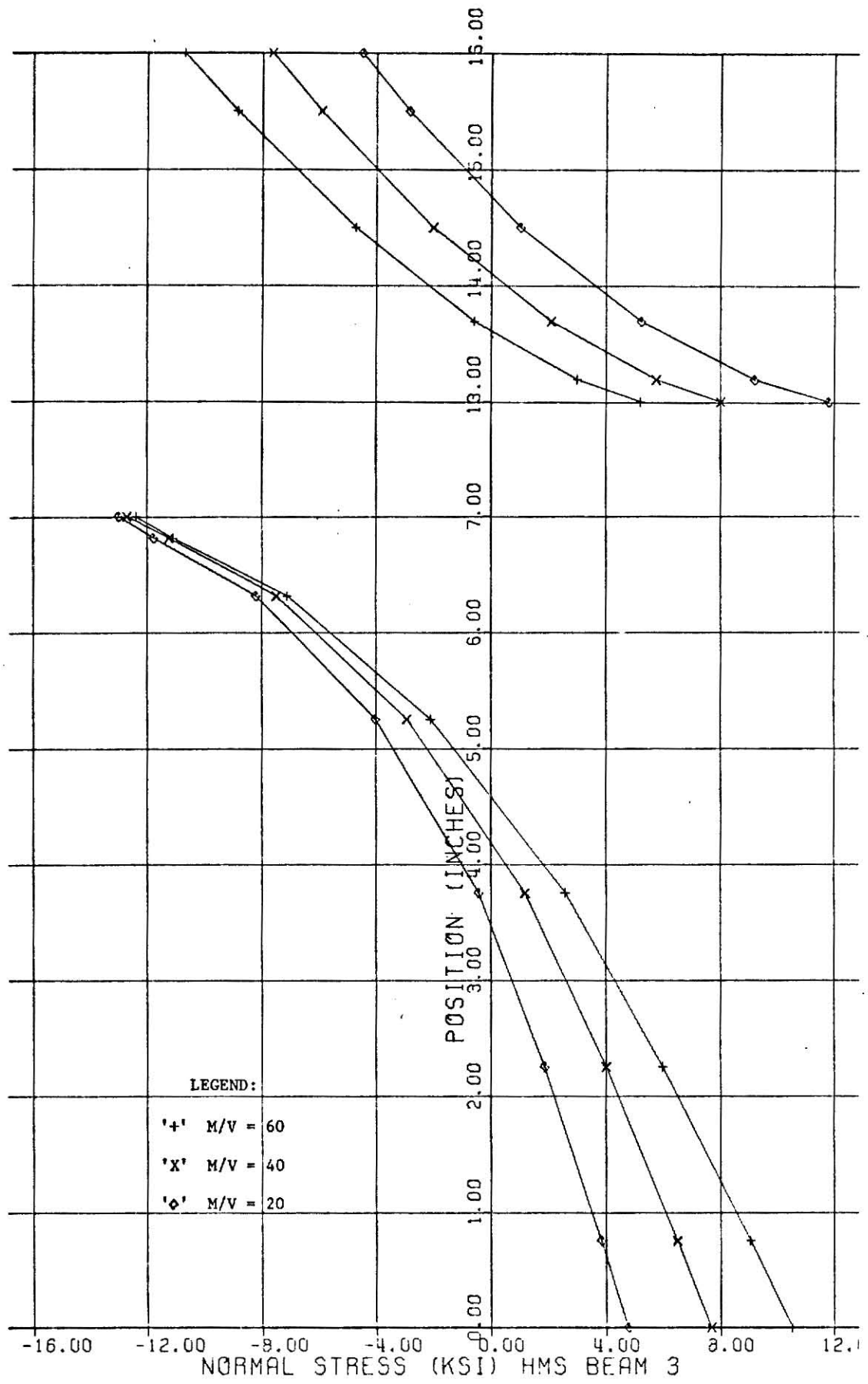
Fig. 21 Finite element stress distribution curves for 20 kip load,
high moment section: Beam 3 (M/V = 20, 40, and 60)
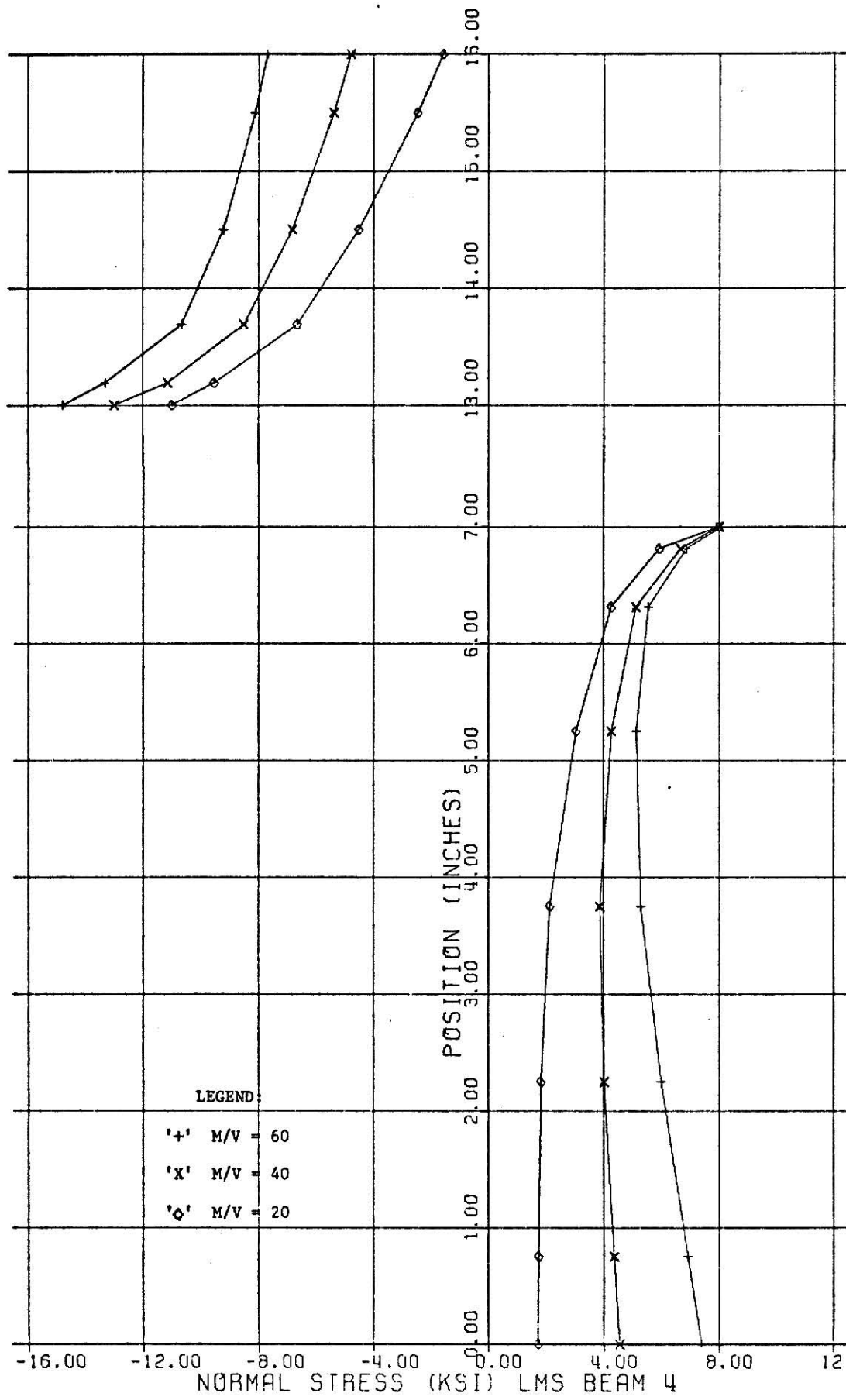
Fig. 22   Finite element stress distribution curves for 20 kip load,
low moment section: Beam 4 (M/V = 20, 40, and 60)
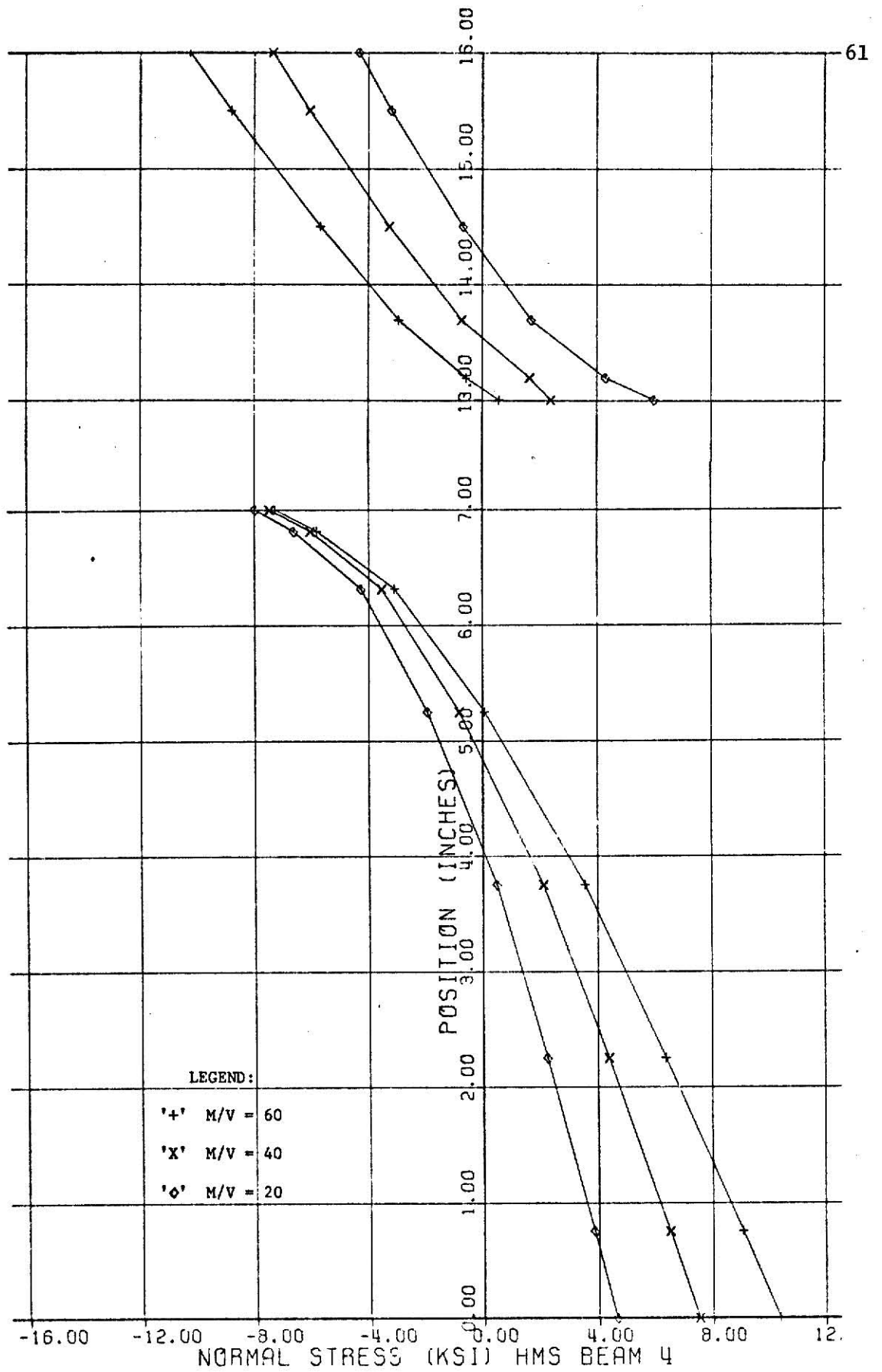
Fig. 23 Finite element stress distribution curves for 20 kip load,
high moment section: Beam 4 (M/V = 20, 40, and 60)
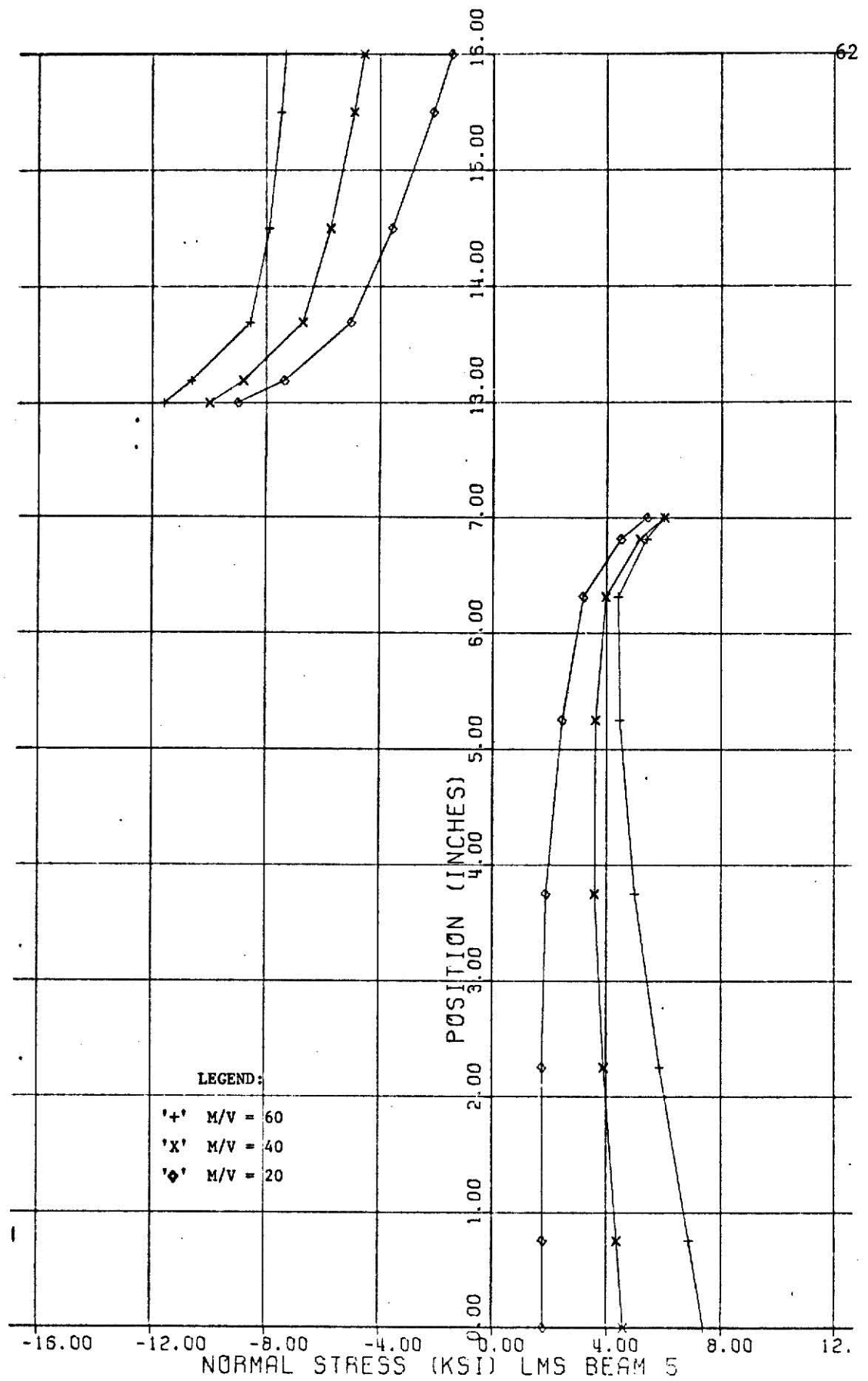
Fig. 24 Finite element stress distribution curves for 20 kip load, low moment section: Beam 5 (M/V = 20, 40 and 60)
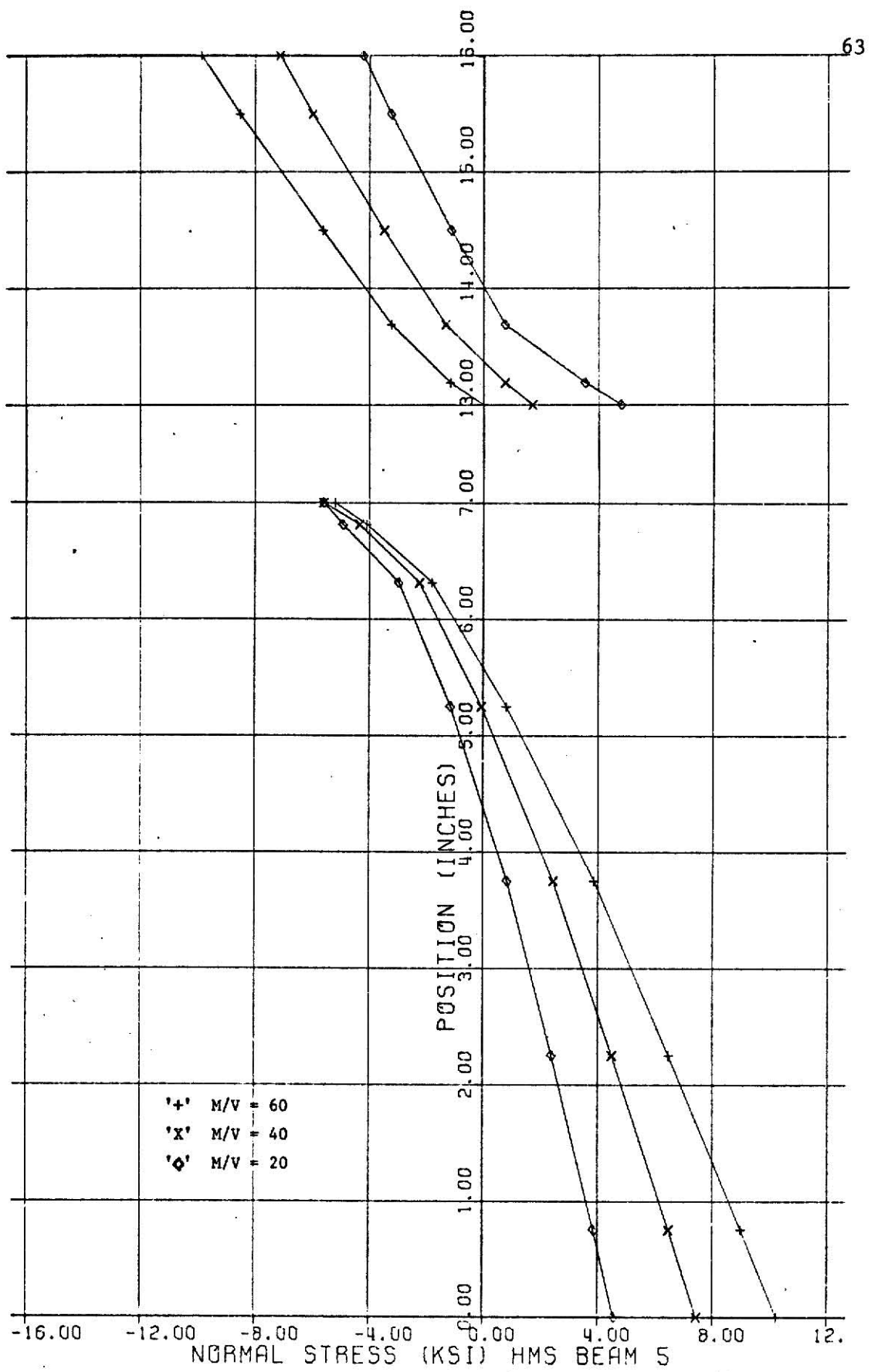
Fig. 25 Finite element stress distribution curves for 20 kip load,
         high moment section: Beam 5 (M/V = 20, 40, and 60)
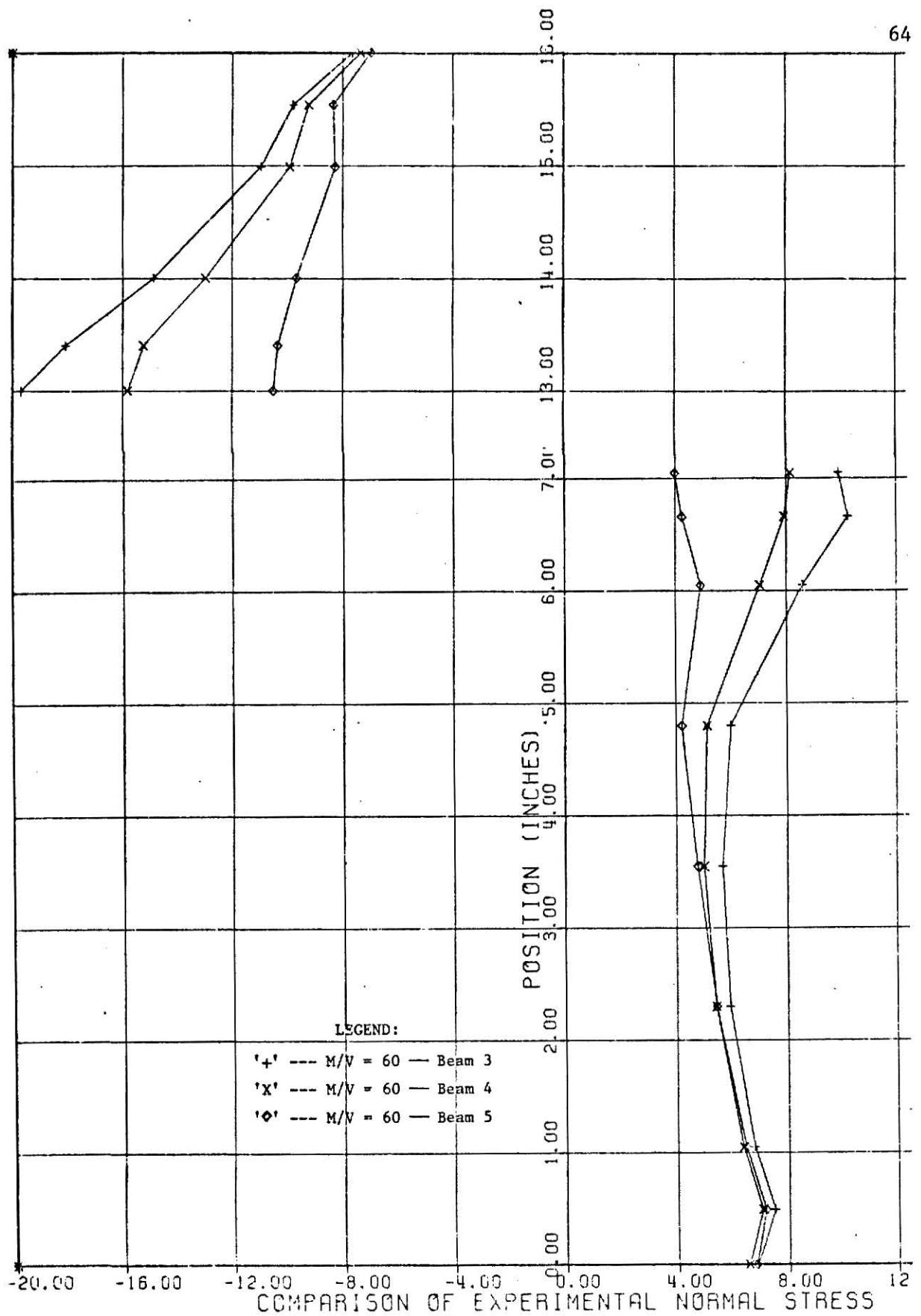
Fig. 26 Comparison of stress distribution curves,
low moment section: Beam 3, 4 and 5 (M/V = 60)
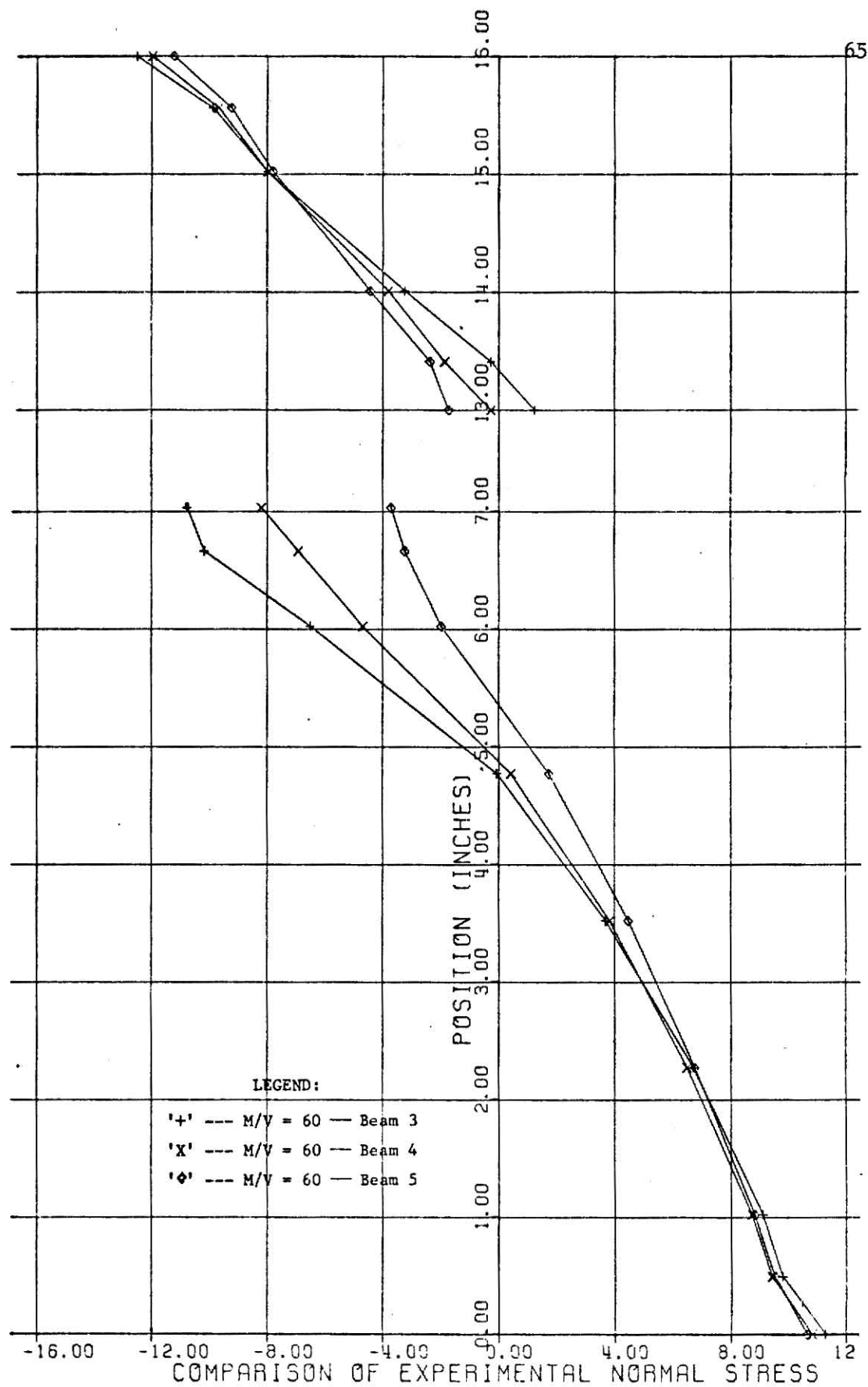
Fig. 27   Comparison of stress distribution curves,
high moment section: Beam 3, 4 and 5 (M/V = 60)
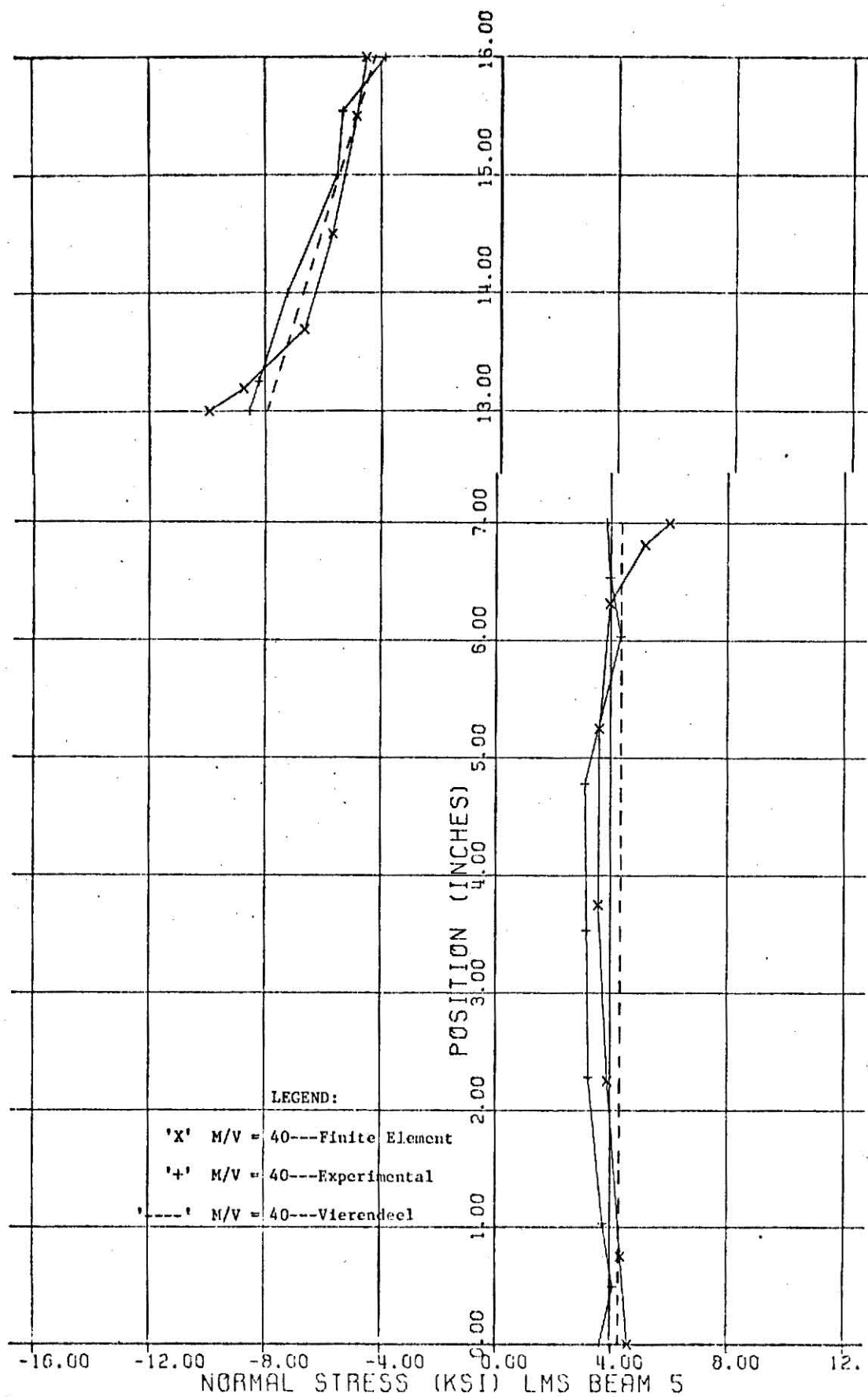
Fig. 28 Comparison of stress distribution curves (Experimental,
finite element, Vierendeel Analysis), low moment section:
Beam 5 (M/V = 40)
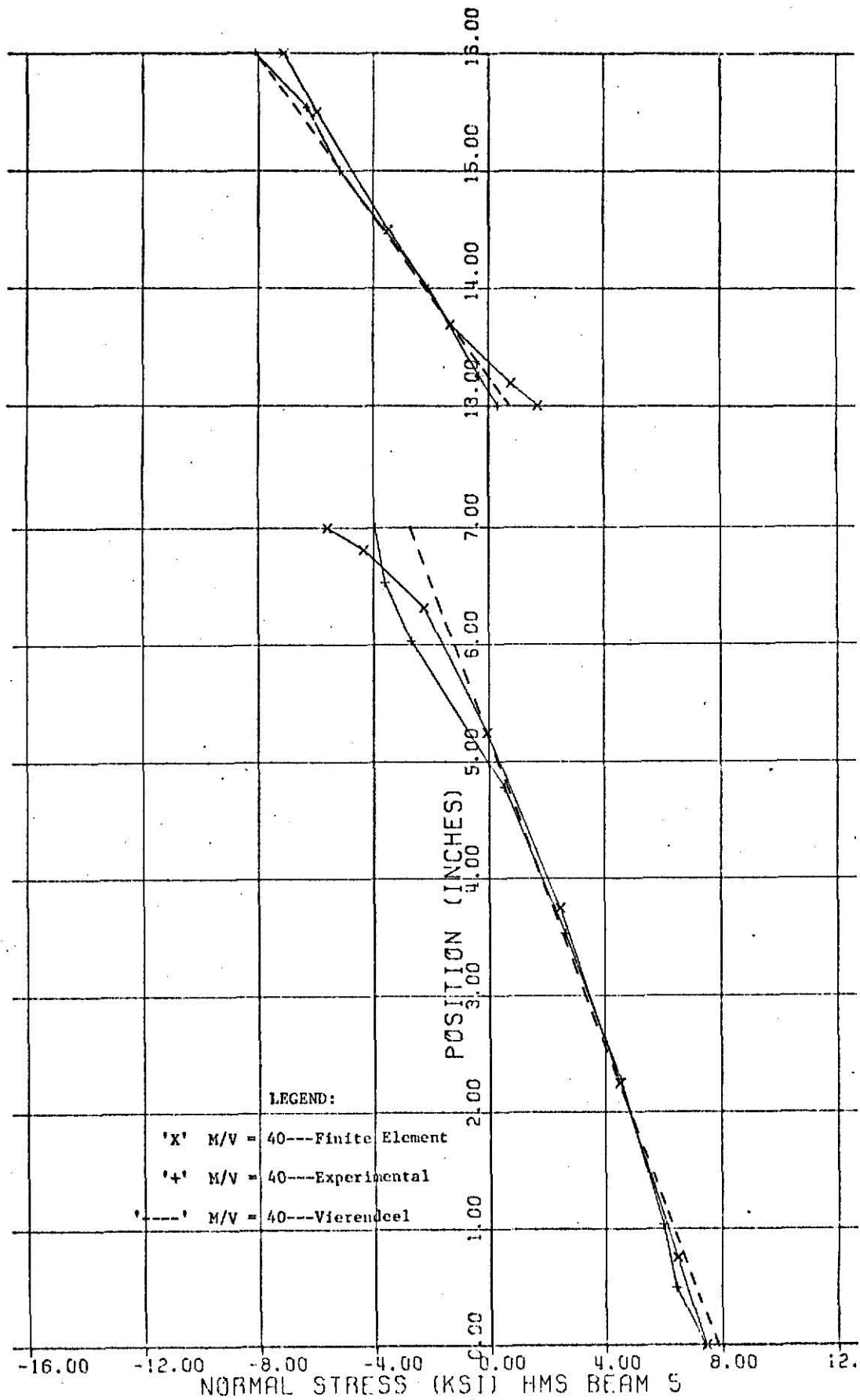
Fig. 29 Comparison of stress distribution curves (Experimental, finite element, Vierendeel Analysis), high moment section:
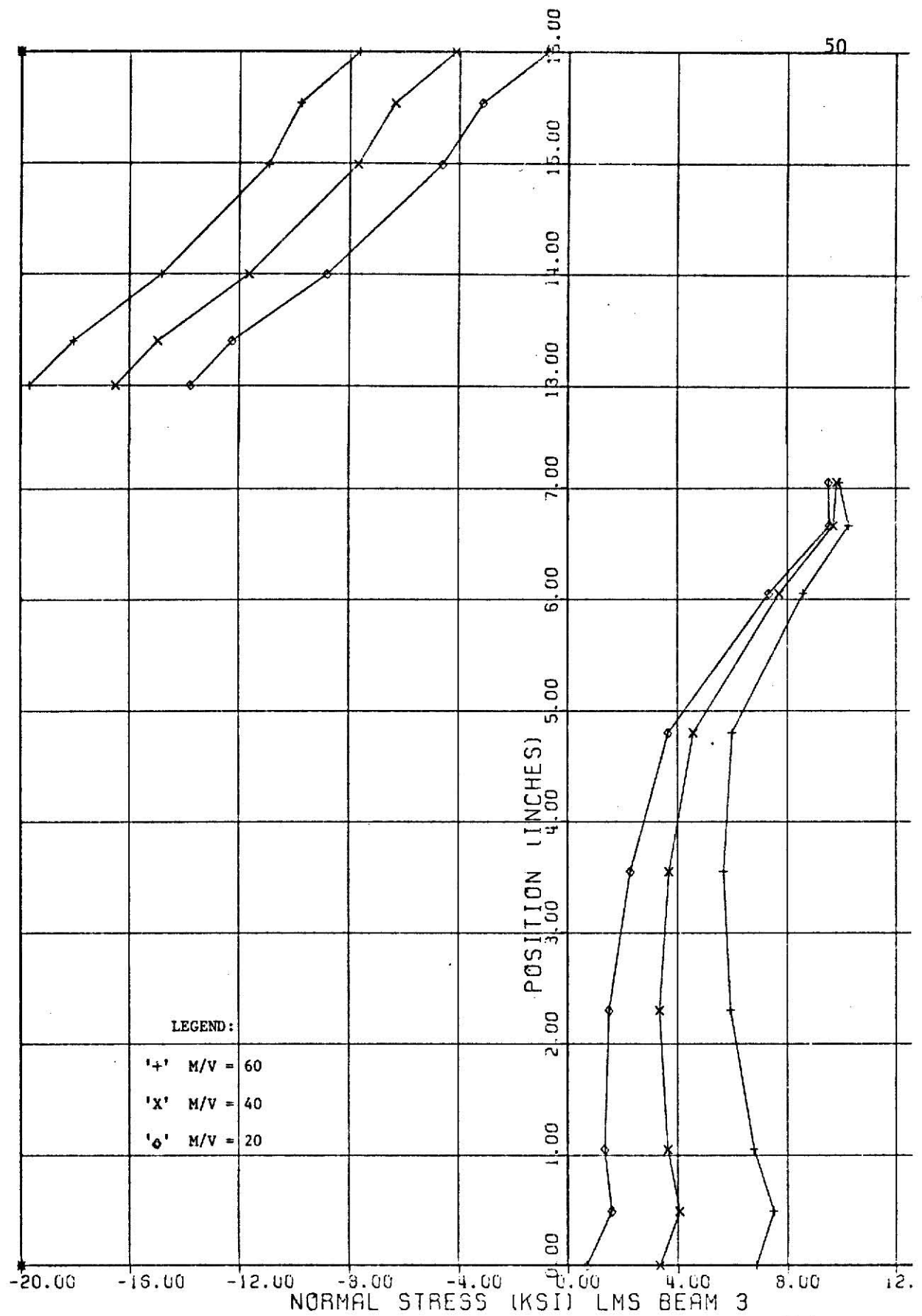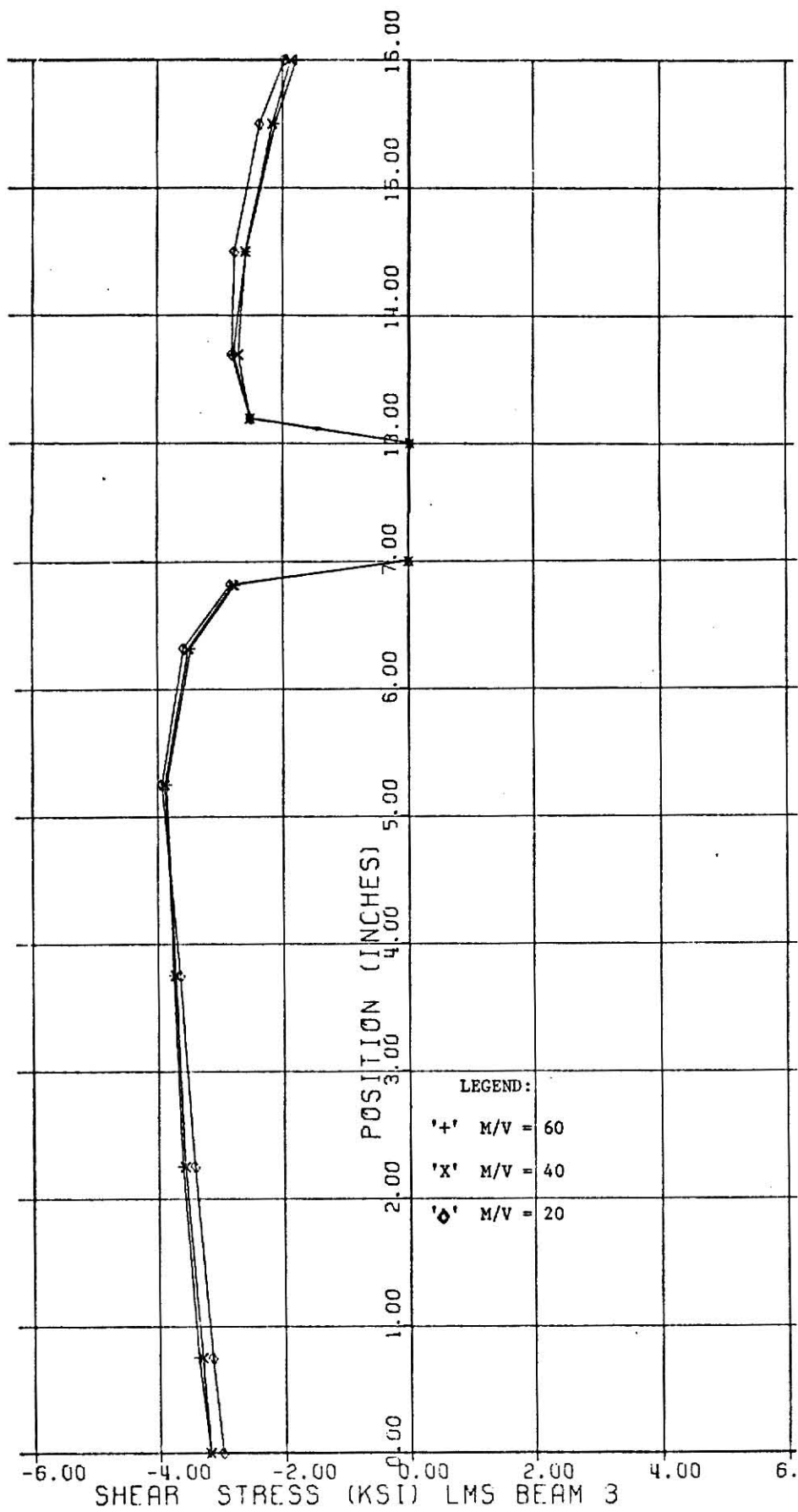
Fig. 30   Finite element shear stress distribution curves for
          20 kip load, low moment section: Beam 3 (M/V = 20,
          40, and 60)
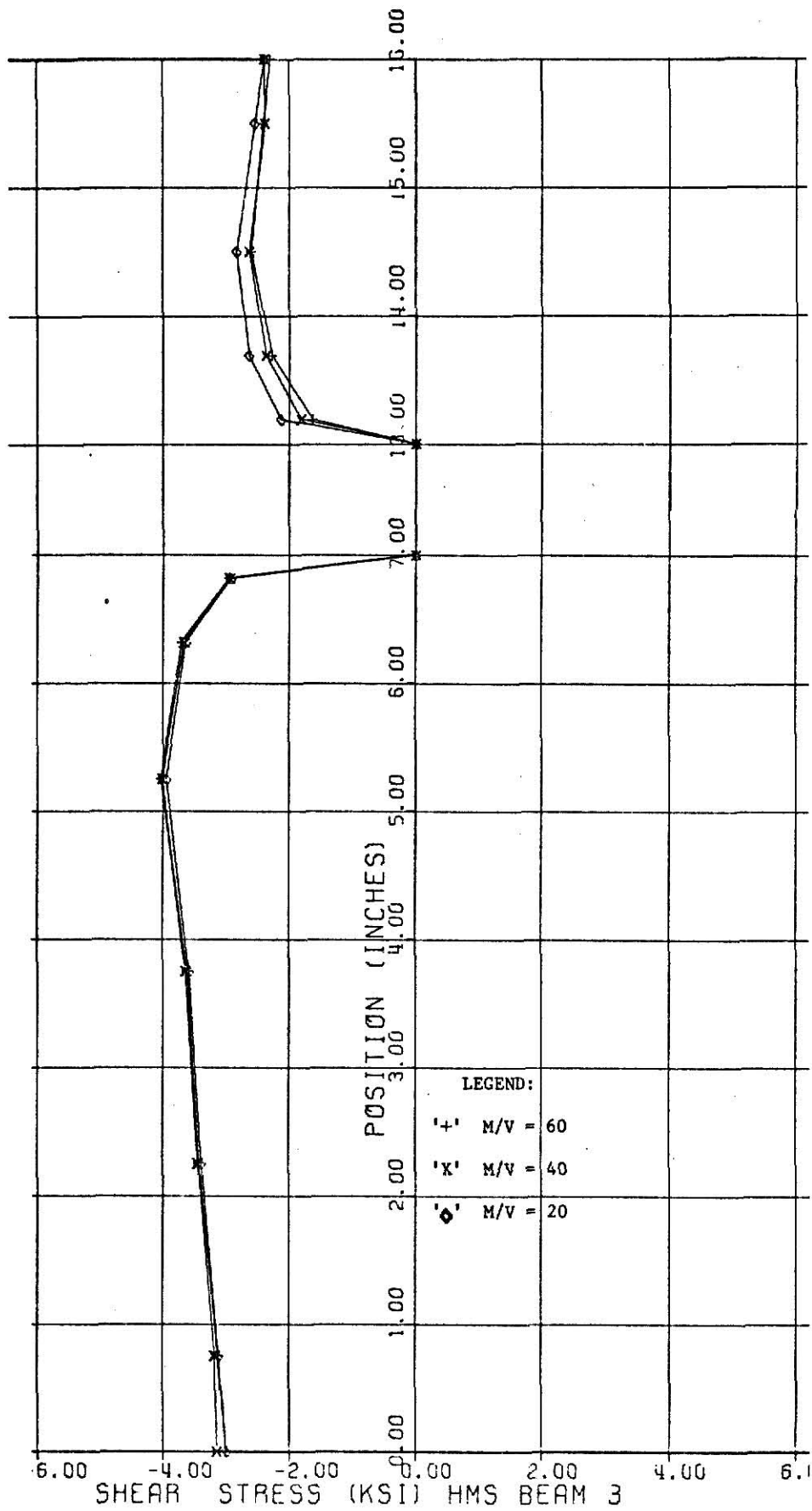
Fig. 31 Finite element shear stress distribution curves for 20 kip load, high moment section: Beam 3 (M/V = 20, 40, and 60)

TABLE 3a. SHEARING FORCES AT THE OPENING, "NORMAL STRESSES" FINITE ELEMENT SOLUTION FOR 20^k LOAD -- BEAMS 1 AND 2.

	M/V	V_T	V_B	$V_T + V_B$	V_T/V_B
BEAM 1 (UNREINFORCED)	20	2.4606^k	7.0153^k	9.4759^k	0.3508
	40	2.2970^k	7.2569^k	9.5538^k	0.3165
	60	2.4137^k	7.1341^k	9.5478^k	0.3383
	80	2.4037^k	7.0410^k	9.4447^k	0.3414
	M/V	V_T	V_B	$V_T + V_B$	V_T/V_B
BEAM 2 (REINFORCED)	20	2.6697^k	7.0292^k	9.6989^k	0.3798
	40	2.4861^k	7.1885^k	9.6746^k	0.3459
	60	2.5938^k	6.9985^k	9.5923^k	0.3706
	80	2.6002^k	6.9740^k	9.5742^k	0.3728

TABLE 3b. SHEARING FORCE AT THE OPENING "NORMAL STRESSES" FINITE ELEMENT, SOLUTION FOR 20^k LOAD -- BEAMS 3, 4 AND 5.

	M/V	V_T	V_B	$V_T + V_B$	V_T/V_B
BEAM 3 (UNREINFORCED)	20	2.2501^k	7.4240^k	9.6741^k	0.3031
	40	2.0853^k	7.5527^k	9.6380^k	0.2761
	60	2.0903^k	7.5162^k	9.6065^k	0.2781
				.	
	M/V	V_T	V_B	$V_T + V_B$	V_T/V_B
BEAM 4 (REINFORCED)	20	2.5162^k	7.1593^k	9.6755^k	0.3515
	40	2.3194^k	7.2482^k	9.5676^k	0.3200
	60	2.3223^k	7.3127^k	9.6350^k	0.3176
	M/V	V_T	V_B	$V_T + V_B$	V_T/V_B
BEAM 5 (REINFORCED)	20	2.6575^k	7.0688^k	9.7263^k	0.3759
	40	2.4248^k	7.2519^k	9.6767^k	0.3344
	60	2.4175^k	7.4829^k	9.9003^k	0.3231

TABLE 4a. SHEARING FORCE AT THE OPENING "SHEARING STRESSES" FINITE ELEMENT SOLUTION FOR 20^k LOAD -- BEAMS 1 AND 2.

BEAM No. 1: (UNREINFORCED)

M/V	LOW MOMENT SECTION				HIGH MOMENT SECTION			
	V_T	V_B	$V_T + V_B$	V_T/V_B	V_T	V_B	$V_T + V_B$	V_T/V_B
20	2.5300^k	7.124^k	9.6540^k	0.3551	2.5600^k	7.2200^k	9.7800^k	0.3546
40	2.3805^k	7.1622^k	9.5427^k	0.3324	2.4428^k	7.2833^k	9.7261^k	0.3354
60	2.4808^k	6.9788^k	9.4596^k	0.3554	2.5604^k	7.1975^k	9.7579^k	0.3557
80	2.4669^k	6.8612^k	9.3281^k	0.3566	2.5881^k	7.2002^k	9.7883^k	0.3594

BEAM No. 2: (REINFORCED)

M/V	LOW MOMENT SECTION				HIGH MOMENT SECTION			
	V_T	V_B	$V_T + V_B$	V_T/V_B	V_T	V_B	$V_T + V_B$	V_T/V_B
20	2.7057^k	6.9235^k	9.6282^k	0.3908	2.7369^k	7.0203^k	9.7572^k	0.3899
40	2.5154^k	7.0619^k	9.5773^k	0.3562	2.5535^k	7.0999^k	9.6534^k	0.3597
60	2.6192^k	6.9096^k	9.5289^k	0.3791	2.6919^k	7.0619^k	9.7538^k	0.3812
80	2.5812^k	6.7401^k	9.3213^k	0.3830	2.7126^k	7.0722^k	9.7848^k	0.3836

TABLE 4b. SHEARING FORCES AT THE OPENING "SHEARING STRESSES" FINITE ELEMENT SOLUTION FOR 20^k LOAD — BEAMS 3, 4 AND 5.

BEAM No. 3: (UNREINFORCED)

M/V	LOW MOMENT SECTION				HIGH MOMENT SECTION			
	V_T	V_B	$V_T + V_B$	V_T/V_B	V_T	V_B	$V_T + V_B$	V_T/V_B
20	2.3981^k	7.1638^k	9.5619^k	0.335	2.3672^k	7.1492^k	9.5164^k	0.331
40	2.2480^k	7.5310^k	9.7790^k	0.299	2.1910^k	7.5046^k	9.6956^k	0.292
60	2.0418^k	7.5669^k	9.6087^k	0.270	2.1377^k	7.4570^k	9.5967^k	0.287

BEAM No. 4: (REINFORCED)

M/V	LOW MOMENT SECTION				HIGH MOMENT SECTION			
	V_T	V_B	$V_T + V_B$	V_T/V_B	V_T	V_B	$V_T + V_B$	V_T/V_B
20	2.6245^k	7.2016^k	9.8261^k	0.364	2.6152^k	7.1888^k	9.8040^k	0.364
40	2.4372^k	7.3418^k	9.7790^k	0.332	2.3991^k	7.4116^k	9.8107^k	0.327
60	2.5192^k	7.1264^k	9.6456^k	0.353	2.3352^k	7.0771^k	9.4123^k	0.330

TABLE 4b. SHEARING FORCES AT THE OPENING "SHEARING STRESSES" FINITE ELEMENT SOLUTION FOR 20^k LOAD -- BEAMS 3, 4 AND 5. (Continued)

BEAM No. 5: (REINFORCED)

M/V	LOW MOMENT SECTION				HIGH MOMENT SECTION			
	V_T	V_B	$V_T + V_B$	V_T/V_B	V_T	V_B	$V_T + V_B$	V_T/V_B
20	2.5706^k	7.1181^k	9.6887^k	0.361	2.6919^k	7.1105^k	9.8024^k	0.379
40	2.5509^k	7.2786^k	9.8295^k	0.350	2.4630^k	7.2716^k	9.7346^k	0.339
60	2.5441^k	7.2830^k	9.8271^k	0.349	2.4200^k	7.2483^k	9.6683^k	0.334

TABLE 5. TOTAL AMOUNT OF SHEAR FORCE ACCOUNTED FOR IN THE FINITE ELEMENT ANALYSIS AND THE EXPERIMENTAL TESTS OF P = 20 kips.

Beam Number	"Normal Stress" Finite Element Solution $V = V_T + V_B$	"Shearing Stress" Finite Element Solution $V = V_T + V_B$	Experimental Results $V = V_T + V_B$
BEAM 1	9.5056^k	9.6304^k	8.583^k / 9.256^k*
BEAM 2	9.6352^k	9.6269^k	9.417^k / 9.394^k*
BEAM 3	9.6395^k	9.6261^k	9.574^k
BEAM 4	9.6260^k	9.7129^k	9.797^k
BEAM 5	9.7677^k	9.7587^k	8.980^k
BEAM 5a			8.733^k

*Revised Results

TABLE 6. COMPARISON OF SHEAR FORCE DISTRIBUTION (V_T/V_B) FOR EXPERIMENTAL AND FINITE ELEMENT SOLUTION.

Beam	Size	Amount of Reinforcement	Size of opening	Eccentricity from mid-depth	Finite Element Normal Stress	Finite Element Shearing Stress	Experimental Normal Stress
1	W16 x 45	None	9" x 6"	2" above	0.360 / 0.337*	0.351	0.375 / 0.303*
2	W16 x 45	0.5 sq.-in.	9" x 6"	2" above	0.380 / 0.367*	0.378	0.32? / 0.342*
3	W16 x 40	None	12" x 6"	2" above	0.286	0.302	0.249
4	W16 x 40	0.5 sq.-in.	12" x 6"	2" above	0.330	0.345	0.272
5	W16 x 40	1.0 sq.-in.	12" x 6"	2" above	0.344	0.352	0.328
5a	W16 x 40	1.0 sq.-in.	12" x 6"	2" below	---	---	2.956 (0.338)

*Revised Results

TABLE 7a. THEORETICAL RATIO OF V_T/V_B FOR W16 x 45 STEEL BEAMS WITH 9" x 6" RECTANGULAR WEB OPENING WITH 2 INCH ECCENTRICITY.

SHEAR FORCE DISTRIBUTION RATIO (V_T/V_B) -- BEAM 1 (UNREINFORCED)

Eccentricity e"	Experimental Results	Finite Element	Theoretical Methods				
			1	2	3	4	5
1"	-----	-----	0.546	0.526	0.508	0.702	0.598
2"	0.375 / 0.303*	0.360 / 0.337*	0.268	0.248	0.231	0.496	0.334
3"	-----	-----	0.099	0.0872	0.079	0.392	0.152

SHEAR FORCE DISTRIBUTION RATIO (V_T/V_B) -- BEAM 2 (REINFORCED)

Eccentricity e"	Experimental Results	Finite Element	Theoretical Methods				
			1	2	3	4	5
1"	-----	-----	0.592	0.573	0.541	0.684	0.593
2"	0.328 / 0.343*	0.380 / 0.367*	0.324	0.301	0.266	0.460	0.325
3"	-----	-----	0.142	0.124	0.099	0.312	0.138

*Revised Results

TABLE 7b. THEORETICAL RATIO OF V_T/V_B FOR W16 x 40 STEEL BEAMS WITH 12" x 6" RECTANGULAR WEB OPENING WITH 2 INCH ECCENTRICITY.

SHEAR FORCE DISTRIBUTION RATIO (V_T/V_B) -- BEAM 3 (UNREINFORCED)

Eccentricity e"	Experimental Results	Finite Element	Theoretical Methods				
			1	2	3	4	5
1"	-----	-----	0.485	0.480	0.466	0.699	0.594
2"	0.249	0.286	0.207	0.203	0.192	0.471	0.329
3"	-----	-----	0.064	0.062	0.057	0.338	0.147

SHEAR FORCE DISTRIBUTION RATIO (V_T/V_B) -- BEAM 4 (REINFORCED)

Eccentricity e"	Experimental Results	Finite Element	Theoretical Methods				
			1	2	3	4	5
1"	-----	-----	0.545	0.541	0.512	0.676	0.590
2"	0.272	0.330	0.269	0.265	0.236	0.444	0.321
3"	-----	-----	0.101	0.098	0.080	0.285	0.135

SHEAR FORCE DISTRIBUTION RATIO (V_T/V_B) -- BEAM 5 (REINFORCED)

Eccentricity e"	Experimental Results	Finite Element	Theoretical Methods				
			1	2	3	4	5
1"	-----	-----	0.569	0.504	0.524	0.669	0.579
2"	0.328	0.340	0.296	0.291	0.248	0.434	0.307
3"	-----	-----	0.120	0.115	0.087	0.269	0.125
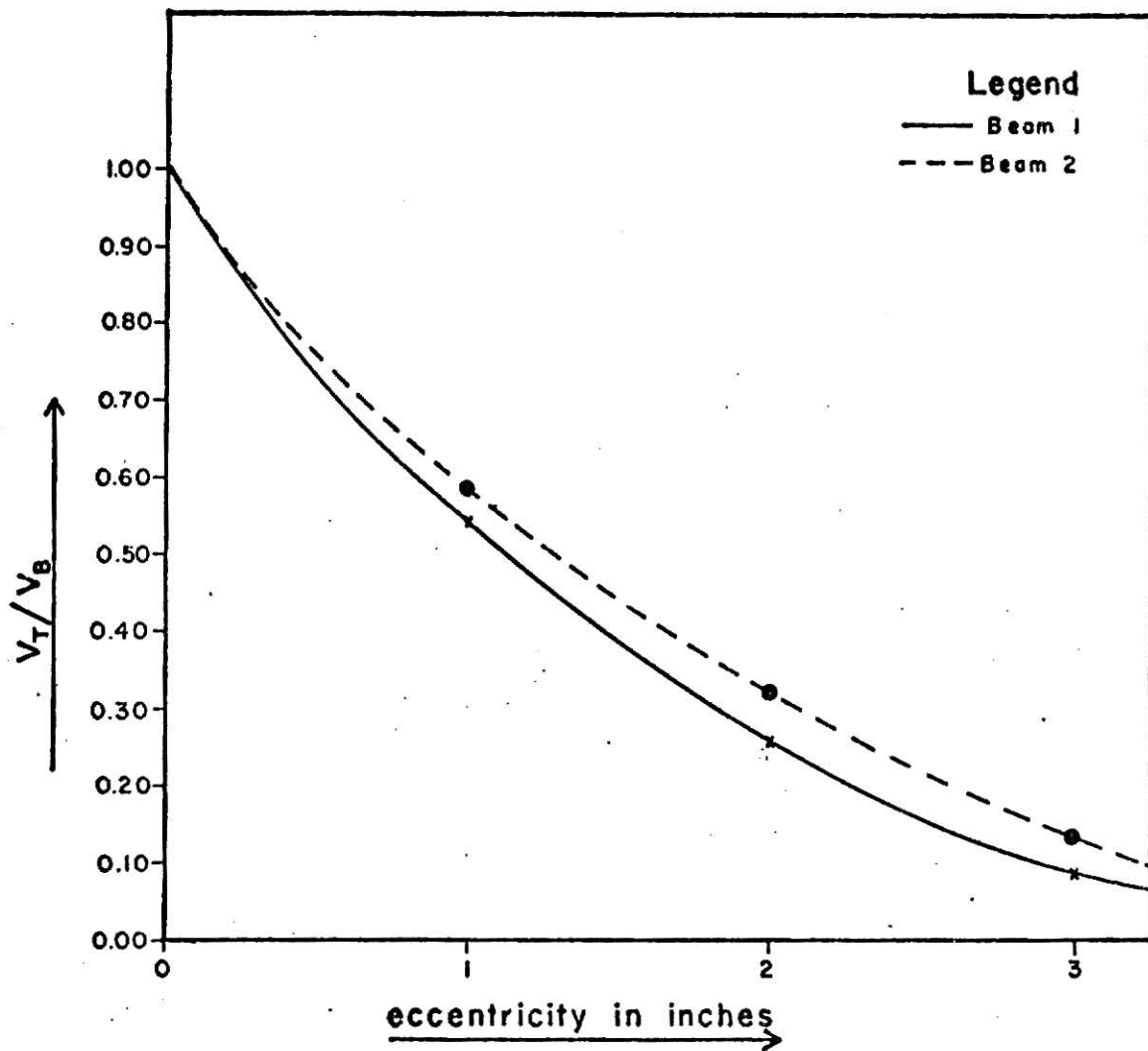
Fig. 32 Eccentricity vs theoretical (V_T/V_B)(Method 1)--Beam 1 and 2
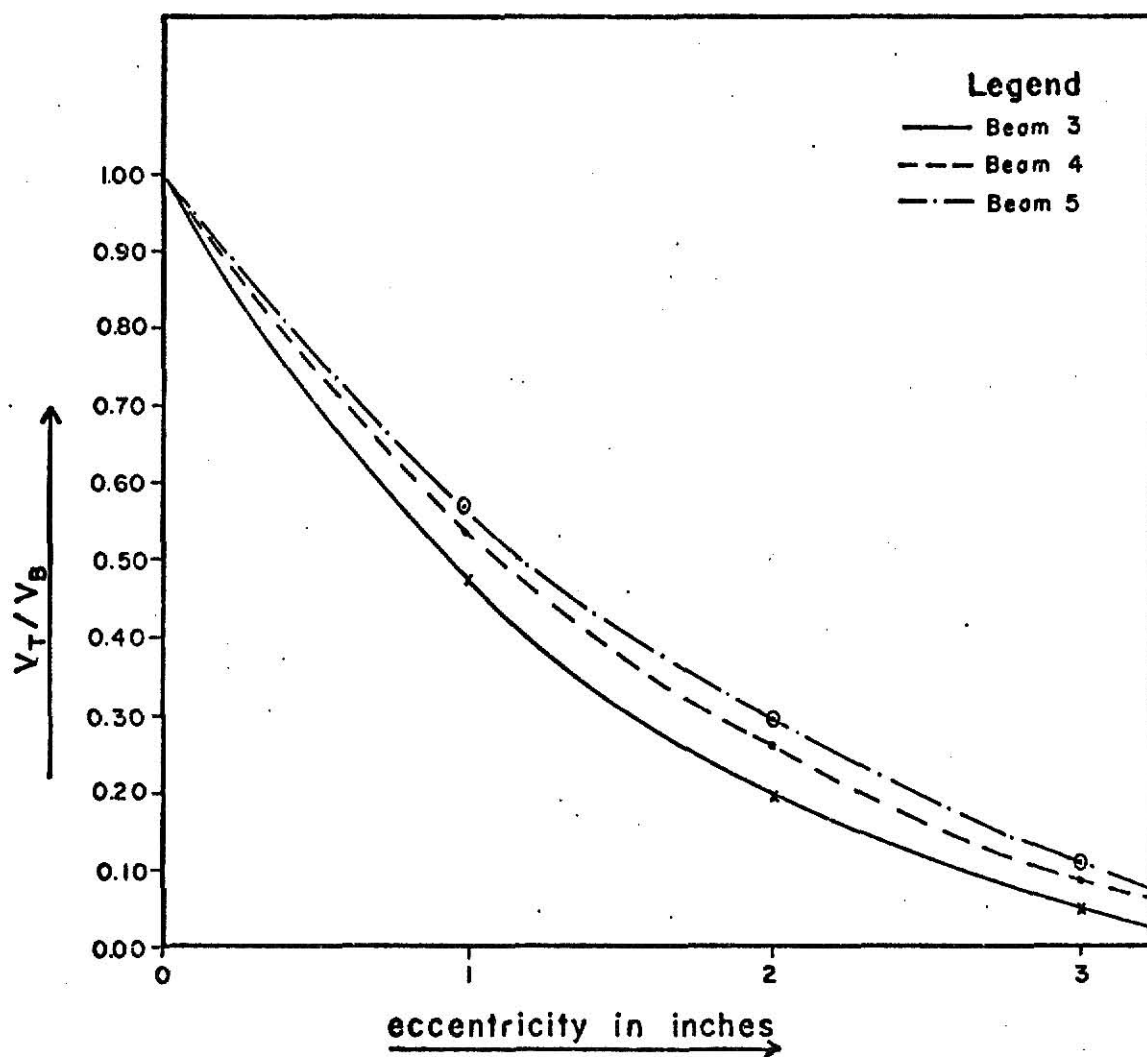
Fig. 33 Eccentricity vs theoretical (V_T/V_B) (Method 1)--Beam 3, 4 and 5

Top Low Moment Section
(TLMS)

Bottom Low Moment Section
(BLMS)
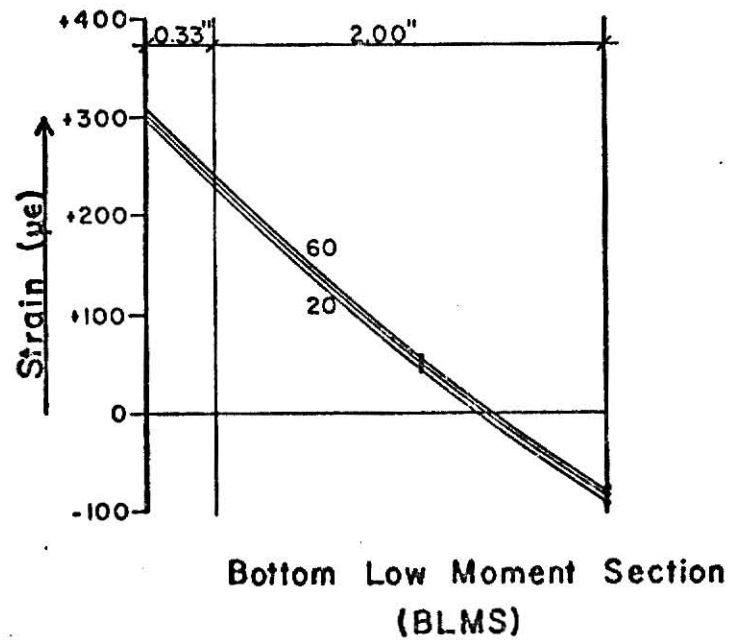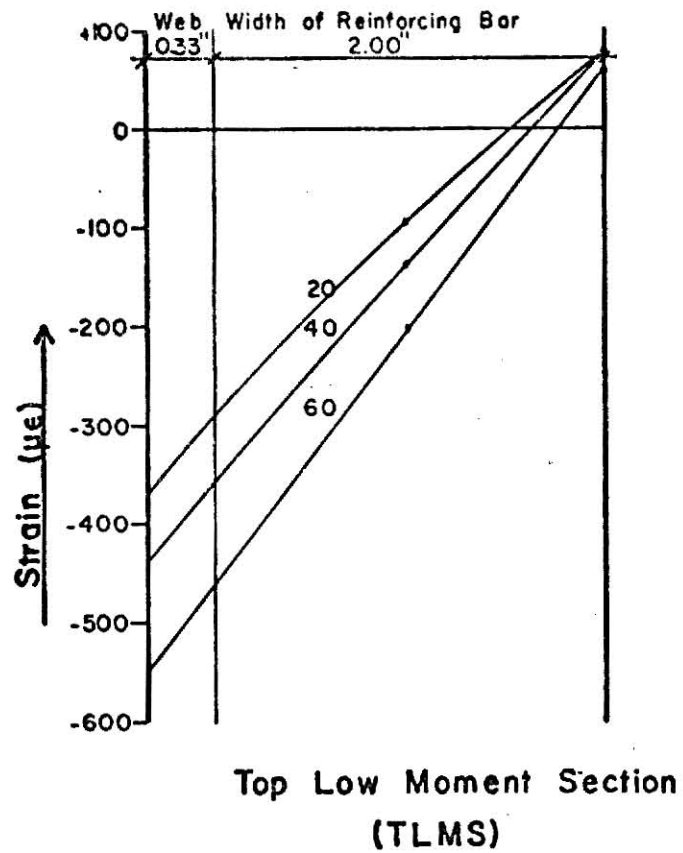
Fig. 34   Strain variation in reinforcing bars, low
moment section: Beam 4; ΔP = 20 kip

Fig. 35 Strain variation in reinforcing bars, high
moment section: Beam 4; $\Delta P = 20$ kip
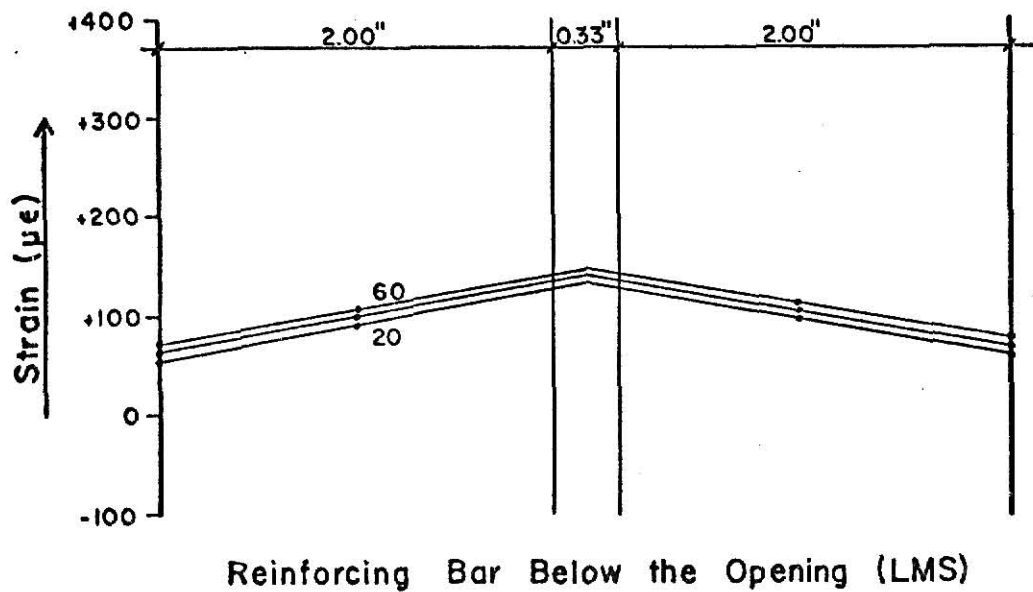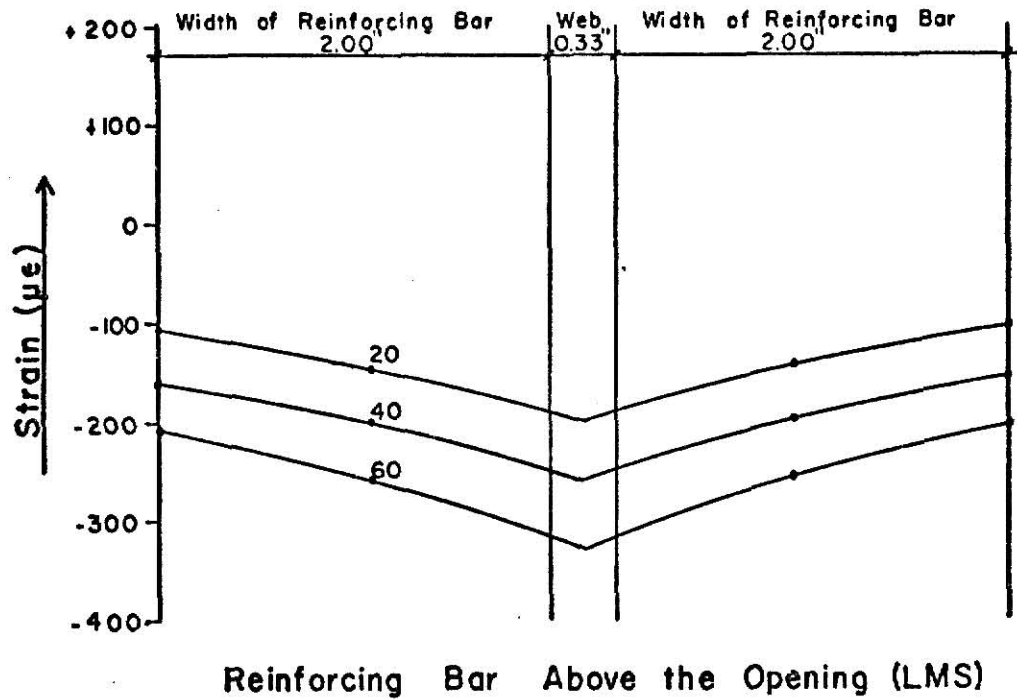
Fig. 36 Strain variation in reinforcing bars, low
moment section: Beam 5; $\Delta P = 20$ kip
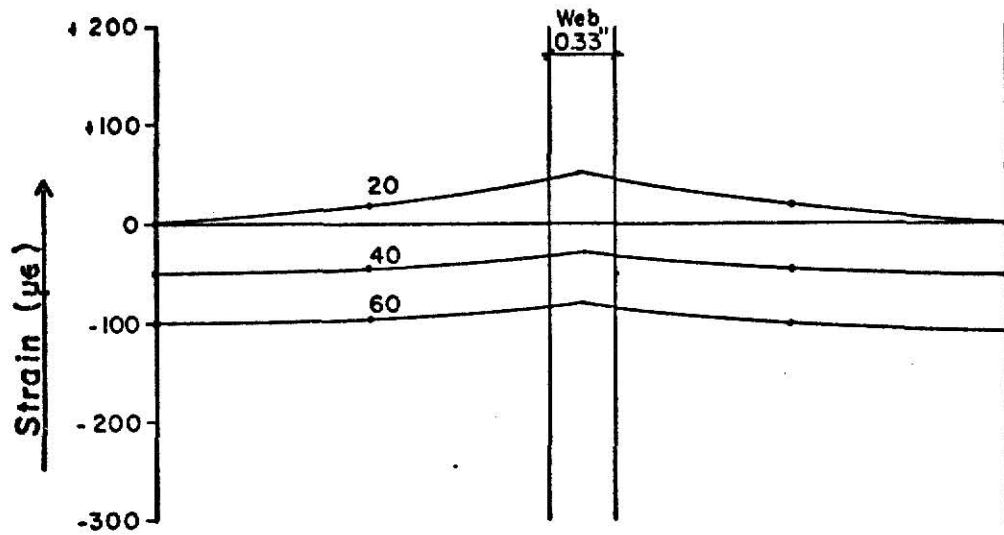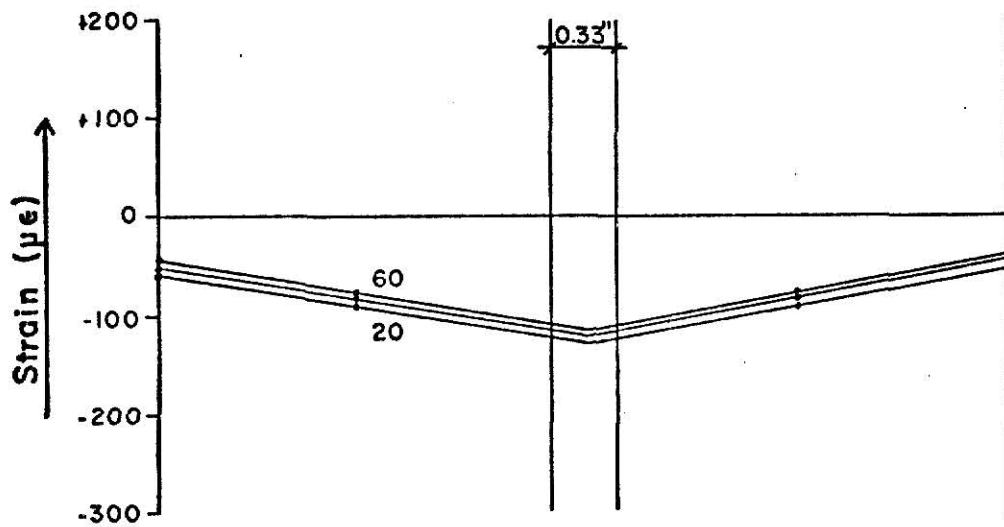
Fig. 37 Strain variation in reinforcing bars, high
moment section: Beam 5; ΔP = 20 kip
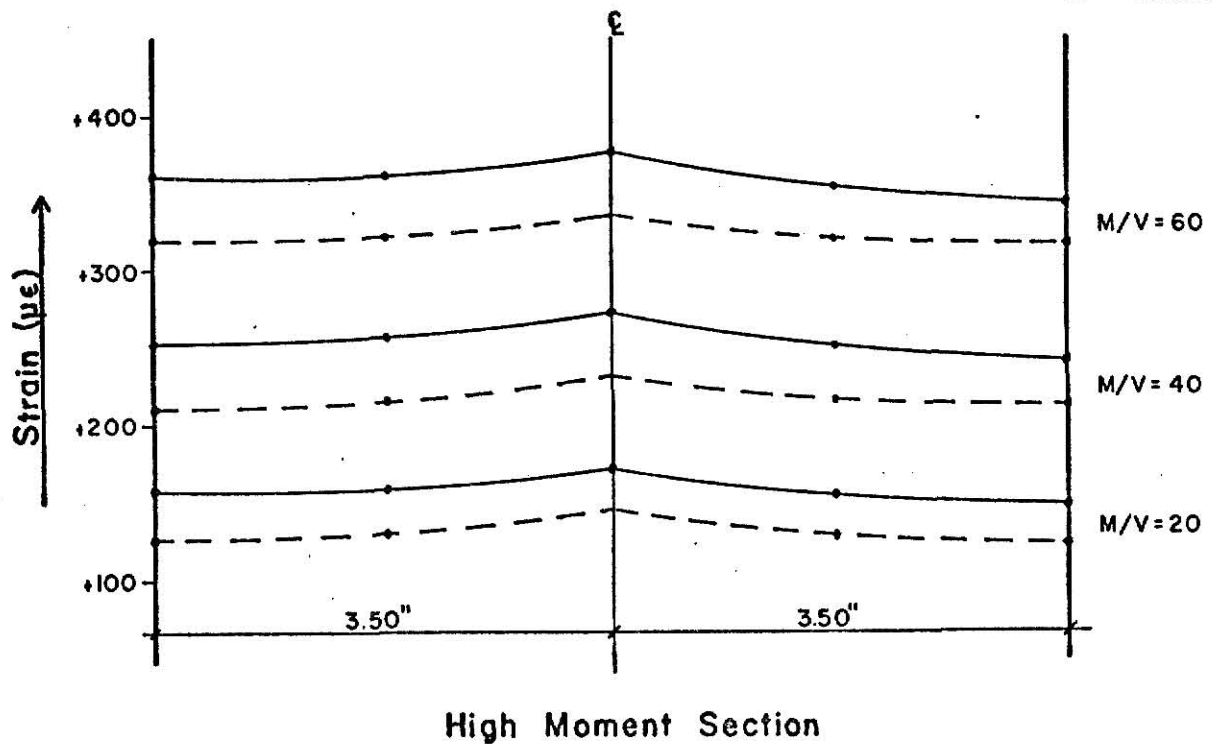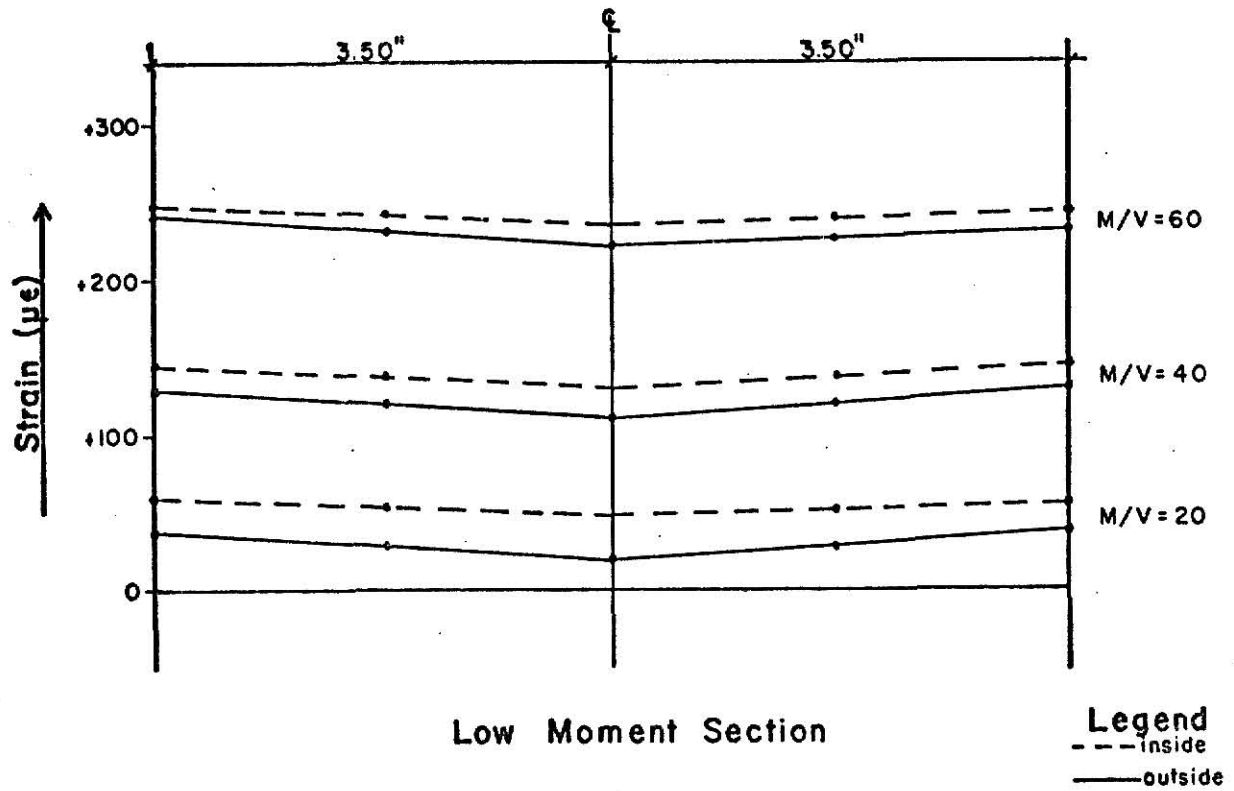
Fig. 38 Strain variation in bottom flange: Beam 5; ΔP = 20 kip
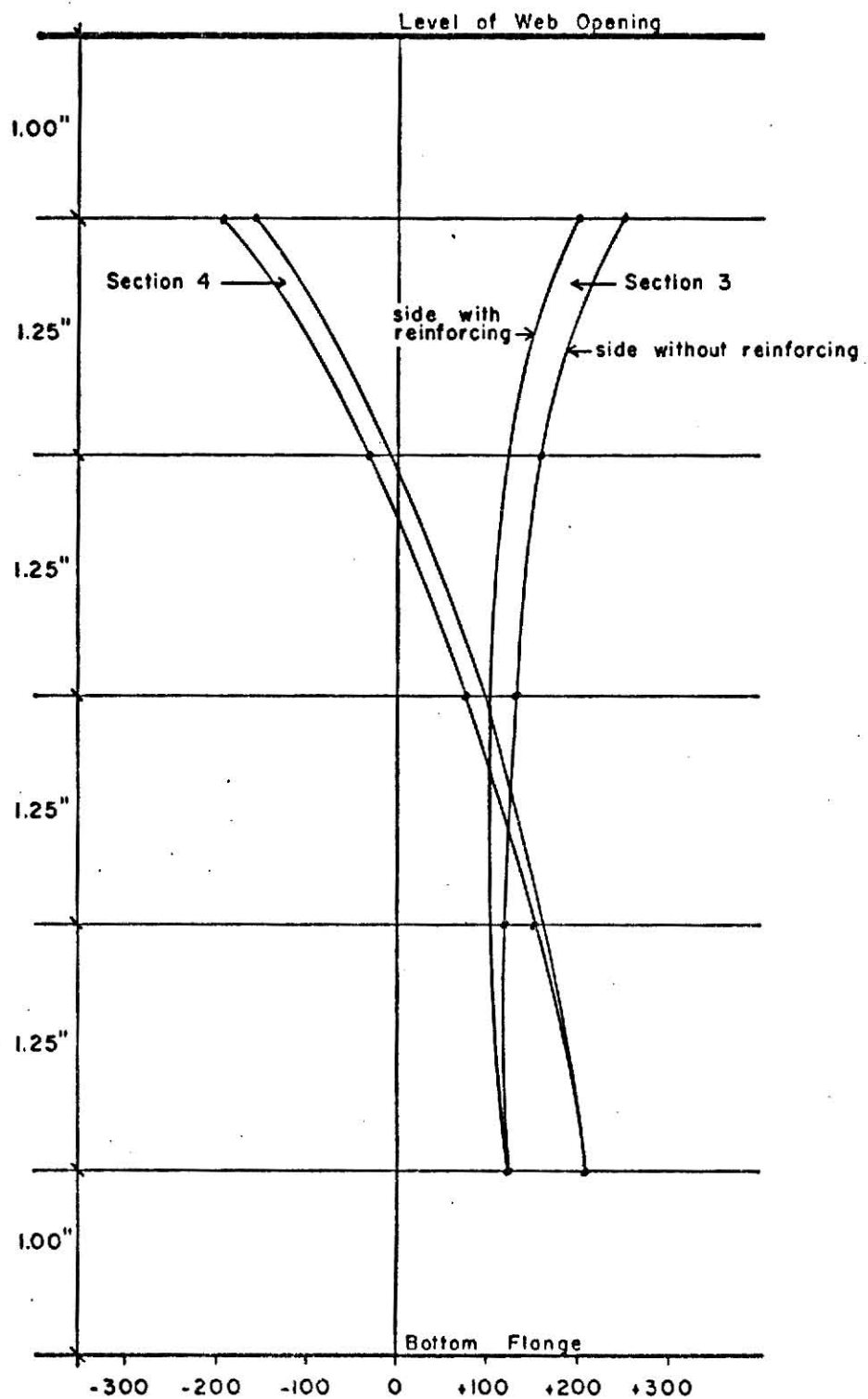
Fig. 39 Typical strain variation in web,
Beam 4, ΔP = 20 kip

TABLE 8. DEFLECTION READING FOR 20^k LOAD.

Eccentricity 2"

Beam 1

M/V	MID-SPAN DEFLECTIONS (INCHES)					RELATIVE DEFLECTION ACROSS THE OPENING (INCHES)	
	Experimental	y_{p_2} Eq. (15)	y_{p_1} Eq. (14)	HME (inches)	LME (inches)	Experimental	Theoretical
80	0.238	0.242	0.239	0.225	0.210	0.015	0.015
60	0.131	0.133	0.130	0.120	0.108	0.012	0.012
40	0.064	0.064	0.061	0.055	0.045	0.010	0.010
20	0.027	0.026	0.023	0.020	0.013	0.007	0.007

Beam 2

M/V							
80	0.223	0.224	0.222	0.210	0.195	0.014	0.013
60	0.118	0.121	0.120	0.110	0.098	0.012	0.011
40	0.060	0.057	0.056	0.049	0.400	0.009	0.008
20	0.023	0.022	0.021	0.019	0.011	0.008	0.006

TABLE 9. DEFLECTION READINGS FOR 20^k LOAD.

Eccentricity 2"

Beam 3

M/V	MID-SPAN DEFLECTIONS (INCHES)					RELATIVE DEFLECTION ACROSS THE OPENING (INCHES)	
	Experimental	y_{p_2} Eq. (15)	y_{p_1} Eq. (14)	HME (inches)	LME (inches)	Experimental	Theoretical
60	0.153	0.157	0.151	0.142	0.121	0.021	0.020
40	0.074	0.077	0.072	0.065	0.048	0.017	0.016
20	0.032	0.033	0.028	0.026	0.012	0.014	0.012

Beam 4

M/V							
60	0.147	0.155	0.151	0.138	0.117	0.021	0.019
40	0.074	0.076	0.072	0.066	0.048	0.018	0.015
20	0.032	0.032	0.028	0.026	0.012	0.014	0.011

TABLE 10. DEFLECTION READINGS FOR 20^k LOAD.

Eccentricity 2"   Beam 5

M/V	MID-SPAN DEFLECTIONS (INCHES)					RELATIVE DEFLECTION ACROSS THE OPENING (INCHES)	
	Experimental	y_{P_2} Eq. (15)	y_{P_1} Eq. (14)	HME (inches)	LME (inches)	Experimental	Theoretical
60	0.147	0.154	0.151	0.137	0.116	0.021	0.019
40	0.072	0.075	0.072	0.064	0.048	0.016	0.015
20	0.031	0.031	0.028	0.025	0.013	0.012	0.011
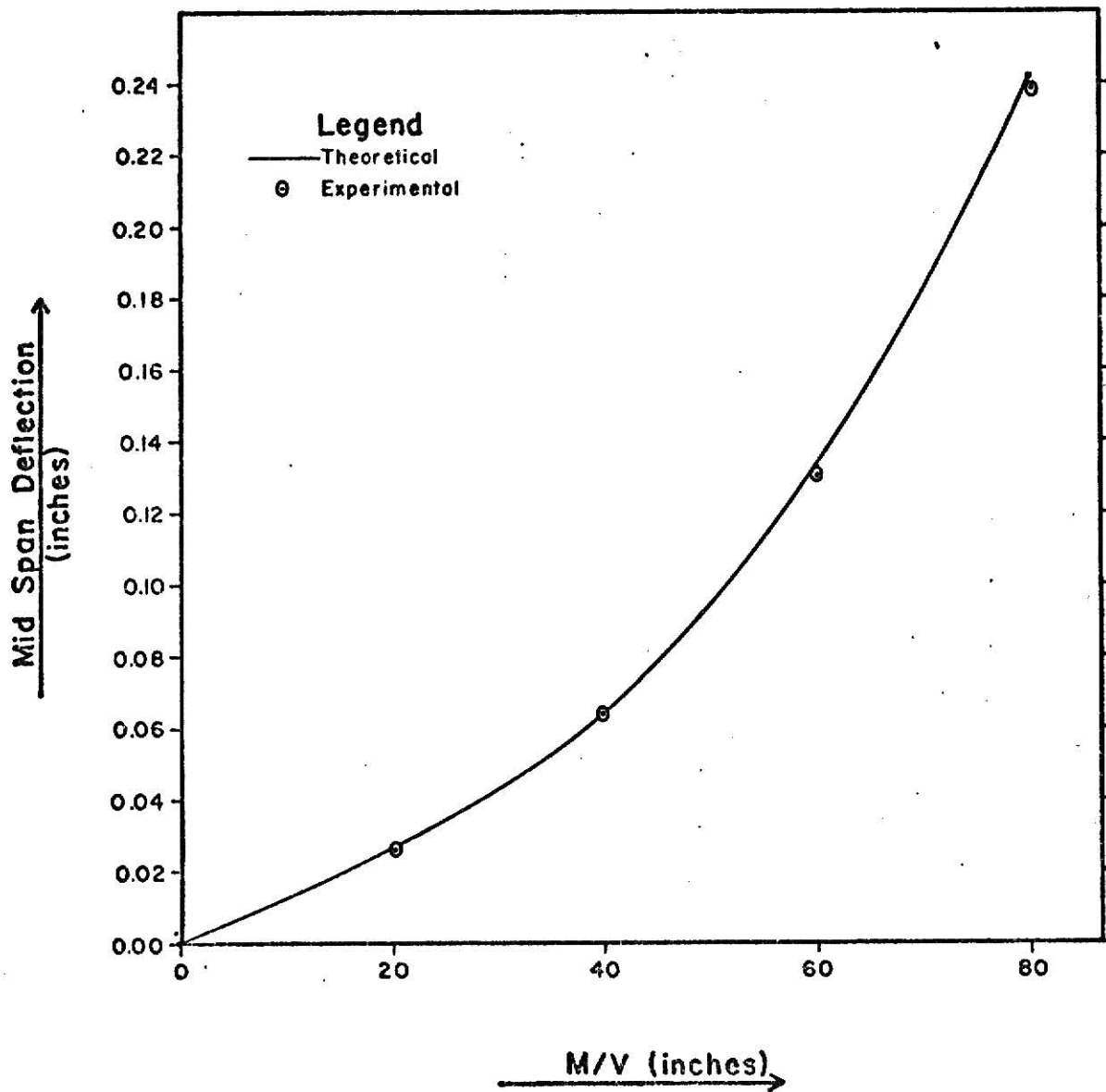
Fig. 40 M/V ratio vs midspan deflection, Beam 1: ΔP = 20 kip
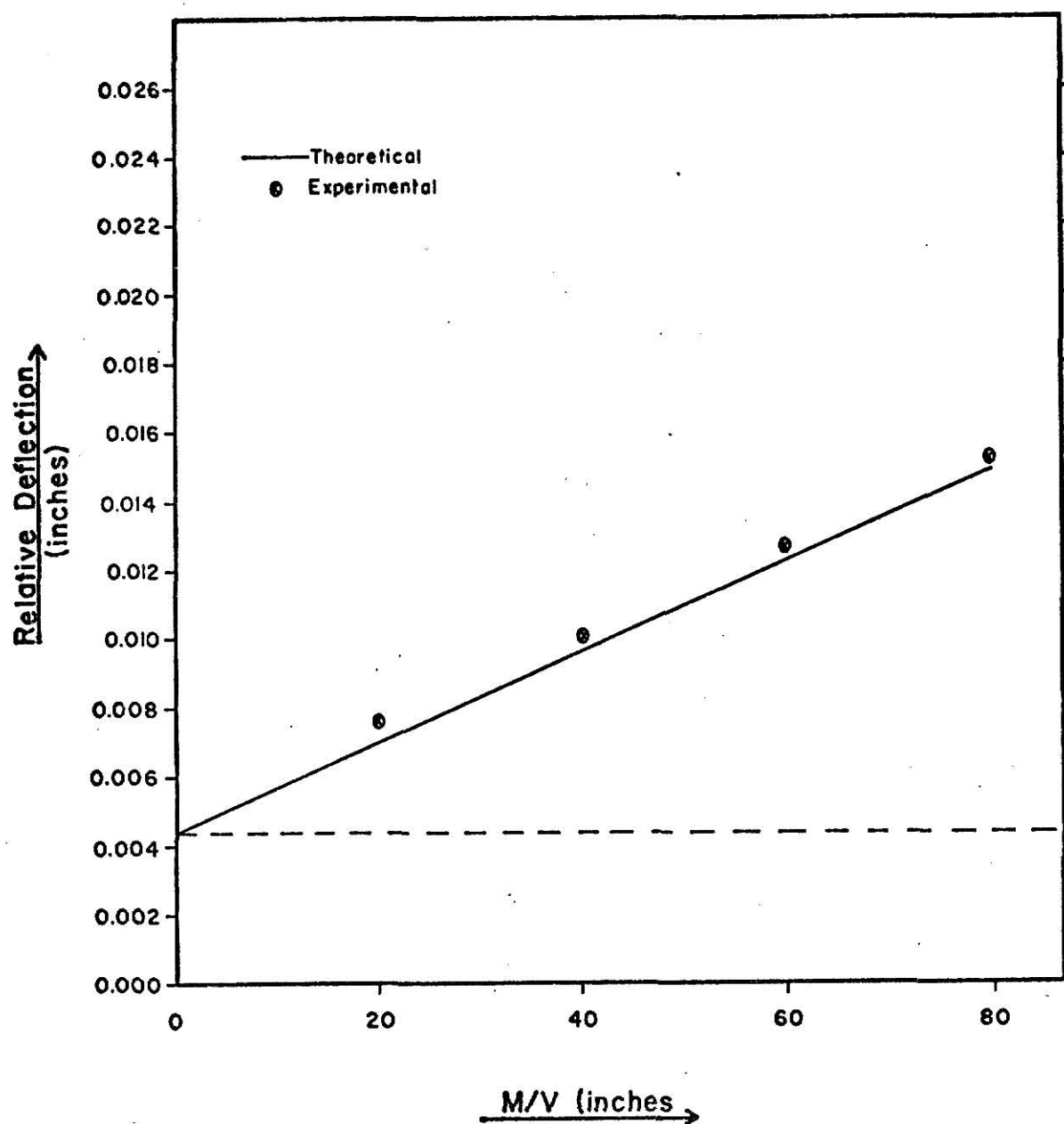
Fig. 41 M/V ratio vs relative deflection across the opening:
Beam 1; ΔP = 20 kip
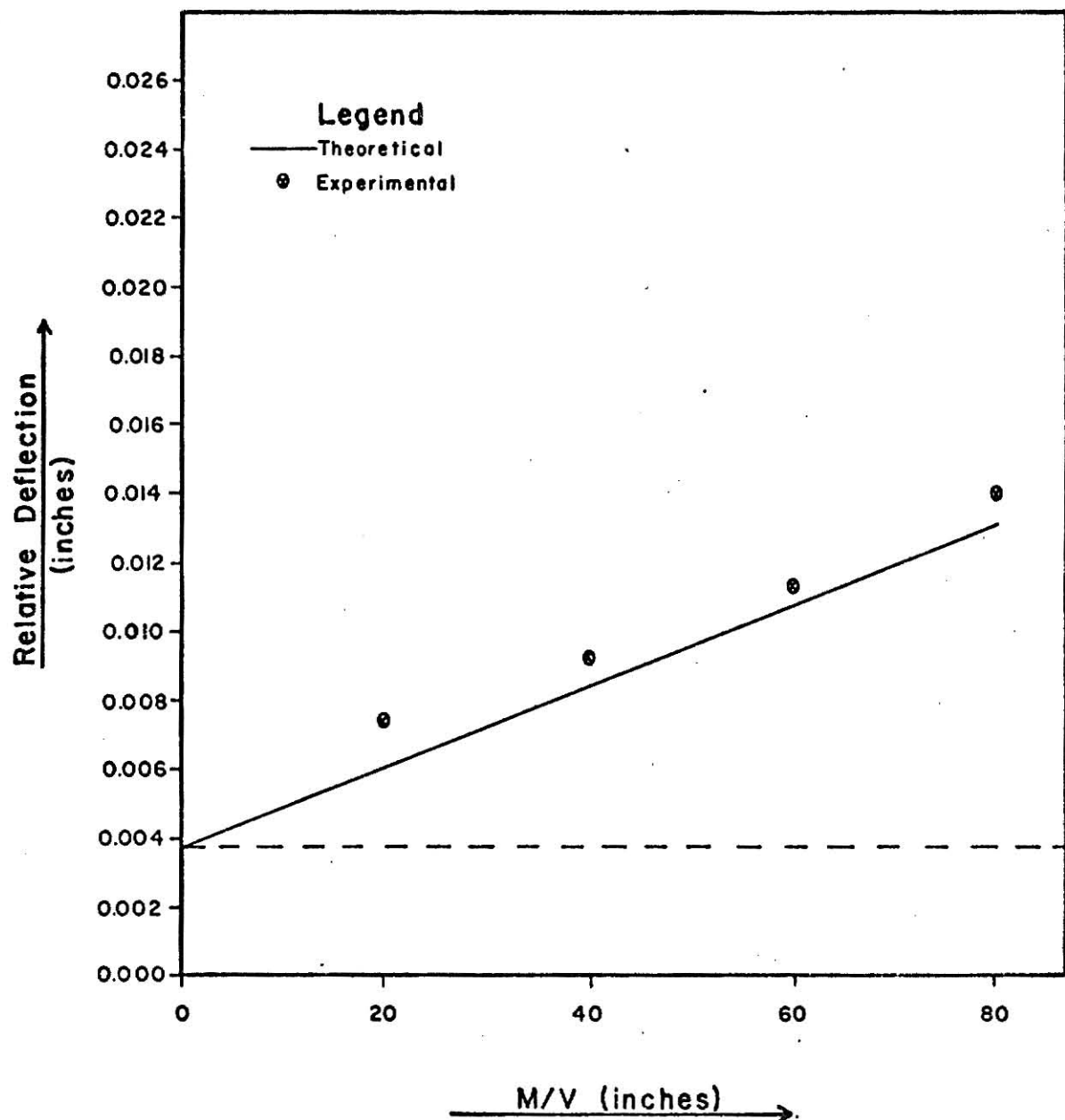
Fig. 42 M/V ratio vs relative deflection across the opening:
Beam 2; ΔP = 20 kip
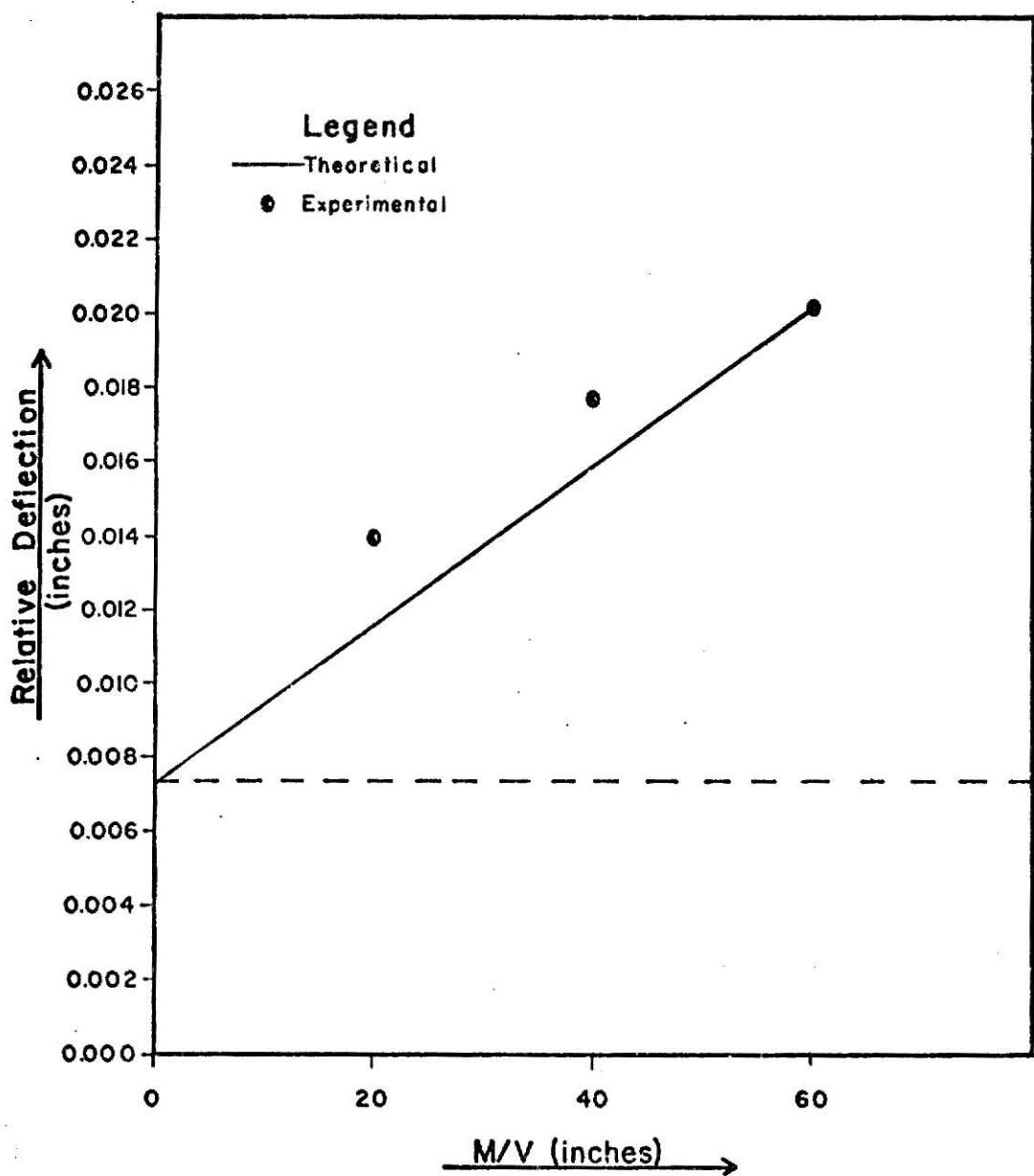
Fig. 43   M/V ratio vs relative deflection across the opening:
Beam 3; $\Delta P = 20$ kip
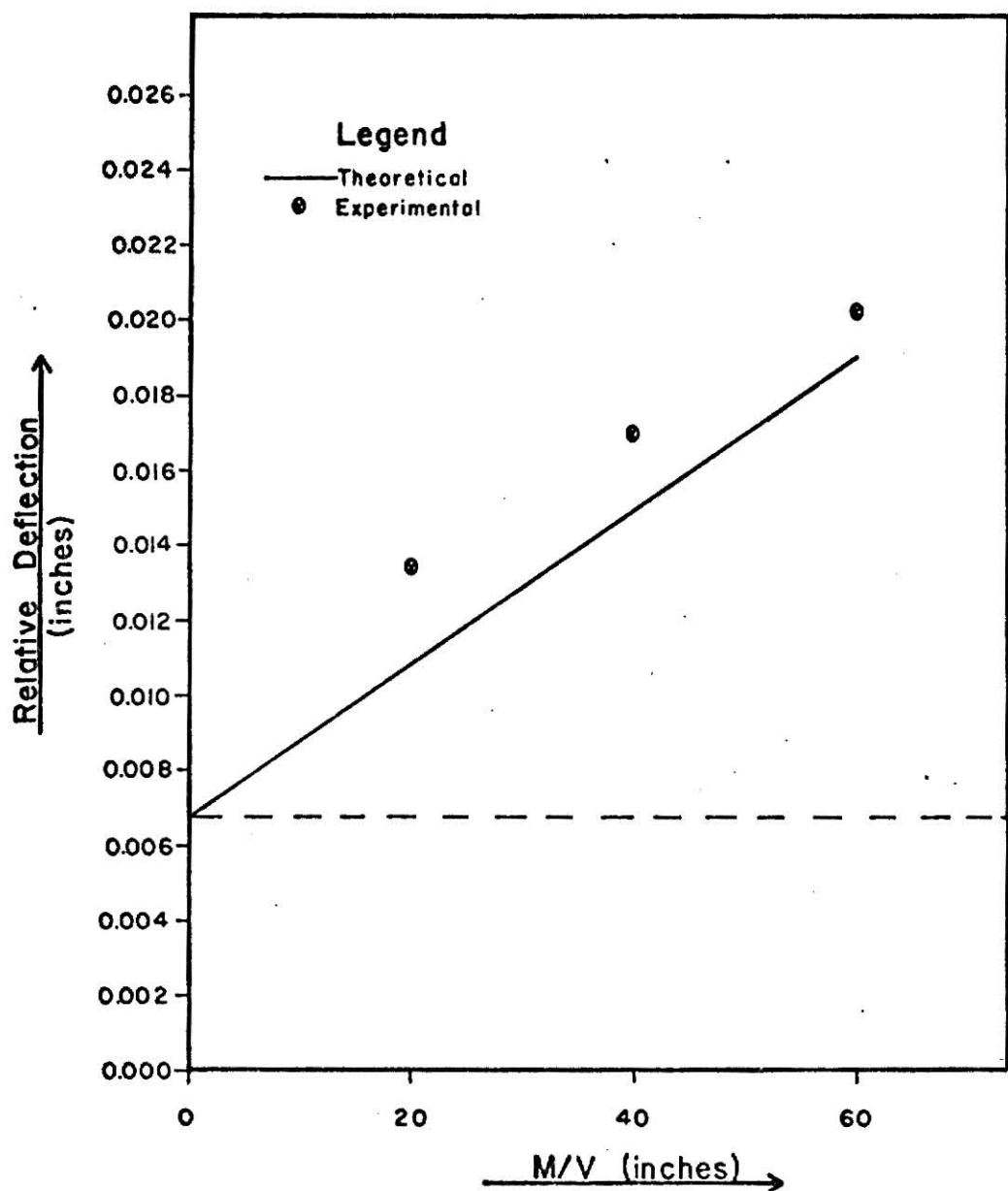
Fig. 44 M/V ratio vs relative deflection across the
opening: Beam 4; ΔP = 20 kip
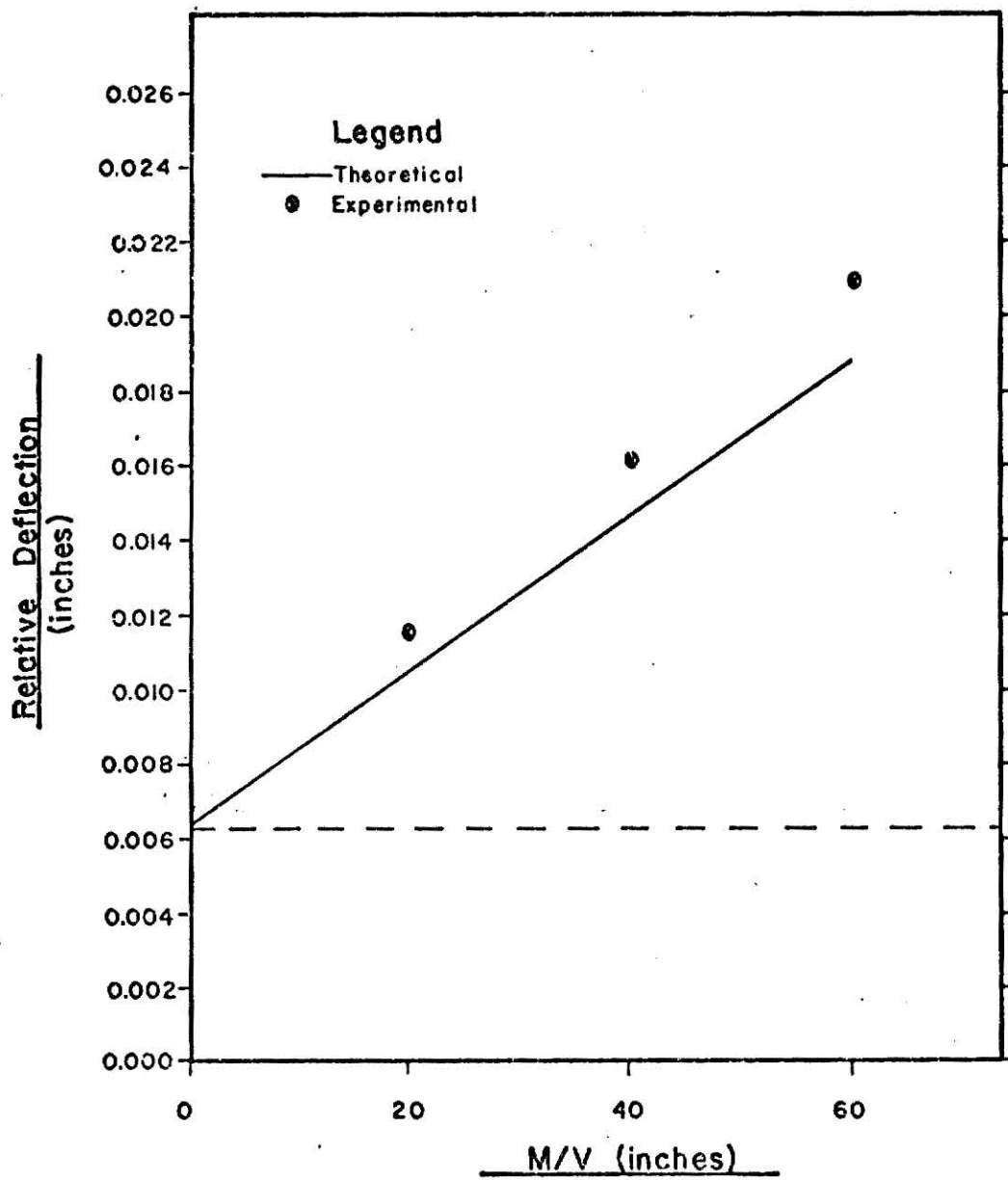
Fig. 45   M/V ratio vs relative deflection across the
opening: Beam 5; ΔP = 20 kip

APPENDIX A

DERIVATION OF THEORETICAL DEFLECTIONS

Relative Deflection Across Web Opening

The problem considered here is finding the deflection at a section in a beam which has a web opening, see Fig. A1. The introduction of the

Fig. A1

opening not only reduces the moment of inertia and cross sectional area, but it also allows secondary bending deflections to be created. The unsymmetrical shape created by cutting the opening also introduces a rigid body rotation term in the deflection equation. So that the secondary deflections can be included in the solution, Castigliano's energy method for finding deflections (Principle of Virtual Forces) is used in this derivation. Both the strain energy due to shearing stresses and normal stresses must be considered.

The notation used in this derivation is as follows:

Symbols

> A - cross-sectional area
>
> C - ratio of shearing forces
>
> E - modulus of elasticity
>
> G - modulus of elasticity for shear
>
> I - moment of inertia

L - length

M - bending moment

P - applied load

Q - integral of the first moment of area to either side of section where shear is desired

R - reaction

U - strain energy

V - shearing force

Y - distance from centroid of section

a - one-half the opening width

k - shear deflection coefficient

v - volume

x - distance from origin

y - deflection

σ - normal stress

τ - shearing stress

Subscripts

A, B, C, D, E, F, G, - vertical cross-sections of beam shown in Fig. Al

B - bottom section at opening

L - left

N - net section

O - refers to vertical centerline of the opening

R - reinforced section or right

T - top section at opening

b - bending

s - shear

The strain energy due to shear is determined by using the equation

$$U_s = \int_o^L \frac{kV^2 dx}{2AG} \quad\text{---} \quad (A1)$$

The basic assumptions in the derivation of this equation is that the shearing

stress and strain are linearly proportional and that the strength of materials

equation for the transverse shearing stress (τ = VQ/It) is sufficiently

accurate. The derivation of Eq. (1) and the shear deflection coefficient

k for the shapes involved in this report are given in Appendix B.

The equation for the strain energy due to normal stress may be written

as

$$U_b = \int_{vol.} \frac{\sigma^2}{2E} \, dv \; \text{--} \quad (A2)$$

where it is assumed that normal stresses and strains are linearly proportional.

When the normal stresses are given by the flexure formula (σ = My/I) the

following more convenient form may be used:

$$U_b = \int_0^L \frac{M^2 dx}{2EI} \; \text{--} \quad (A3)$$

The fictious loads P_B and P_C shown in Fig. 1 are used to determine the

deflection at those two sections. According to Castigliano's theorem the

deflection at B is given by $y_B = \partial U / \partial P_B$ where P_B and P_C are set equal to

zero after differentiating. Since the fictious loads are set to zero after dif-

ferentiating it is often simpler to differentiate before integrating. For ex-

ample consider the region A-B, the strain energy can easily be determined from

Eqs. (A1) and (A3) where

$$V = R_L$$

$$M = R_L \cdot x$$

$$R_L = \frac{P}{2} + P_B \, (\frac{L-x_B}{L}) + P_C \, (\frac{L-x_C}{L})$$

By differentiating we obtain

$$\frac{\partial U_{AB}}{\partial P_B} = \int_0^{x_B} \frac{M}{EI} \frac{\partial M}{\partial P_B} \, dx + \int_0^{x_B} \frac{kV}{AG} \frac{\partial V}{\partial P_B} \, dx$$

now setting P_B and P_C equal to zero and substituting from above we get

$$\frac{\partial U_{AB}}{\partial P_B} = \int_0^{x_B} \frac{(\frac{P}{2} \cdot x)}{EI} \, (\frac{L-x_B}{L}) \, dx + \int_0^{x_B} \frac{k(\frac{P}{2})}{AG} \, (\frac{L-x_B}{L}) \, dx$$

After integrating the equation becomes

$$\frac{\partial U_{AB}}{\partial P_B} = \frac{Px_B^3}{6EI} \left(\frac{L-x_B}{L}\right) + \frac{kPx_B}{2AG} \left(\frac{L-x_B}{L}\right) \rule{3cm}{0.4pt} \text{(A4-a)}$$

Following the same prodcedure we obtain for the other regions, except region B-C, the following Eqs:

Region C-D:

$$\frac{\partial U_{CD}}{\partial P_B} = \frac{Px_B}{2EIL} \left[\frac{Lx_D^2}{2} - \frac{x_D^3}{3} - \frac{Lx_C^2}{2} + \frac{x_C^3}{3}\right] - \frac{kPx_B}{2AGL} (x_D - x_C) \rule{1.5cm}{0.4pt} \text{(A4-b)}$$

Region D-E:

$$\frac{\partial U_{DE}}{\partial P_B} = \frac{Px_B}{2EI_RL} \left[\frac{L^3}{12} - \frac{Lx_D^2}{2} + \frac{x_D^3}{3}\right] - \frac{kPx_B}{2A_RGL} \left(\frac{L}{2} - x_D\right) \rule{1.5cm}{0.4pt} \text{(A4-c)}$$

Region E-F:

$$\frac{\partial U_{EF}}{\partial P_B} = \frac{Px_B}{6EI_RL} \left(\frac{L^3}{8} - x_D^3\right) + \frac{kPx_B}{2A_RGL} \left(\frac{L}{2} - x_D\right) \rule{2cm}{0.4pt} \text{(A4-d)}$$

Region F-G:

$$\frac{\partial U_{FG}}{\partial P_B} = \frac{Px_B x_D^3}{6EIL} + \frac{kPx_B x_D}{2AGL} \rule{3cm}{0.4pt} \text{(A4-e)}$$

To account for the strain energy in the region BC certain assumptions must be made about the normal stresses and the amount of the shearing force carried above and below the opening. In this derivation the normal stresses are assumed to be correctly predicted by the Vierendeel method of analysis as explained in Ref. (11). According to this theory the normal stresses in the sections above and below are given by the equation

$$\sigma_T = \frac{M_O Y_N}{I_N} \pm \frac{V_T x_O Y_T}{I_T} \rule{3cm}{0.4pt} \text{(A5-a)}$$

$$\sigma_B = \frac{M_0 Y_N}{I_N} \pm \frac{V_B x_0 Y_B}{I_B} \ \text{------------------------------------} \ (A5-b)$$

where positive values of the distance y are measured down. To the left of the opening centerline the negative sign applies to Eqs. (A5) and the positive to the right. By substituting Eqs. (A5) into Eq. (A2) and simplifying we obtain

$$U_{BC} = \int_o^a \int_A \frac{1}{E} \left(\frac{M_0 Y_N}{I_N}\right)^2 dA \ dx + \int_o^a \int_{A_T} \frac{1}{E} \left(\frac{V_T^2 x_0^2}{I_T^2} Y_T^2\right) dA_T \ dx$$

$$+ \int_o^a \int_{A_B} \frac{1}{E} \left(\frac{V_B^2 x_0^2}{I_B^2} Y_B^2\right) dA_B \ dx$$

and integrating gives the strain energy due to bending as

$$(U_{BC})_{bending} = \frac{M_0^2 a}{EI_N} + \frac{V_T^2 a^3}{3EI_T} + \frac{V_B^2 a^3}{3EI_B} \ \text{------------------------} \ (A6)$$

From Eq. (A1) the shearing strain energy may be written as

$$(U_{BC})_{shear} = \frac{k_T V_T^2 (2a)}{2A_T G} + \frac{k_B V_B^2 (2a)}{2A_B G} \ \text{------------------------} \ (A7)$$

Now by combining Eqs. (A6) and (A7), differentiating with respect to P_B and then setting P_B and P_C equal to zero we obtain

$$\frac{\partial U_{BC}}{\partial P_B} = \frac{PL_0 a x_B}{EI_N L} (L - L_0) - C_T^2 \frac{Px_B}{2L} \left(\frac{2}{3} \frac{a^3}{EI_T} + \frac{k_T (2a)}{A_T G}\right)$$

$$- C_B^2 \cdot \frac{Px_B}{2L} \left(\frac{2}{3} \frac{a^3}{EI_B} + \frac{k_B (2a)}{A_B G}\right) \ \text{------------------------} \ (A8)$$

where C_T and C_B are constants representing the precent of the total shearing force in region BC distributed to the sections above and below the opening

respectively. In order to simplify Eq. (A8) it is necessary to know the shear distribution ratio V_T/V_B. To determine this ratio the sections above and below the opening are treated as beams which must deflect equally. The deflections of these beams as determined by assuming fixed ends with points of inflection at their centers are

$$(y_{BC})_T = \frac{2}{3} \frac{V_T a^3}{EI_T} + \frac{k_T V_T (2a)}{A_T G}$$

$$(y_{BC})_B = \frac{2}{3} \frac{V_B a^3}{EI_B} + \frac{k_T V_B (2a)}{A_B G} \quad \text{--- (A9)}$$

Equating these two deflections we obtain the shearing force ratio to be

$$\frac{V_T}{V_B} = \frac{\dfrac{a^2}{3I_B E} + \dfrac{k_B}{A_B G}}{\dfrac{a^2}{3I_T E} + \dfrac{k_T}{A_T G}} \quad \text{--- (A10)}$$

Now since the deflections given by Eq. (A9) are equal we can rearrange Eq. (A8) to

$$\frac{\partial U_{BC}}{\partial P_B} = \frac{PL_0 a x_B}{EI_N L} (L - L_0) - \frac{Px_B}{2L} \left(\frac{2}{3} \frac{a^3}{EI_T} + \frac{k_T (2a)}{A_T G}\right) \left(C_T^2 + \frac{V_T}{V_B} C_B^2\right) \quad \text{----- (A11)}$$

By substituting for the constants C_T and C_B, the last term in Eq. (A11) becomes

$$C_T^2 + \frac{V_T}{V_B} C_B^2 = \frac{V_T^2}{V^2} + \frac{V_T}{V_B} \frac{V_B^2}{V^2} = \frac{V_T}{P/2}$$

and the partial derivative of the strain energy in region BC reduces to

$$\frac{\partial U_{BC}}{\partial P_B} = \frac{PL_0 a x_B}{EI_N L} (L - L_0) - V_T \cdot \frac{x_B}{L} \left(\frac{2}{3} \frac{a^3}{EI_T} + \frac{k_T (2a)}{A_T G}\right) \quad \text{------------------ (A12)}$$

Adding Eqs. (A4) and (A12) and reducing gives the deflection at B as

$$y_B = \frac{Px_B L^2}{EI_R} + \frac{Px_B x_D^2}{4EI} \left(1 - \frac{I}{I_R}\right) + \frac{Px_B^3}{6EI} \left(1 - \frac{x_B}{L}\right)$$

$$+ \frac{kPx_B}{2AG} \left(1 - \frac{x_B}{L}\right) + \frac{PL_0^2 a}{EI_N} \left(1 - \frac{x_B}{L}\right) - \frac{PL_0 a^2}{EI_N}$$

$$+ \frac{Px_B}{2EIL} \left(\frac{x_C^3}{3} - \frac{Lx_C^2}{2}\right) + \frac{kPx_B}{2AGL} x_C$$

$$- V_T \frac{x_B}{L} \left(\frac{2}{3} \frac{a^3}{EI_T} + \frac{k_T(2a)}{A_T G}\right) \text{ ----------------------------- (A13)}$$

The deflection at section C is given by the partial derivative of the strain energy with respect to P_C. Hence following the same procedure as before we find the partial derivatives for the different portions to be as follows:

$$\frac{\partial U_{AB}}{\partial P_C} = \frac{Px_B^3}{6EI} \left(1 - \frac{x_C}{L}\right) + \frac{kPx_B}{6AG} \left(1 - \frac{x_C}{L}\right) \text{ --------------------------- (A14-a)}$$

$$\frac{\partial U_{BC}}{\partial P_C} = \frac{PL_0^2 a}{EI_N} \left(1 - \frac{x_C}{L}\right) + V_T \left(\frac{2}{3} \frac{a^3}{EI_T} + \frac{k_T(2a)}{A_T G}\right) \left(1 - \frac{x_C}{L}\right) \text{ ------------- (A14-b)}$$

$$\frac{\partial U_{CD}}{\partial P_C} = \frac{Px_C}{2EIL} \left(\frac{Lx_D^2}{2} - \frac{x_D^3}{3} - \frac{Lx_C^2}{2} + \frac{x_C^3}{3}\right) - \frac{kPx_C}{2AGL} (x_D - x_C) \text{ ----------- (A14-c)}$$

$$\frac{\partial U_{DE}}{\partial P_C} = \frac{Px_C}{2EI_R L} \left(\frac{L^3}{12} - \frac{Lx_D^2}{2} + \frac{x_D^3}{3}\right) - \frac{kPx_C}{2A_R GL} \left(\frac{L}{2} - x_D\right) \text{ ------------------ (A14-d)}$$

$$\frac{\partial U_{GF}}{\partial P_C} = \frac{Px_D^3}{6EI} \cdot \frac{x_C}{L} + \frac{kPx_D}{2AG} \frac{x_C}{L} \text{ ------------------------------------- (A14-e)}$$

$$\frac{\partial U_{EF}}{\partial P_C} = \frac{Px_C}{L} \left(\frac{L^3}{48EI_R} + \frac{kL}{4A_R G} - \frac{x_D^3}{6EI_R} - \frac{kx_D}{2A_R G} \right) \text{----------------} \quad (A14\text{-}f)$$

By adding Eqs. (A14) and canceling terms the deflection at C maybe written as

$$y_C = \left[\frac{Px_B^3}{6EI} + \frac{kPx_B}{2AG} + \frac{PL_0^2 a}{EI_N} + V_T \left(\frac{2a^3}{3EI_T} + \frac{2k_T a}{A_T G} \right) \right] \left(1 - \frac{x_C}{L} \right)$$

$$+ \frac{Px_C L^2}{16EI_R} + \frac{Px_C x_D^2}{4EI} \left(1 - \frac{I}{I_R} \right) + \frac{Px_C}{2EIL} \left(\frac{x_C^3}{3} - \frac{Lx_C^2}{2} \right) + \frac{kPx_C^2}{2AGL} \quad \text{------} \quad (A15)$$

Then subtracting Eq. (A13) from Eq. (A15) we obtain the equation for the relative opening deflection to be

$$y_{BC} = \frac{2Pa}{E} \left[\frac{x_C^3 - x_B^3}{6IL} - \frac{x_C^2}{4I} + \frac{L_0 a}{I_N L} \left(\frac{L}{2} - L_0 \right) \right.$$

$$+ \frac{kaE}{ALG} + \frac{L^2}{16I_R} + \frac{x_D^2}{4I} \left(1 - \frac{I}{I_R} \right) \right]$$

$$+ V_T \left(\frac{2}{3} \frac{a^3}{EI_T} + \frac{k_T (2a)}{A_T G} \right) \left(1 - \frac{2a}{L} \right) \text{----------------------} \quad (A16)$$

Deflection at the Point of Load

The less difficult problem of determining the deflection under the load is accomplished by finding the partial derivative of the strain energy with respect to the applied load P. This solution takes into account the web opening and the flange reinforcing as shown in Fig. A1. By evaluating the regions of the beam separately, the following equations for the partial derivatives of the strain energy were obtained:

$$\frac{\partial U_{AB}}{\partial P} = \frac{Px_B^3}{12EI} + \frac{kPx_B}{4AG} \text{-----------------------------------} \quad (A17\text{-}a)$$

$$\frac{\partial U_{BC}}{\partial P} = \frac{PL_0^2 a}{2EI_N} + V_T \left(\frac{2a^3}{3EI_T} + \frac{k_T(2a)}{A_T G}\right) \text{---------------------------------} \quad \text{(A17-b)}$$

$$\frac{\partial U_{CD}}{\partial P} = \frac{P}{12EI} (x_D^3 - x_C^3) + \frac{kP}{4AG} (x_D - x_C) \text{---------------------} \quad \text{(A17-c)}$$

$$\frac{\partial U_{DE}}{\partial P} = \frac{P}{12EI_R} \left(\frac{L^3}{8} - x_D^3\right) + \frac{k_R P}{4A_R G} \left(\frac{L}{2} - x_D\right) \text{---------------------} \quad \text{(A17-d)}$$

$$\frac{\partial U_{EF}}{\partial P} = \frac{\partial U_{DE}}{\partial P} \text{--} \quad \text{(A17-e)}$$

$$\frac{\partial U_{FG}}{\partial P} = \frac{Px_D^3}{12EI} + \frac{kPx_D}{4AG} \text{---} \quad \text{(A17-f)}$$

By adding all the terms in Eqs. (A17) and reducing the deflection under the load P may be written as

$$y_P = \frac{P}{12EI} (x_B^3 + 2x_D^3 - x_C^3) + \frac{P}{6EI_R} \left(\frac{L^3}{8} - x_D^3\right)$$

$$+ \frac{PL_0^2 a}{2EI_N} + V_T \left(\frac{2a^3}{3EI_T} + \frac{k_T(2a)}{A_T G}\right)$$

$$+ \frac{kP}{4AG} (x_B + 2x_D - x_C) + \frac{k_R P}{4A_R G} \left(\frac{L}{2} - x_D\right) \text{---------------------} \quad \text{(A18)}$$

APPENDIX B

Shear Deflection Coefficient

To determine the distribution of shearing force to the tee sections above and below the web opening on the basis of equal deflections, the deformation due to shearing strains as well as bending strains must be considered. To correct for the variation in the shearing strain over the cross section, a shear deflection coefficient k is generally applied to the simple shear deflection formula based on the deflection of the neutral axis. Letting y_S represent the shear deformation of the neutral axis we can write

$$\frac{dy_S}{dx} = \gamma_{xy}\Big|_{y=0} = \frac{1}{G}\,\tau_{xy}\Big|_{y=0} = \frac{kV}{AG} \quad\text{-----------------------------------} \quad (B1)$$

where V is the shearing force, A is the area of the cross section and G is the shear modulus. Then if the cross section and shearing force are constant, the shear deformation over the length L is

$$y_S = \frac{kVL}{AG} \quad\text{---} \quad (B2)$$

The shear deflection coefficient k depends upon the shearing stress distribution and hence the shape of the cross section. For a linearly elastic material the strain energy may be used to determine the coefficient k.

The shearing strain energy per unit volume in terms of the shearing stress τ and the shearing strain γ is

$$U_0 = \int_0^\gamma \tau d\gamma = G\int_0^\gamma \gamma d\gamma = \frac{G\gamma^2}{2} = \frac{\tau^2}{2G}$$

and for the whole volume v we have

$$U = \int_v \frac{\tau^2}{2G}\, dv \quad\text{---} \quad (B3)$$

Now assuming that the shearing stress distribution given by the strength of materials approach ($\tau_{xy} = VQ/It$) is sufficiently accurate for our purposes the total shear strain energy becomes

$$U = \int_0^L \frac{V^2}{2AG} \left[\frac{A}{I^2} \int_A \frac{Q^2}{t^2} \, dA \right] dx \text{ --- (B4)}$$

where t is the thickness and I is the centroidal moment of inertia. The term Q represents the first moment of the cross sectional area to either side of the section where the shearing stress is being determined. By setting the bracket term in Eq. (B4), which is dimensionless and independent of the integration over the length, equal to the constant

$$k = \frac{A}{I^2} \int_A \frac{Q}{t^2} \, dA \text{ --- (B5)}$$

the strain energy due to shearing stress may be written as

$$U_S = \int_0^L \frac{kV^2}{2AG} \, dx \text{ -- (B6)}$$

Then by applying Castigliano's theorem on deflections we again obtain Eq. (B2). Hence the k given by Eq. (B5) is the proper equation for the shear deflection coefficient when the assumptions are those stated above.

Although the values of the shear deflection coefficient k have been found for a number of cross sections, those required for a tee section or a reinforced tee section don't seem to be available. The integration of Eq. (B5) for the shear deflection coefficient is broken down into four parts; the flange, the web between the flange and the reinforcing bar, the reinforcing bar including the web at that level, and the web portion outside the reinforcing. By integrating and using the notation shown in Fig. B1 the following equations

were obtained for the reinforced tee section:

$$k = \frac{A}{I^2} (k_1 + k_2 + k_3 + k_4) \text{ --} \quad (B7)$$

where

$$k_1 = \frac{b}{4} (S_1^4(S_1-S_3) - \frac{2}{3} S_1^2(S_1^3 - S_3^3) + \frac{1}{5} (S_1^5 - S_3^5)$$

$$k_2 = \frac{w}{4} [S_3^4(S_3 + S_4) - \frac{2}{3} S_3^2(S_3^3 + S_4^3) + \frac{1}{5} (S_3^5 + S_4^5)]$$

$$+ A_f \cdot \overline{Y}_f [S_3^2(S_3 + S_4) - \frac{1}{3} (S_3^3 + S_4^3)]$$

$$+ (A_f \cdot \overline{Y}_f)^2 (S_3 + S_4)/w$$

$$k_3 = \frac{c}{4} [S_5^4 (S_5 - S_4) - \frac{2}{3} S_5^2 (S_5^3 - S_4^3) + \frac{1}{5} (S_5^5 - S_4^5)]$$

$$+ A_3 \cdot \overline{Y}_3 [S_5^2 (S_5 - S_4) - \frac{1}{3} (S_5^3 - S_4^3)]$$

$$+ (A_3 \cdot \overline{Y}_3)^2 (S_5 - S_4)/c$$

$$k_4 = \frac{w}{4} [S_2^4 (S_2 - S_5) - \frac{2}{3} S_2^2 (S_2^3 - S_5^3) + \frac{1}{5} (S_2^5 - S_5^5)]$$

$$A_f = b \cdot t$$

$$\overline{Y}_f = (S_1 + S_3)/2$$
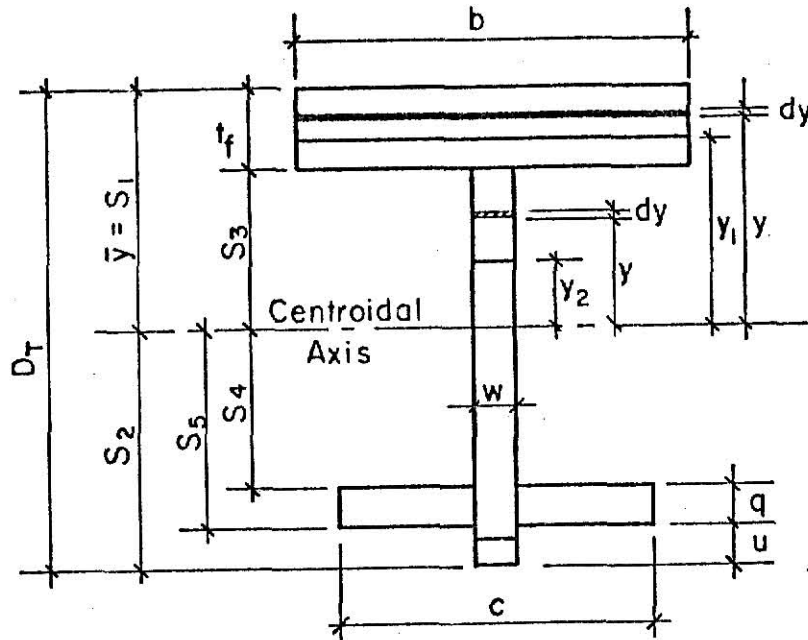
$$A_3 = u \cdot w$$

$$\overline{Y}_3 = (S_2 + S_5)/2$$

Fig. B1.

By making u and q in Fig. B1 zero and setting c equal to the width of the web w, the same equations apply to the unreinforced tee section. After working a number of numerical examples the conclusion was reached that the only significant term in the shear coefficient was k_2, that for the web between the flange and the reinforcing.

Shearing Force Distribution

One way to determine the theoretical distribution of shearing force to sections above and below the web opening is on the basis of equal secondary deflections. The secondary deflection of the beam between the edges of the opening depends upon both bending stresses and shearing stresses. By assuming the tee sections to have fixed ends with points of inflection at the middle, the bending deflection is found to be

$$y_b = \frac{2Va^3}{3EI}$$

where V is the shearing force and 2a equals *the width of the opening.*

Hence the total secondary deflection becomes

$$y = y_b + y_S = \frac{2}{3}\frac{Va^3}{EI} + \frac{2kVa}{AG} \quad\text{--} \quad (B8)$$

Now equating the secondary deflections of the sections above and below

the opening we write

$$\frac{2}{3}\frac{V_Ta^3}{EI_T} + \frac{2k_TV_Ta}{A_TG} = \frac{2}{3}\frac{V_Ba^3}{EI_B} + \frac{2k_BV_Ba}{A_BG}$$

and solving for the shear force ratio gives

$$\frac{V_T}{V_B} = \frac{\dfrac{a^2}{3I_B\ E/G} + \dfrac{k_B}{A_B}}{\dfrac{a^2}{3I_T\ E/G} + \dfrac{k_T}{A_T}} \quad\text{--} \quad (B9)$$

where the subscripts T and B refer to the sections above and below the opening

respectively.

This equation for the shearing force distribution ratio is essentially

the same as those presented by Frost (9) and by Douglas and Gambrell (8).

Frost's version uses only the area of the web along with a shear deflection

coefficient of 1.2, while Douglas and Gambrell suggest using *the shear*

coefficient defined by Cowper (7). Although based on the Vierendeel analysis,

the assumptions of the derviation presented in Douglas and Gambrell appear

to be somewhat different than those used here.

ELASTIC TESTS ON STEEL BEAMS WITH ECCENTRIC
RECTANGULAR WEB OPENINGS

by

SHUAIB HAROON AHMAD

B.S., N.E.D. Engineering College, Karachi, Pakistan, 1974

AN ABSTRACT OF A MASTER'S THESIS

submitted in partial fulfillment of the

requirements of the degree

MASTER OF SCIENCE

Department of Civil Engineering

KANSAS STATE UNIVERSITY
Manhattan, Kansas

1975

ABSTRACT

Frequently openings are cut in the web of the beams for passage of utility ducts in the building frames. Because of the insufficient information on the strength of beams and the structural behavior of beams with eccentric web openings, a theoretical and experimental investigation of such beams was conducted.

For the experimental investigation, four W16 x 40 steel beams with 12 inch long by 6 inch deep rectangular openings were tested elastically. All the beams had eccentricities of 2 inches with three of the openings being above mid-depth and one below. One beam was unreinforced, one was reinforced only on one side of the web, and two were reinforced symmetrically. Both deflections and strains were recorded during the elastic tests. The experimental stresses were compared with those obtained by the finite element and Vierendeel solution, and were used to determine the ratio of shear force carried by the section above and below the opening V_T/V_B. The experimental values of the ratio V_T/V_B were used to determine the theoretical stresses by the Vierendeel method.

The three beams with the opening centered above mid-depth were modeled by the finite element method and solutions were obtained for moment shear ratios of 20, 40 and 60. These solutions give shearing stresses as well as normal stresses, which allows the shear force distribution V_T/V_B to be determined in two ways.

Several theoretical methods of calculating the shear force distribution were studied and compared with the experimental results. None of the methods seemed to give the accuracy desired, but some methods were definitely better

than others. The derivation of a shear deflection coefficient based on strain energy, which is used in one of the theoretical methods, is given in Appendix B.

Theoretical equations for mid-span deflection and relative deflection across the opening, which take into account the web opening, the opening reinforcement, and the flange reinforcement, are derived in Appendix A. The theoretically predicted mid-span deflections and relative deflections across the opening have been compared with the experimental results.